AWARD NUMBER: W81XWH-20-1-0755

TITLE: Subset of Preexisting, Poly-Resistant Cancer Stem Cells in High-Grade Serous Ovarian Cancer

PRINCIPAL INVESTIGATOR: Dr. Wa Xian

CONTRACTING ORGANIZATION: University of Houston, Houston, TX

REPORT DATE: October 2021

TYPE OF REPORT: Annual

PREPARED FOR: U.S. Army Medical Research and Materiel Command
Fort Detrick, Maryland 21702-5012

DISTRIBUTION STATEMENT: Approved for Public Release; Distribution Unlimited

The views, opinions and/or findings contained in this report are those of the author(s) and should not be construed as an official Department of the Army position, policy or decision unless so designated by other documentation.

REPORT DOCUMENTATION PAGE

Form Approved
OMB No. 0704-0188

Public reporting burden for this collection of information is estimated to average 1 hour per response, including the time for reviewing instructions, searching existing data sources, gathering and maintaining the data needed, and completing and reviewing this collection of information. Send comments regarding this burden estimate or any other aspect of this collection of information, including suggestions for reducing this burden to Department of Defense, Washington Headquarters Services, Directorate for Information Operations and Reports (0704-0188), 1215 Jefferson Davis Highway, Suite 1204, Arlington, VA 22202-4302. Respondents should be aware that notwithstanding any other provision of law, no person shall be subject to any penalty for failing to comply with a collection of information if it does not display a currently valid OMB control number. **PLEASE DO NOT RETURN YOUR FORM TO THE ABOVE ADDRESS.**

1. REPORT DATE	**2. REPORT TYPE**	**3. DATES COVERED**
October 2021	Annual	01Sep2020-31Aug2021

4. TITLE AND SUBTITLE

Subset of Preexisting, Poly-Resistant Cancer Stem Cells in High-Grade Serous Ovarian Cancer

5a. CONTRACT NUMBER
W81XWH-20-1-0755

5b. GRANT NUMBER

5c. PROGRAM ELEMENT NUMBER

6. AUTHOR(S)

Dr. Wa Xian

E-Mail:

5d. PROJECT NUMBER

5e. TASK NUMBER

5f. WORK UNIT NUMBER

7. PERFORMING ORGANIZATION NAME(S) AND ADDRESS(ES)

University of Houston
Houston, TX

8. PERFORMING ORGANIZATION REPORT NUMBER

9. SPONSORING / MONITORING AGENCY NAME(S) AND ADDRESS(ES)

U.S. Army Medical Research and Development Command
Fort Detrick, Maryland 21702-5012

10. SPONSOR/MONITOR'S ACRONYM(S)

11. SPONSOR/MONITOR'S REPORT NUMBER(S)

12. DISTRIBUTION / AVAILABILITY STATEMENT

Approved for Public Release; Distribution Unlimited

13. SUPPLEMENTARY NOTES

14. ABSTRACT

High-grade ovarian cancer responds very well to primary chemotherapy and yet almost always returns in 6-24 months and often in a form that is resistant to chemotherapy. Using novel technologies for cloning the plurality of cancer stem cells from HGOC tumors, we have identified a minority of cancer stem cells in each tumor that are resistant to a wide range of chemotherapeutic drugs to which they have never been exposed. Based on the hypothesis that these "polyresistant" cells drive recurrent disease, the present proposal seeks to clone polyresistant cells in an additional 20 cases of ovarian cancer, understand the molecular mechanisms by which these cells evade a broad array of chemotherapeutic drugs, and to identify drugs that circumvent and even leverage this resistance mechanism to selectively eliminate these preexisting cells that likely drive recurrent disease in these patients. Important new data suggest that the resistance driven by these polyresistance cancer stem cell variants may be a tractable problem. The first is that all polyresistant cells share, in common, a broad pattern of gene expression previously implicated in ancient mechanisms that respond to exogenous chemicals, or "xenobiotics", in the environment. The second is that the pattern of polyresistance- down to the specific chemotherapeutic drugs, is identical not only in different cancer stem cells within a patient but across patients, suggesting that the polyresistance phenomenon is surprisingly uniform. The last is that our initial attempts to find drugs that circumvent the polyresistance mechanism in one case successfully eliminates polyresistant clones from other tumors. Working with our clinical collaborators we will ask of these data based on five cases can be extending to a cohort of 20 additional cases of high-grade ovarian cancer. We anticipate these studies will lead to new approaches to the prevention of recurrent disease in women with this aggressive cancer.

15. SUBJECT TERMS
None listed.

16. SECURITY CLASSIFICATION OF:			**17. LIMITATION OF ABSTRACT**	**18. NUMBER OF PAGES**	**19a. NAME OF RESPONSIBLE PERSON**
					USAMRMC
a. REPORT	**b. ABSTRACT**	**c. THIS PAGE**	Unclassified		**19b. TELEPHONE NUMBER** *(include area code)*
Unclassified	Unclassified	Unclassified			

TABLE OF CONTENTS

	Page
1. Introduction	2
2. Keywords	2
3. Accomplishments	3
4. Impact	9
5. Changes/Problems	10
6. Products	10
7. Participants & Other Collaborating Organizations	11
8. Special Reporting Requirements	12
9. Appendices	12

REPORT OUTLINE

1. INTRODUCTION

Chemotherapy resistance is a common feature of recurrent high-grade ovarian cancer and underlies the poor outcome for this disease. The present program seeks to understand the molecular basis of this chemotherapy resistance through the use of novel technologies that capture the spectrum of stem cells from HGOC for a clonal analysis of chemotherapy resistance. Surprisingly, our analysis of multiple cases of HGOC reveals that each has a minor subset of cancer stem cells that are resistant to a wide range of oncology drugs that otherwise kill the majority of stem cells in these patients. In Aim 1, that asks whether these resistant clones are present in these patients prior to chemotherapy, we have found affirmative results for each case we have examined indicating this is a common if not universal feature of HGOC. We are now poised, in collaboration with our key clinical collaborators, to determine whether these preexisting resistant clones are in fact the same cells that drive recurrent disease in HGOC patients. In Aim 2, we have now firmly established that the differential gene expression profiles between the minor resistant clones and the majority sensitive clones are similar both within particular cases and show distinct similarities in gene expression profiles between distinct patients. Remarkably, the differential gene expression in resistant clones across cases indicate gene sets involving 1,200 to 1.600 genes that are heavily biased to nuclear receptor signaling found in pathways linked to xenobiotic handling. The xenobiotic pathways are ancient features of cells devoted to degrading toxic molecules found in the environment, and likely explain the robust chemotherapy resistance of these cells. In exciting work enabled by adapting these resistant and sensitive cancer stem cells to high-throughput drug screening, we have found that the resistant clones are "polyresistant" to an array of oncology drugs. In particular, we have found that this pattern of polyresistance is the same across all resistant clones within a case, and that this similarity extends to all cases of high-grade serous ovarian cancer (HGSOC) that we have examined. This key finding suggests the possibility that resistance is not polymorphic but indeed highly uniform, and raises the hope that the molecular basis for resistance can be defined and successfully drugged. Lastly, Aim 3 seeks to identify drugs that target cells with high levels of xenobiotic degradation activity. By successfully adapting cancer stem cell clones to high-throughput drug screening platforms, we have now identified a set of overlapping lead compounds that specifically target resistant clones while having only minor or no effect on paclitaxel-carboplatin sensitive clones. We are presently testing these and related compounds for their ability to eliminate resistant clones in xenograft models with the goal of interdicting recurrent disease early in therapeutic efforts.

2. KEYWORDS

High-grade Serous Ovarian Cancer

Chemotherapy Resistance

Cancer Stem Cells

Clonogenic Analysis

Xenobiotic Resistance

Recurrent Disease

3. Accomplishments

3.1. Major Goals of the Project

Aim 1. Identifying Pre-existing, Poly-Resistant Clones Across Cohort of HGSOC cases

Hypothesis: The presence of pre-existing, polyresistant clones in HGSOC is a common and perhaps universal feature of this cancer. The goal in Task 1 is to extend our preliminary clonal analysis of five HGSOC tumors to 20 additional cases to assess the generality of our basic conclusions on the presence and properties of pre-existing, polyresistant clones in therapy-naive tumors. In particular, it is critical to determine if pre-existing, polyresistant clones are present in most or all of HGSOC, and if so whether all pre-existing, polyresistant clones in these cases show the same intra-case uniformity as that five cases assessed to date. This analysis will require the generation of large clone libraries from 20 additional, therapy-naive HGSOC tumors, the generation of two 384-well plates of single cell-derived clones for each library via FACS-based flow sorting, and the replica-plating of these clones for analysis of standard-of-care resistance and polyresistance. Six polyresistant and six sensitive clones from each case will be analyzed by whole genome expression analysis by RNA-seq and by xenografting in immunodeficient mice for tumorigenicity and resistance to paclitaxel and unrelated chemotherapeutic drugs within the resistance profile. These clones will be the substrates for the analyses presented in Aims 2 and 3 concerning epigenetic profiling and drug screening for agents that circumvent resistance in each case.

Major Task 1 Resistant Clones in 20 HGSOC

Subtask 1 Collect 20 pre-therapy HGSOC tumors

Subtask 2 Generate libraries of clonogeneic cells from each of 20 HGSOC samples

Subtask 3 Identify resistant clones for each of 20 HGSOC tumors

Milestone to be achieved: Pre-existing resistant clone analysis across 20 HGSOC tumors

Local IRB/IACUC Approval

Milestone to be achieved: HRPO/ACURO Approval

Major Task 2 Molecular Analysis of Patient Matched Resistant and Sensitive Clones

Subtask 1 RNAseq of patient-matched resistant and sensitive clones

Subtask 2 Xenografting and histopathology of resistant and sensitive clones in xenografts

Milestone to be achieved: Resistance gene expression profiles of 20 HGSOC tumors

Aim 2. Establish the Epigenetic Basis of Polyresistance within Each Case

Hypothesis: The stability, uniformity, and broadness of the polyresistance profiles within a given case are the result of an epigenetically enforced program. The goal of Task 2 is to define the molecular mechanisms underlying the immense stability of the polyresistant properties of the pre-existing clonal variants in therapy-naive HGSOC. The uniformity of the differential gene profiles among the resistant clones within a patient, coupled with the excess representation of unusual transcription factor genes, suggests that epigenetic mechanisms ensure the programming of such cells across proliferative time. This notion is further supported by the fact that the polyresistant features of these clones cannot be predicted by their genetic heterogeneity which, as for the clones across a given library, is vast. Therefore we anticipate that a distinct set of epigenetic marks at the level of chromatin modifications and DNA methylation define the programming of such cells, and will exploit chromatin immunoprecipitation (ChIP-Seq), DNA methylation, and analysis of open chromatin patterns to characterize such patterns. These patterns will be compared with the whole-genome expression analyses performed on the same clones assess the presence of epigenetically controlled networks.

Major Task 3 Epigenetic Basis of Resistance

Subtask 1 Whole genome profiling of chromatin modifications in resistant clones

Subtask 2 Bioinformatics analysis of RNAseq and epigenetic data to mechanistic model

Milestone to be achieved: Epigenetic basis of pre-existing and stable resistance to chemotherapeutic drugs

Aim 3: Mechanisms Underlying and Therapeutic Targeting of Poly-Resistance

Hypothesis: Despite the broad spectrum of chemotherapeutic drug resistance displayed by the polyresistant variant clones, high-throughput small molecule screens can nevertheless identify vulnerabilities that could form the basis of patient-specific or cohort-specific therapies to prevent recurrent disease. The overarching goal of this research is to understand the incidence of and key drivers underlying poly-resistant clones and target them for therapeutic effect. Aim 3 leverages a key advantage of the cloning technology that provides unlimited numbers of clonally-derived lines for high-throughput screening against a broad array of approved, IND, and experimental small molecules in a short time frame. One of the goals of this work aside from molecular characterization of polyresistance is developing a rapid and efficient means of identifying resistant clones from a new case and using them to identify drugs or drug combinations that specifically target them for elimination. And while the data from Aims 1 and 2 may in the end implicate a common pathway essential for poly-resistant clones across cases, we have to be prepared for addressing resistance in a personalized, case-by-case approach.

Major Task 4 Targeting the Polyresistance Mechanism

Subtask 1 Characterization of polyresistance profiles to established oncology drugs for all 20 HGSOC cases

Subtask 2 Identification of drugs that interfere with the resistance program as probes to the mechanism and potential therapeutic leads

Milestones to be achieved: Precise definition of scope and variation of polyresistance in HGSOC

Milestone(s) Achieved: Identification of lead compounds that abrogate or bypass resistance phenotype to eliminate resistant clones

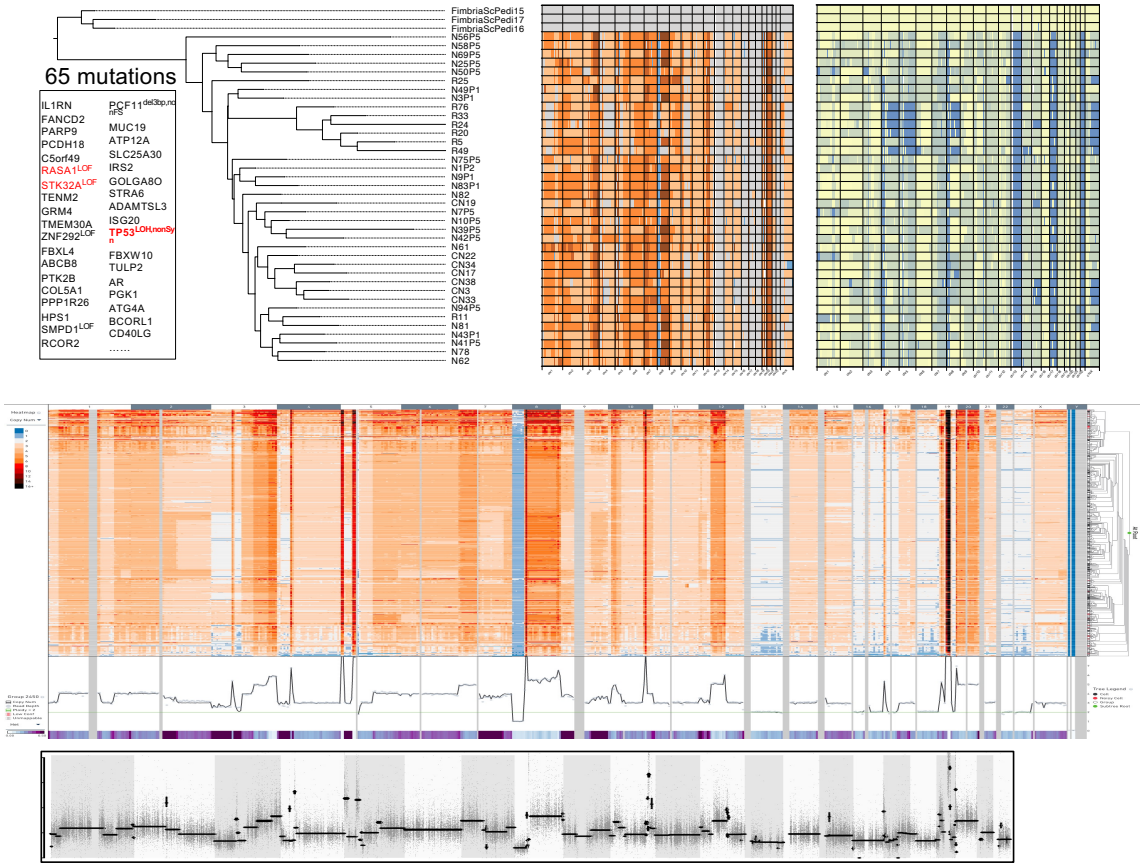


Fig. 1. Clonal analysis of stem cells from a single case of HGSOC depicting their phylogenetics based on copy number variation and inter-clonal variation. Below, a single-cell DNA sequencing profile of multiple cells from the library of cancer stem cells from this case showing that we have, by clonal sampling, captured the heterogeneity in this case.

3.2 What was accomplished under these goals?

The team has made tremendous progress in streamlining the analysis and identification of the minor fraction of resistant clones in HOSOCs that will greatly speed the analysis of the cohort of HGSOCs to be assessed in this program. In addition, the team has made important advances in the analysis of the bioinformatics of differential gene expression of the resistant clones in our five original cases that is detailing the common overexpression of pathways involved in the resistance to xenobiotics. Lastly, we have fully adopted these resistant and sensitive clones to high-throughput drug screening and have identified drugs that interfere with the "polyresistant" mechanisms in these resistant cells.

Specific Aim 1: Major Task 1- Identification of Resistant Clones in HGSOC

To achieve this goal, it is essential to streamline the process from the "random sampling" of clones to identify resistant clones that typically represent 1:50 to 1:200 of all cancer stem cell (CSC) clones in a library of a given tumor. We in fact used random sampling for the first five cases we examined and, in the process, had to individually clone and expand thousands of clones to isolate only several resistant clones from each case. The requirement for this random sampling was predicated on the fear and wide expectation that alternative approaches, such as selection for paclitaxel/carboplatin-resistant clones, would be accompanied by genetic changes in any resistant variants. Given the widespread intratumor heterogeneity among these clones that we had observed in any given tumor (**Fig. 1**), the expectation for genomic instability among these clones, especially in the presence of chemotherapeutic drugs, was a real possibility. Balancing this concern was other studies in the lab that showed that clones of esophageal adenocarcinoma, another cancer that also shows tremendous intratumor heterogeneity among CSC clones we generated, that showed that individual clones were in fact remarkably stable despite extensive passaging *in vitro* and even in clonal xenografts in immunodeficient mice (**Fig. 2**). In fact the esophageal adenocarcinoma clones showed almost no copy

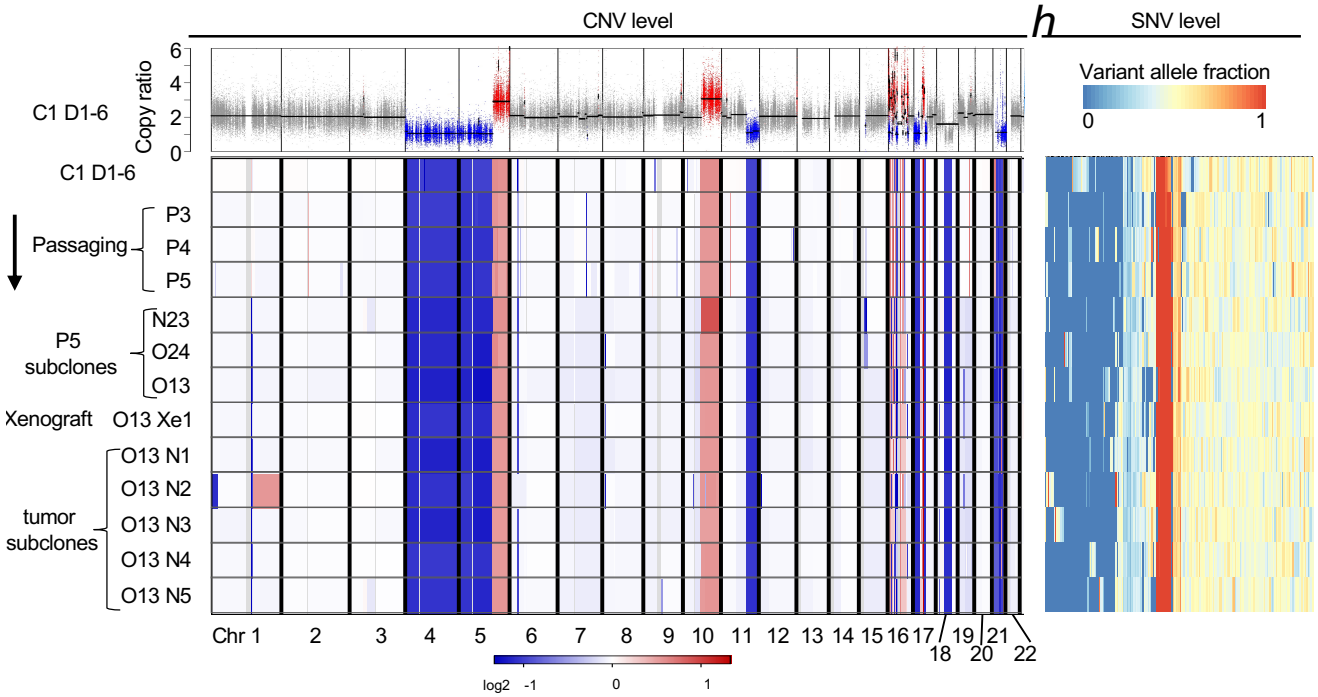


Fig. 2. Immense genomic stability of a single clone of esophageal adenocarcinoma across serial passaging in vitro and through tumor growth following xenografting to immunodeficient mice. In subclones derived after each of these procedures, very few copy number variation events or single nucleotide changes were found.

number variation events and only a handful of new non-synonymous mutations despite several months of tumor formation. Armed with these data, we asked how paclitaxel/carboplatin treatment would affect

the genomic structure of resistant clones versus the whole library of clones from a therapy-naive HGSOC. Unlike the whole library, which as expected undergoes tremendous changes with the elimination of sensitive clones, resistant clones are essentially unchanged by extensive passaging in the presence of chemotherapeutic drugs (**Fig. 3**). This is a major finding in that it demonstrates that we can use paclitaxel/carboplatin *selection* to identify the minor population of resistant clones instead of labor-intensive, *random sampling* of hundreds and perhaps thousands of clones that we have traditionally done to isolate these clones. From a wider perspective, this finding that chemotherapy does not "generate"

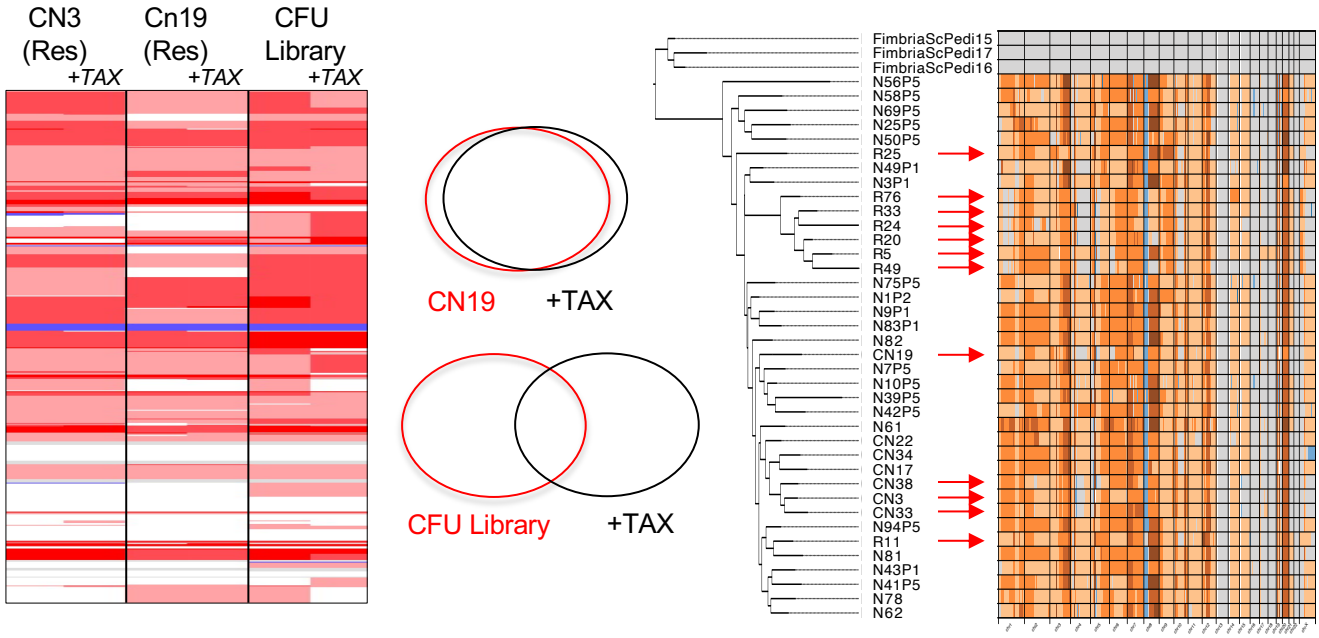


Fig. 3. Genomic stability of sampled resistant clones to paclitaxel/carboplatin (TAX) treatment compared with whole library that shows considerable changes as the majority of sensitive clones drop out. Right, red arrows indicate copy number variation profiles of resistant clones among sampled clones highlighting lack of correlation with genomics.

isolation from the 20 HGSOC tumors targeted by this proposal. We estimate that this new approach to the isolation of minor populations of resistant clones will save us the efforts of an entire FTE devoted to sampling and expansion now freed up for molecular analysis of the polyresistant clones.

Aim 2. Establish the Epigenetic Basis of Polyresistance within Each Case
Major Task 3- Major Task 3 Epigenetic Basis of Resistance

Our bioinformatics analysis of gene expression datasets of resistant versus sensitive clones across our original five cases has led to major insights into the basis of the polyresistance features of the resistant subsets. In particular, there is considerable overlap in the resistance gene expression profiles between these cases of HGSOC, so much so that discrete pathways can be identified (Fig. 4). These pathways are dominated by nuclear receptors marked by the Vitamin D pathway, the Nuclear Receptors Meta-Pathway, and nuclear receptors governing cellular differentiation such as the retinoids involved in epidermal differentiation (Hair Follicle Development) and fat cell differentiation (Transcription Factor Regulation of Adipogenesis). These nuclear receptors overlap the pathways involved in nuclear receptors governing the Response to Xenobiotics, a pathway responsible for the P450-mediated degradation of xenobiotics and pharmaceutical drugs in general. These data support the possibility that an epigenetically enforced expression of these nuclear receptors and their downstream programs of P450 degradation pathways is the basis of the ability of the polyresistant cells to identify and degrade a broad set of oncology drugs that make up the therapeutic options for HGSOC. Unlike most xenobiotic pathways, which are thought to be "induced" by exposure to a xenobiotic drug via their binding to

promiscuous nuclear receptors, these pathways appear to be constitutively "on" in these polyresistant HGSOC cells, and likely dictate the ability of these cells to evade these drugs.

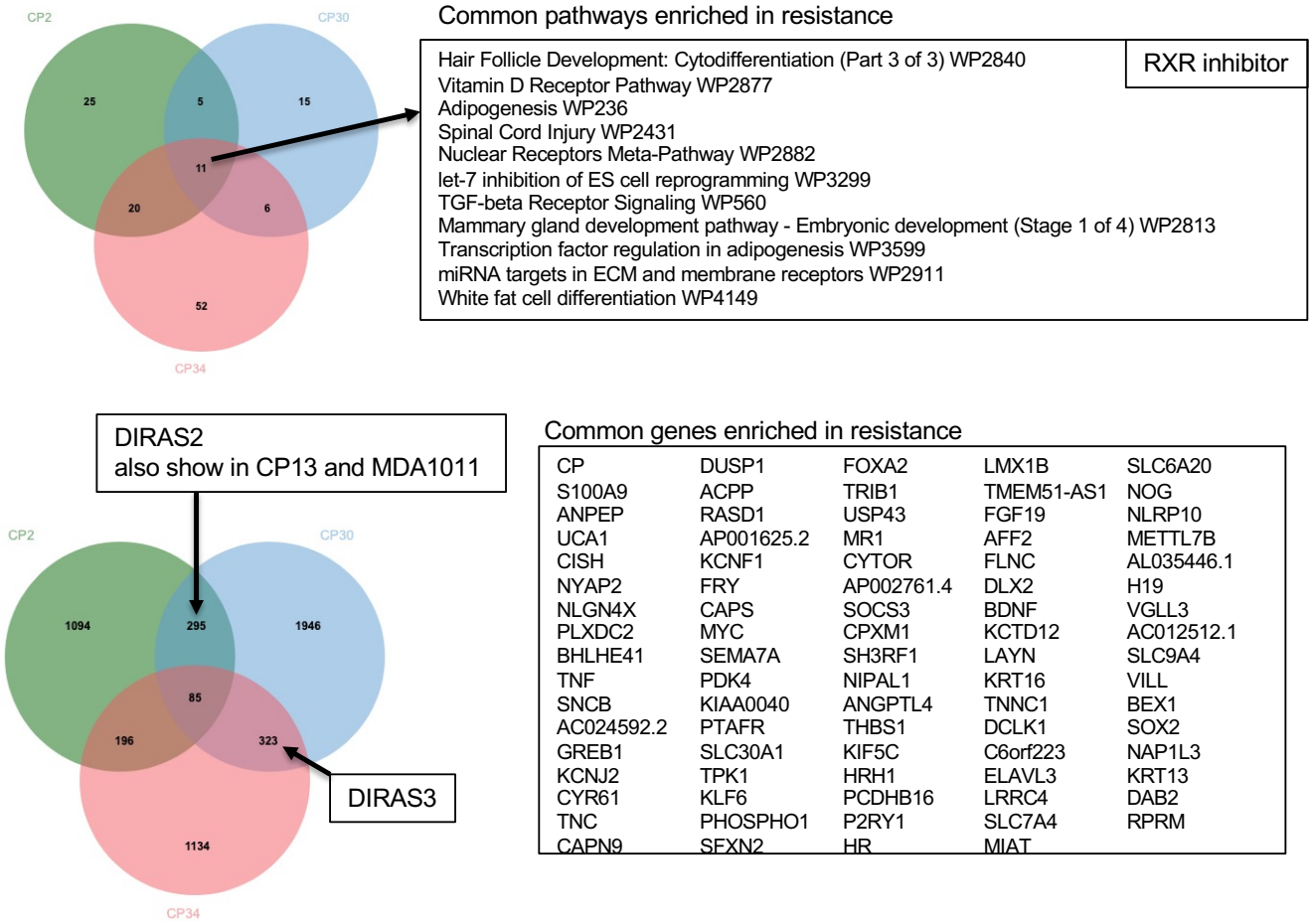


Fig. 4. Major signaling pathways overrepresented in common among resistant clones in HGSOC cases include those involving nuclear receptors regulating the degradation of steroids and xenobiotics in general.

Perhaps the most positive realization from these data relates to the nature of the polyresistance phenomenon within and across patients with HGSOC. Whereas the discovery of "polyresistance" in a subset of clones within HGSOC is important from a mechanistic standpoint, the key question is how many forms this polyresistance takes within an individual patient or across patients. If, for instance, each polyresistant clone is resistant to different drugs, it might be possible to block one of these types but other clones conceivably would be resistant to that treatment because they express a "different" type of polyresistance. We addressed this problem by directly assessing the polyresistant profiles of clones within and across HGSOC cases. Significantly, both within cases and across cases the pattern of polyresistance, as judged by specific molecules that comprise the polyresistance profile, are nearly identical (Fig. 5). Side-by-side comparisons of the specific polyresistance profiles of resistant-sensitive pairs of clones from two cases show a common pattern of drugs (blue) that do not kill the resistant clones but do eliminate the sensitive clones. These drugs vary widely in function and chemical structure, and suggest that despite the complexity of the resistance, the overall pattern is nearly identical across these patients. These data provide a basis and motivation for thinking that resistance is potentially simpler than we had anticipated and therefore a process that could be susceptible to therapeutic targeting. That being said we are aware of the challenges of attempting to target a process that is intrinsically designed to degrade exogenous chemical entities.

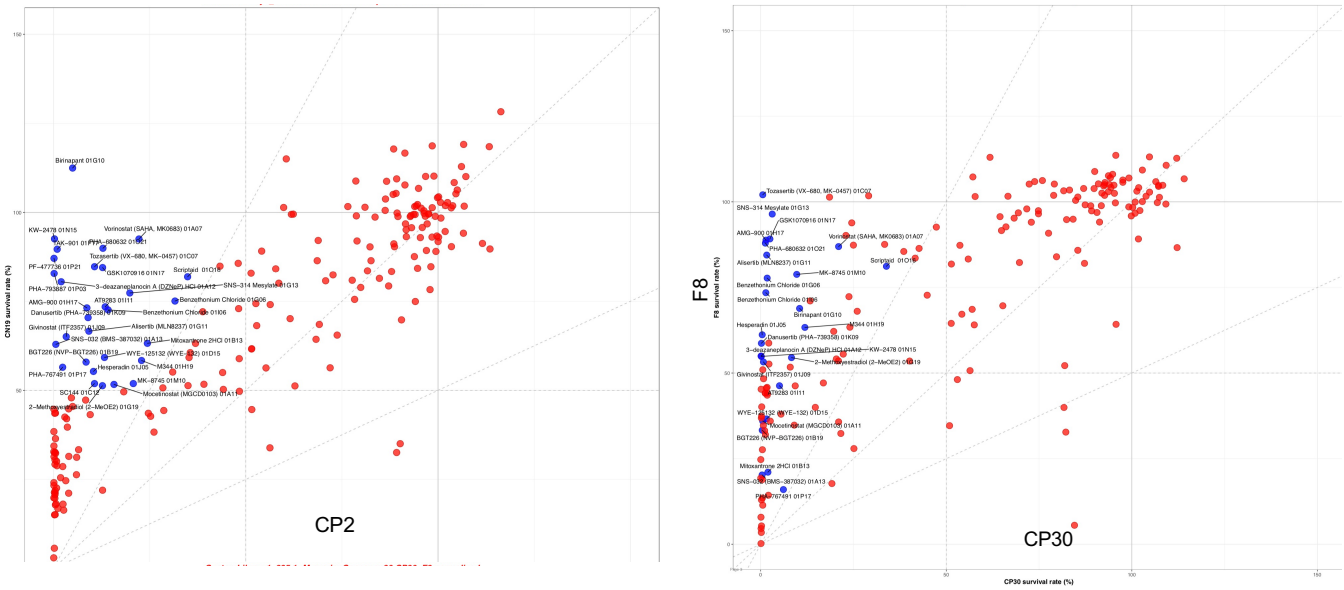
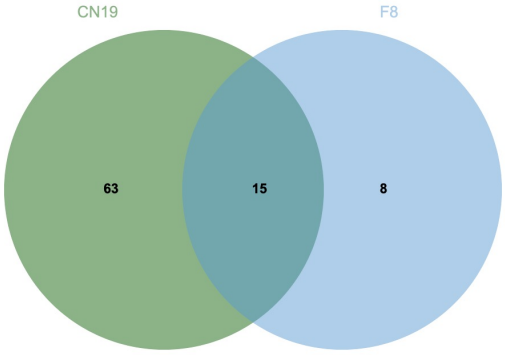


Fig. 5. Similarity in polyresistance profiles in paclitaxel/carboplatin resistant clones from two patients indicating that they are nearly identical (blue-marked compounds).

Aim 3: Task 4: Targeting the Polyresistance Mechanism

With the adaptation of the CSC clones to 384-well screening formats, we now have the potential to identify compounds that might circumvent the resistance mechanism. Through screening multiple collections of small molecules, we have now identified a number of leads that can enable paclitaxel/carboplatin lethality. As expected, some of the "hits" we obtained were known inhibitors of the ABC transporters that act to remove taxol from the cell (Fig. 6). However, we also identified multiple compounds that target epigenetic mechanisms and discrete pathways, suggesting the possibility that these drugs are targeting more general features of the polyresistance mechanism. We believe there will be a learning curve for understanding the basis of circumventing the polyresistance mechanism where we will have to introduce additional molecules from the resistance profile into the test platform. We are set to do this especially as success in this effort will be fundamental in address the resistance problem that represents the key barrier to treatment of patients with HGSOC.



Common hits

Posaconazole, CYP3A4 inhibitor, P450 inhibitor, Metabolism
Cyclosporine, phosphatase inhibitor & Immunology & Inflammation related inhibitor
SRT1720, SIRT1 inhibitor, Epigenetics
SANT-2, Smoothened inhibitor, WNT
GDC-0152, IAP inhibitor, Apoptosis
R428 (BGB324), Axl inhibitor, Protein Tyrosine Kinase
AZD3463, ALK/IGF-1R inhibitor, Protein Tyrosine Kinase
NVP-ADW742, IGF-1R, Protein Tyrosine Kinase
PD173074, FGFR/VEGFR inhibitor, Angiogenesis
Ponatinib (AP24534), Abl, PDGFRα, VEGFR2, FGFR1 and Src inhibitor, Angiogenesis
Lapatinib (GW-572016) Ditosylate, EGFR/HER2 inhibitor, Protein Tyrosine Kinase
Afatinib (BIBW2992), EGFR/HER2 inhibitor, Protein Tyrosine Kinase
Elacridar, ABCB1 inhibitor
Tariquidar, ABCB1 inhibitor
Zosuquidar (LY335979) 3HCl, ABCB1 inhibitor

Fig. 6. Early lead compounds that enable paclitaxel/carboplatin to kill resistant clones. Multiple pathways are implicated by these compounds, including epigenetics, Hedgehog signaling, receptor tyrosine kinases, and ABC transporters, the latter of which are known to enhance the activity of taxol compounds.

Opportunities for Training and Professional Development

Nothing to report.

Dissemination to Communities of Interest

Nothing to report.

Plans for Next Reporting Period

Adaptation of advanced technologies for resistant clone isolation from 20 additional cases of HGSOC
Profiling of epigenetic chromatin modifications in resistant clones versus sensitive clones
Testing lead compounds that circumvent polyresistance profiles of resistant clones
Demonstration that lead compounds prevent recurrent disease in xenograft models

IMPACT

Impact on the Development of the Principal Disciplines of the Project

The studies performed here have shown that all HGSOC cases have polyresistant clones, and importantly that these clones can be rapidly isolated by straightforward and rapid screening of cancer stem cell libraries with paclitaxel/carboplatin without worry that these treatments would alter the genomics of the resistant survivors. This concept, which we address and validate at a clonogenic level, is contrary to commonly repeated concepts for which there is no supporting data at the clone level. This finding will greatly enhance the speed and therefore scope of the studied here.

The identification of polyresistant clones in therapy naive tumors will ultimately impact our understanding of the origins of recurrent disease. These findings suggest that chemotherapy does not alter clones as much as eliminates the majority population of sensitive clones and enables the expansion of minor but ultimately dominant resistant clones.

Lastly, the observation that the polyresistance profiles of resistant clones within patients and across patients suggests that resistance may be a uniform process amenable to therapeutic interdiction. This finding provides much optimism that this problem can be solved through drug-screening efforts outlined in this proposal.

Impact On Other Disciplines

We anticipate that the insights we have gained into the mechanisms of chemotherapy in HGSOC will be germane to other human cancers such as lung, pancreatic, and gastrointestinal cancers.

Impact On Technology Transfer

The technologies we have developed to enable the cloning and manipulation of cancer stem cells in HGSOC are generally applicable to the cloning of cancer stem cells in general and will likely figure in the screening and identification of small molecules that specifically target CSCs in multiple human cancers. Patents for this technology have been filed and new ones will come from this work. I am one of several founders of a startup company (Tract Pharmaceuticals) to bring these technologies to drug development for patients with highly lethal cancers.

Impact On Society

Nothing to report.

5. CHANGES/PROBLEMS

Changes in Approach

None.

Actual or Anticipated Problems or Delays

While the project has made significant advances in advancing the technology for cloning resistant cells from HGSOC and in understanding the molecular mechanisms of chemotherapy resistance and drugs that overcome this process, the IRB approval to obtain additional HGSOC samples has been delayed and is the subject of intense discussions between the DOD, the University of Houston, the Brigham and Women's Hospital, and the University of South Florida School of Medicine. The discussions have been very productive, there is complete agreement between the DOD and the participating organizations, and we anticipate approval of the IRB within the month.

Changes with significant impact on expenditures

None.

Significant changes in use or care of human subjects, vertebrate animals, biohazards

None.

PRODUCTS

Journal Publications

Rao W, Niroula S, Wang S, Vincent M, McKeon F, Xian W. Protocol for Cloning Epithelial Stem Cell Variants from Human Lung. STAR Protoc. 2020 Sep 18;1(2):100063. PMID: 33015646

Rao W, Wang S, Duleba M, Niroula S, Goller K, Xie J, Mahalingam R, Neupane R, Liew AA, Vincent M, Okuda K, O'Neal WK, Boucher RC, Dickey BF, Wechsler ME, Ibrahim O, Engelhardt JF, Mertens TCJ, Wang W, Jyothula SSK, Crum CP, Karmouty-Quintana H, Parekh KR, Metersky ML, McKeon FD, Xian W. Regenerative Metaplastic Clones in COPD Lung Drive Inflammation and Fibrosis. Cell 2020 May 14;181(4):848-864. PMID: 32298651

Duleba M, Yamamoto Y, Neupane R, Rao W, Xie J, Qi Y, Liew AA, Niroula S, Zhang Y, Mahalingam R, Wang S, Goller K, Ajani JA, Vincent M, Ho KY, Hou JK, Hyams JS, Sylvester FA, Crum CP, McKeon F, Xian W. Cloning of ground-state intestinal stem cells from endoscopic biopsy samples. Nat Protoc. 2020 May;15(5):1612-1627. PMID: 32238950

Technologies or techniques

Our stem cell cloning technologies have been published in methods and protocol journals such as STAR protocols and Nature Protocols for dissemination to researchers in multiple areas.

Inventions, patent applications, and/or licenses

Patent Applications

1. Title of Invention: "Feeder-Free Stem Cell Culture Systems For Columnar Epithelial Stem Cells, And Uses Related Thereto," PCT Patent No.: PCT/US2018/067858; UHID:2020-026 Inventors: Frank McKeon, Marcin Duleba, Matt Vincent, Wa Xian

2. Title of Invention: "Feeder-Based and Feeder-Free Stem Cell Culture Systems For Stratified Epithelial Stem Cells, and Uses Related Thereto," U.S. Application No: 62/913,226; UHID: 2020-027. Inventors: Frank McKeon, Marcin Duleba, Matt Vincent, Wa Xian.

3. Title of Invention: "Methods and Compositions for Treating Epithelial Metaplasia, Dysplasia and Carcinomas, including Barrett's Esophagus and Epithelial Tumors," US Patent Application: 62/839,152UHID: 2019-027. Inventors: Frank McKeon, Marcin Duleba, Yanting Zhang, Jingzhong Xie, Wa Xian, Matthew Vincent

4. Title of Invention: "Methods and Compositions for Treating Inflammatory pulmonary disorders" US Application Number: 62992282; UHID: 2019-025. Inventors: Frank McKeon, Wei Rao, Marcin Duleba, Jingzhong Xie, Shan Wang, Wa Xian, Matthew Vincent

Patents licensed to Tract Pharmaceuticals, January 11, 2021.

Other Products

New Business creation: Tract Pharmaceuticals is a new startup devoted to a clonal analysis of cancers and associated chronic inflammatory diseases.

PARTICIPANTS AND OTHER COLLABORATING ORGANIZATIONS

Name:	**Wa Xian**
Project Role:	**PI**
Research Identifier	0000-0001-6315-8858
Nearest Person Month Worked:	**5**
Contribution to Project:	**Design and perform the experiments. Analyze the data and prepare the manuscript and report.**

Name:	**Frank McKeon**
Project Role:	**Co-investigator**
Research Identifier	**0000-0002-7747-9983**
Nearest Person Month Worked:	**0.1**
Contribution to Project:	**Consult on overall direction of this project including its experimental designs, analyzing and interpreting data.**

Name:	**Chris Crum**
Project Role:	**Co-investigator**
Research Identifier	0000-0002-0511-7756
Nearest Person Month Worked:	**0.1**

Contribution to Project:	**Consult on overall direction of this project including its experimental designs, analyzing and interpreting data.**

Name:	**Matt Anderson**
Project Role:	**Co-investigator**
Research Identifier	0000-0002-2081-4672
Nearest Person Month Worked:	**0.1**
Contribution to Project:	**Consult on overall direction of this project including its experimental designs, analyzing and interpreting data.**

Has there been a change in active other support?

Nothing to Report.

Other organizations?

Nothing to Report.

COLLABORATIVE REPORTS

Not applicable.

APPENDIX

Copies of the following papers:

Rao W, Niroula S, Wang S, Vincent M, McKeon F, Xian W. Protocol for Cloning Epithelial Stem Cell Variants from Human Lung. STAR Protoc. 2020 Sep 18;1(2):100063. PMID: 33015646

Rao W, Wang S, Duleba M, Niroula S, Goller K, Xie J, Mahalingam R, Neupane R, Liew AA, Vincent M, Okuda K, O'Neal WK, Boucher RC, Dickey BF, Wechsler ME, Ibrahim O, Engelhardt JF, Mertens TCJ, Wang W, Jyothula SSK, Crum CP, Karmouty-Quintana H, Parekh KR, Metersky ML, McKeon FD, Xian W. Regenerative Metaplastic Clones in COPD Lung Drive Inflammation and Fibrosis. Cell 2020 May 14;181(4):848-864. PMID: 32298651

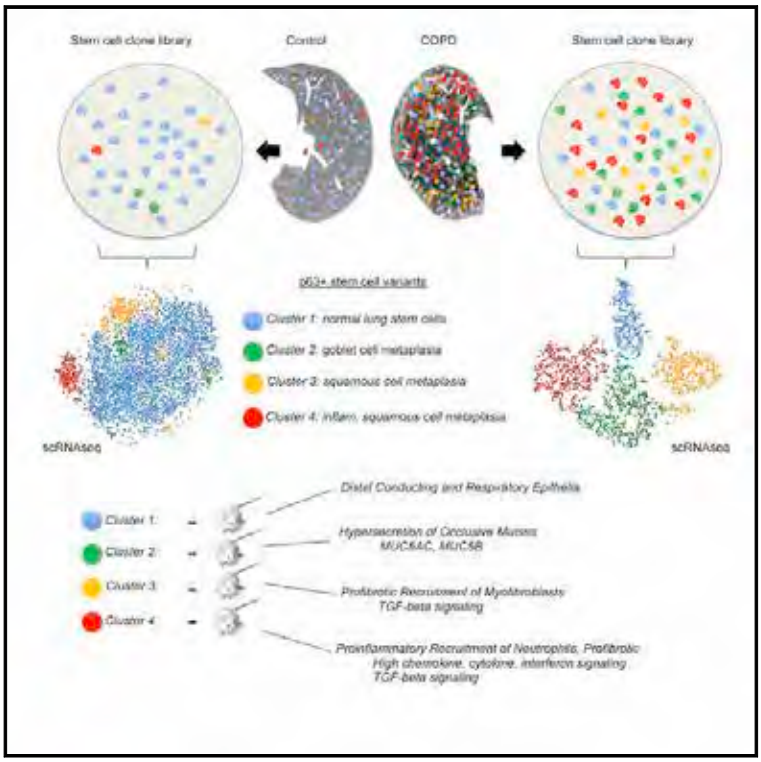
Duleba M, Yamamoto Y, Neupane R, Rao W, Xie J, Qi Y, Liew AA, Niroula S, Zhang Y, Mahalingam R, Wang S, Goller K, Ajani JA, Vincent M, Ho KY, Hou JK, Hyams JS, Sylvester FA, Crum CP, McKeon F, Xian W. Cloning of ground-state intestinal stem cells from endoscopic biopsy samples. Nat Protoc. 2020 May;15(5):1612-1627. PMID: 32238950

Article

Cell

Regenerative Metaplastic Clones in COPD Lung Drive Inflammation and Fibrosis

Graphical Abstract



Highlights

- COPD lung is dominated by three pathogenic stem cell variants
- These variants are epigenetically committed to metaplastic lesions found in COPD
- Variants drive key COPD features of inflammation, fibrosis, and airway obstruction
- Similar variants in fetal and normal lung likely serve sentinel functions

Authors

Wei Rao, Shan Wang, Marcin Duleba, ..., Mark L. Metersky, Frank D. McKeon, Wa Xian

Correspondence

fdmckeon@uh.edu (F.D.M.), wxian@uh.edu (W.X.)

In Brief

The hallmark features of COPD (inflammation, fibrosis, and mucus hypersecretion) are driven by distinct pathogenic progenitors which pre-exist as minor populations in healthy lungs but dominate in the disease state relative to normal lung stem cells.

Rao et al., 2020, Cell *181*, 1–17
May 14, 2020 © 2020 Elsevier Inc.
https://doi.org/10.1016/j.cell.2020.03.047

CellPress

Please cite this article in press as: Rao et al., Regenerative Metaplastic Clones in COPD Lung Drive Inflammation and Fibrosis, Cell (2020), https://doi.org/10.1016/j.cell.2020.03.047

Article

Cell

Regenerative Metaplastic Clones in COPD Lung Drive Inflammation and Fibrosis

Wei Rao,[1,12] Shan Wang,[1,12] Marcin Duleba,[1] Suchan Niroula,[1] Kristina Goller,[1] Jingzhong Xie,[1] Rajasekaran Mahalingam,[1] Rahul Neupane,[1] Audrey-Ann Liew,[1] Matthew Vincent,[2] Kenichi Okuda,[3] Wanda K. O'Neal,[3] Richard C. Boucher,[3] Burton F. Dickey,[4] Michael E. Wechsler,[5] Omar Ibrahim,[6] John F. Engelhardt,[7] Tinne C.J. Mertens,[8] Wei Wang,[8] Soma S.K. Jyothula,[9] Christopher P. Crum,[10] Harry Karmouty-Quintana,[8] Kalpaj R. Parekh,[7,11] Mark L. Metersky,[6,13] Frank D. McKeon,[1,13,14,*] and Wa Xian[1,13,14,15,*]

[1]Stem Cell Center, Department of Biology and Biochemistry, University of Houston, Houston, TX 77003, USA
[2]Nüwa Medical Systems, Houston, TX 77479, USA
[3]Marsico Lung Center, University of North Carolina, Chapel Hill, NC 27599, USA
[4]Department of Pulmonary Medicine, University of Texas MD Anderson Cancer Center, Houston, TX 77030, USA
[5]Department of Medicine, National Jewish Health, Denver, CO 80206, USA
[6]Department of Medicine, Division of Pulmonary, Critical Care, and Sleep Medicine, University of Connecticut School of Medicine, Farmington, CT 06032, USA
[7]Department of Anatomy and Cell Biology, University of Iowa Carver College of Medicine, Iowa City, IA 52242, USA
[8]Department of Biochemistry and Molecular Biology, McGovern Medical School, University of Texas Health Science Center at Houston, Houston, TX 77030, USA
[9]Department of Internal Medicine, McGovern Medical School, University of Texas Health Science Center at Houston, Houston, TX 77030, USA
[10]Department of Pathology, Harvard Medical School and Brigham and Women's Hospital, Boston, MA 02215, USA
[11]Department of Surgery, Division of Cardiothoracic Surgery, University of Iowa Carver College of Medicine, Iowa City, IA 52242, USA
[12]These authors contributed equally
[13]Senior author
[14]Present address: Stem Cell Center, Department of Biology and Biochemistry, University of Houston, Houston, TX 77004, USA
[15]Lead Contact
*Correspondence: fdmckeon@uh.edu (F.D.M.), wxian@uh.edu (W.X.)
https://doi.org/10.1016/j.cell.2020.03.047

SUMMARY

Chronic obstructive pulmonary disease (COPD) is a progressive condition of chronic bronchitis, small airway obstruction, and emphysema that represents a leading cause of death worldwide. While inflammation, fibrosis, mucus hypersecretion, and metaplastic epithelial lesions are hallmarks of this disease, their origins and dependent relationships remain unclear. Here we apply single-cell cloning technologies to lung tissue of patients with and without COPD. Unlike control lungs, which were dominated by normal distal airway progenitor cells, COPD lungs were inundated by three variant progenitors epigenetically committed to distinct metaplastic lesions. When transplanted to immunodeficient mice, these variant clones induced pathology akin to the mucous and squamous metaplasia, neutrophilic inflammation, and fibrosis seen in COPD. Remarkably, similar variants pre-exist as minor constituents of control and fetal lung and conceivably act in normal processes of immune surveillance. However, these same variants likely catalyze the pathologic and progressive features of COPD when expanded to high numbers.

INTRODUCTION

Chronic obstructive pulmonary disease (COPD) is an inflammatory condition of the lung marked by chronic bronchitis, small airway occlusion, inflammation, fibrosis, and emphysematous destruction of alveoli (Barnes et al., 2015; Decramer et al., 2012; Hogg et al., 2004; McDonough et al., 2011). The global impact of COPD is enormous as evidenced by the 250 million patients with this condition and the 50%, 5-year survival of those with Global Initiative for Chronic Obstructive Lung Disease (GOLD) stage 3 and 4 disease (FEV_1<50%) (Barnes et al., 2015; Decramer et al., 2012; Hogg et al., 2004; McDonough et al., 2011; Quaderi and Hurst, 2018; Singh et al., 2019). Risk factors include chronic exposure to cigarette smoke and environmental pollutants; early-life respiratory illnesses such as asthma, viral pneumonia, and perinatal bronchopulmonary dysplasia; as well as genetics (Busch et al., 2017; Fletcher and Peto, 1977; Martinez, 2016; Martinez et al., 2018; McGeachie et al., 2016). Given that 80% of COPD cases are associated with long-term chronic smoking, absolute abstinence will limit risk for this disease. However, the success of smoking cessation programs on patients with established COPD has been disappointing (Barnes, 2016; Fletcher and Peto, 1977; Gamble et al., 2007; Hogg and Timens, 2009; Miller et al., 2011; Scanlon et al., 2000; Wen et al., 2010), and most people with moderate COPD progress to severe disease (FEV_1<30) in a 5- to 20-year interval despite tobacco cessation. The mechanistic basis for

Please cite this article in press as: Rao et al., Regenerative Metaplastic Clones in COPD Lung Drive Inflammation and Fibrosis, Cell (2020), https://doi.org/10.1016/j.cell.2020.03.047

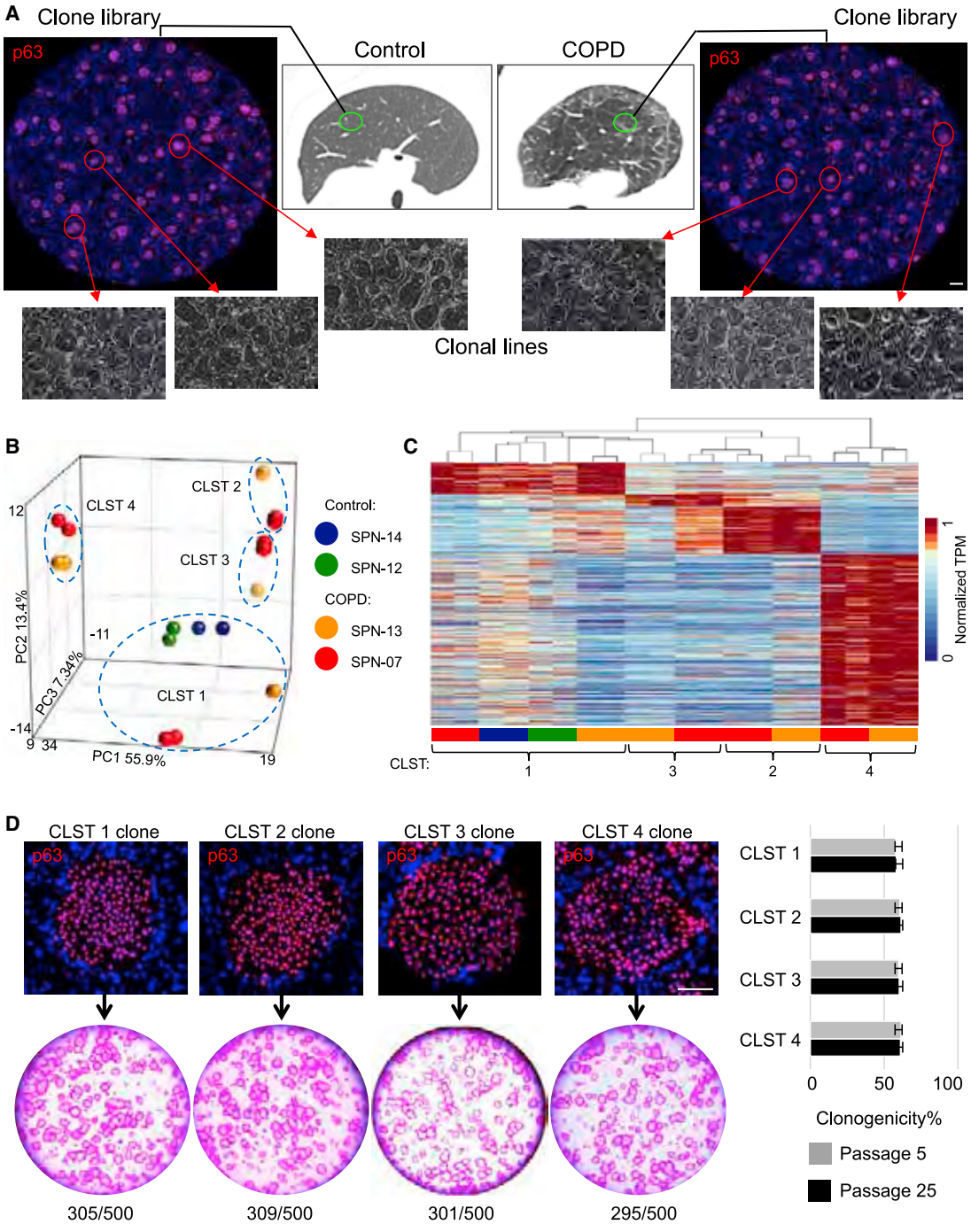


Figure 1. Epithelial Clone Heterogeneity in COPD

(A) Schematic depicting workflow of generating p63+ epithelial colony pools from resected normal and COPD lung tissue. Individual colonies are captured and expanded individually to generate clonal cell lines. Scale bar, 500 μm.

(B) Principal component analysis of RNA-seq differential expression genes (DEGs) (false discovery rate [FDR] < 0.05) derived from multiple clones from control (SPN-12, -14) and COPD (SPN-13, -07) lungs.

(C) RNA-seq expression heatmap of the clones depicted in the principal-component analysis (PCA) plot is shown highlighting cluster 1 (control) versus clusters 1–4 in COPD (detailed in Table S4).

(legend continued on next page)

this dogged progression of COPD is unclear, but multiple studies have shown that lung inflammatory pathways remain activated years after smoking cessation (Barnes, 2016; Gamble et al., 2007; Miller et al., 2011; Scanlon et al., 2000; Wen et al., 2010).

The predisposing influences of early-life pulmonary disease, coupled with the general irreversibility of this condition in previous smokers, suggest that inertial processes may drive COPD. Consistent with this notion, squamous cell metaplasia (SCM) and goblet cell metaplasia (GCM) typically observed in COPD likewise are not fully abolished by smoking cessation (Hogg and Timens, 2009; Lapperre et al., 2007; Raju et al., 2016; Zhou-Suckow et al., 2017). This persistence was surprising, as metaplasia has been tied to acute effects of cigarette smoke and inflammatory cytokines on normal airway progenitors (Araya et al., 2007; Schamberger et al., 2015; Wills-Karp et al., 1998). Removal of these toxicants was expected to enable distal airway progenitors to resume their roles in restoring tissue homeostasis in small airways and terminal bronchioles (Kumar et al., 2011; Ray et al., 2016; Tanaka et al., 2018; Vaughan et al., 2015; Yang et al., 2018; Zuo et al., 2015). In this context, we speculated that some irreversible alterations in distal airway progenitors explain their inability to restore airway and lung homeostasis following smoking cessation.

In the present study, we leveraged robust technologies that enable the cloning of distal airway epithelial cells (Kumar et al., 2011; Zuo et al., 2015) to perform a comparative analysis of clonogenic cells in patients with and without COPD. The data revealed that the COPD distal airways are populated by a highly stereotyped triad of clonogenic cells in addition to the normal clonogenic cell type that predominates control lungs. We show here these variants are stably committed to metaplastic fates and autonomously drive proinflammatory and pro-fibrotic programs akin to those implicated in COPD pathology. Lastly, we show that a similar triad of clonogenic cells in COPD also exists in control adult and 13-, 14-, and 17-week fetal lung, albeit at low ratios to the predominant distal airway clone type seen in normal lung. Thus, the variant clones predate any disease state and yet have features that could contribute to the emergence, pathology, or progression of COPD as a function of their numbers.

RESULTS

Heterogeneity of Clonogenic Cells in COPD

Libraries of clonogenic epithelial cells from resected lung tissue of 19 COPD and 11 control patients (Table S1) were generated by selective colony growth on lawns of irradiated, 3T3-J2 feeder cells (Kumar et al., 2011; Zuo et al., 2015; detailed in STAR Methods). In brief, approximately 0.85 ± 0.04% of all enzymatically digested lung cells yielded colonies from COPD patients and 0.15 ± 0.02% from controls (Table S2). These libraries have a complexity of 2,000 to 20,000 independent colonies per cubic centimeter of lung tissue and consist exclusively of cells that co-express E-cadherin and p63 (Ecad+/p63+). Single cells from these patient-specific libraries have a clonogenicity of greater than 50% as judged by single cell sorting to 384-well plates and give rise to discrete lines of highly immature epithelial cells characterized by a long-term (> 1 year) proliferative potential. Randomly sampled clones from libraries of control patients (SPN-12, -14) displayed whole genome expression profiles consistent with previously characterized clonogenic cells of distal airways (Kumar et al., 2011; Zuo et al., 2015) (Figures 1B and 1C). In contrast, sampled clones from libraries derived from COPD patients (SPN-7, -13) yielded a more complex spectrum of gene expression profiles. In addition to the normal distal airway clones (hereafter "cluster 1"), the majority of sampled clones showed whole genome expression profiles that diverged from cluster 1 and readily segregated into three additional distinct clusters (clusters 2, 3, and 4) (Figures 1B and 1C). Despite this clonal heterogeneity in COPD, all clones from clusters 1–4 shared the expression of established markers of distal airway progenitors (p63, KRT5), displayed a clonogenicity of 60 ± 1.4%, and showed a long-term proliferative potential of at least 25 passages (> 8 months) while maintaining a clonogenicity of 59.9 ± 1.6% (Figure 1D). Herein we leverage the regenerative properties of these patient-specific libraries of clonogenic cells and the single cell-derived clones from them to assess the properties of epithelial progenitors in COPD and control cases.

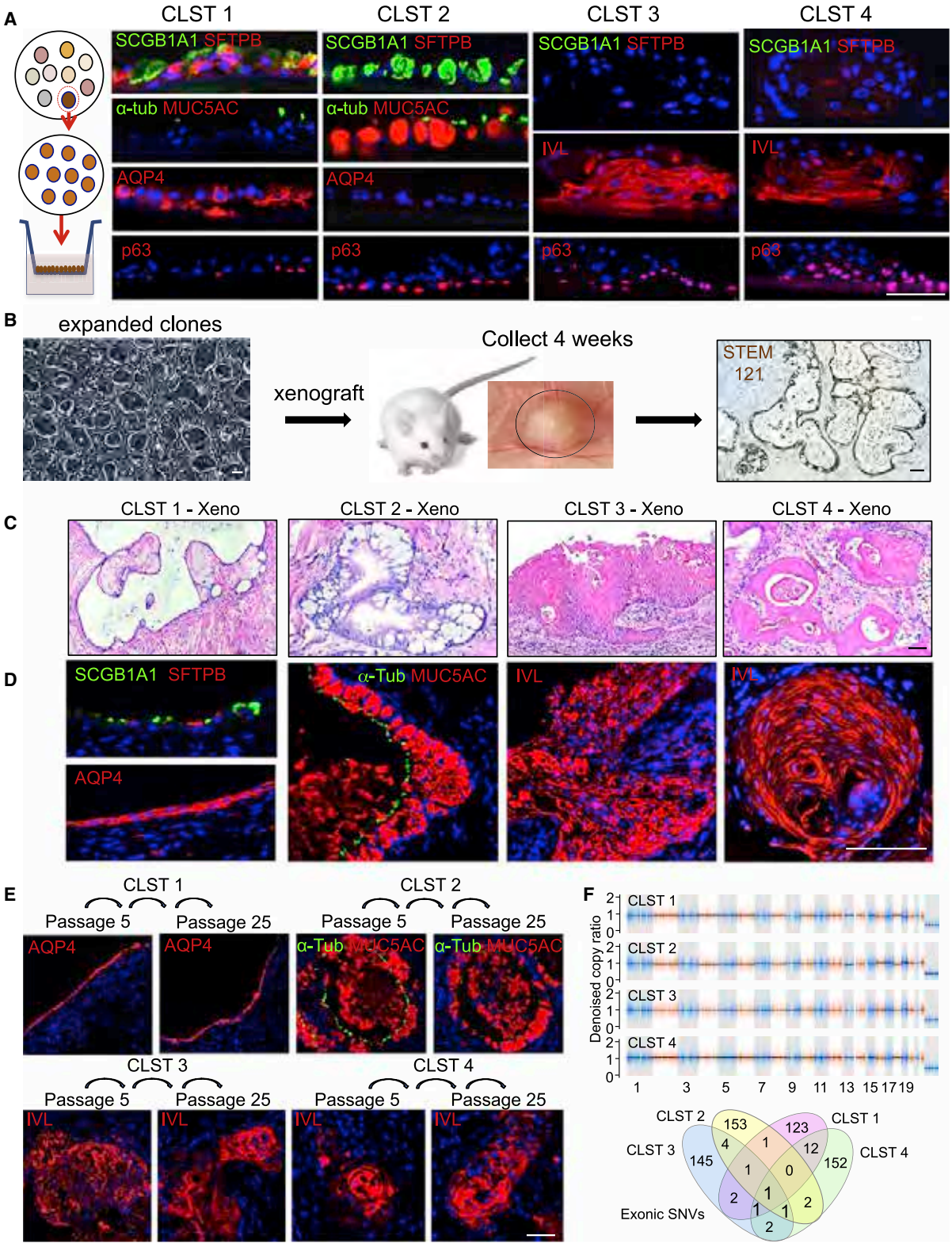
Metaplastic Fate Commitment of COPD Clones

In vitro differentiation of cluster 1 clones from both COPD and control libraries yielded normal epithelia (NM) marked by p63+ basal cells and suprabasal, differentiated cells expressing SCGB1A1, SFTPB, and AQP4, similar to human epithelia of small airways and terminal bronchioles (Figures 2A, S1A, and S1B). In contrast, clones of cluster 2 differentiated to a GCM marked by p63+ basal cells and differentiated goblet cells co-expressing SCGB1A1, MUC5AC, and MUC5B, whereas clones from clusters 3 and 4 gave rise to SCM marked by immature p63 cells and differentiated keratin 10 (Krt10)- and involucrin (IVL)-expressing cells (Figures 2A and S1A).

We further tested the fates of cluster-specific clones *in vivo* by transplanting discrete clones into highly immunodeficient NSG (*NODscidIL2ra*^{null}) (Shultz et al., 1995) mice. Briefly, 1 million cells of a designated clone were mixed with 50% *Matrigel* and injected subcutaneously, and the resulting xenograft nodule was examined four weeks later (Figure 2B). Significantly, normal control clones, as well as those from cluster 1 of COPD patients, assembled into a polarized epithelium *in vivo* comprised of cells positive for p63, KRT5, SCGB1A1, AQP4, AQP5, SFTPB, and SFTPC (Figures 2C and 2D) like that of normal human terminal bronchioles (Figure S1B) or that produced by *in vitro* differentiation of cluster 1 clones (Figures 2A and S1A). Also mirroring the *in vitro* air-liquid interface (ALI) cultures, the xenografts of cluster 2 clones from COPD libraries formed an epithelium dominated by large goblet cells (Figures 2C, 2D, and S1D) expressing MUC5AC and MUC5B (Fahy and Dickey, 2010; Kesimer et al., 2017; Okuda et al., 2019), and both cluster 3 and 4 clone

(D) Top: individual colonies from cloned representatives of clusters 1–4 stained with antibody to p63 showing uniform nuclear staining. Scale bar, 100 μm. Bottom: rhodamine red-stained colonies arising on lawns of irradiated 3T3-J2 fibroblasts from 500 cells from each of cloned representatives of clusters 1–4. Right: histogram of clonogenicity based on percentage of plated cells that formed colonies using representative clones from clusters 1–4 at passage 5 (P5) and 25 (P25). Data represented as mean ± SEM; See also Tables S1 and S4.

Please cite this article in press as: Rao et al., Regenerative Metaplastic Clones in COPD Lung Drive Inflammation and Fibrosis, Cell (2020), https://doi.org/10.1016/j.cell.2020.03.047



(legend on next page)

xenografts yielded SCM-expressing IVL and Krt10 (Figures 2C, 2D, S1E, and S1F). Despite their commitment to histologically similar SCM, cluster 3 and 4 clones exhibit distinct gene expression profiles (Figures 1B and 1C). cluster 4 clones in particular constitutively express a broad array of genes related to inflammation and are denoted herein as 'inflammatory SCM' or 'iSCM' versus 'SCM' for cluster 3 clones. Importantly, the respective differentiation fates of these clone types in xenografts proved to be remarkably stable to 250 days of continuous propagation *in vitro*, suggesting that these metaplasia are the consequences of highly stable, cell-autonomous fate programs (Figure 2E). Lastly, whole exome DNA sequencing of cluster 2, 3, and 4 clones derived from these COPD patients showed an absence of copy number variation events greater than 10Kb (Figure 2F). Moreover, the 127–157 single nucleotide variation (synonymous, nonsynonymous, indels) events in these clones were consistent in number with other somatic cells (Lee-Six et al., 2018) and did not impact known tumor suppressors or oncogenes such as p16 or p53 (Figures 2G and S1G; Table S5), arguing against the possibility these clones are related to neoplastic lesions.

Metaplastic Lesions Dominate End-Stage COPD Lung

Given the observation that the cluster 1–4 clones expressed p63 and yet differentiated to cluster-specific metaplasia *in vitro* and *in vivo*, we asked if metaplasia in the distal airways of COPD lung exhibited a similar association with p63+ basal cells. To address this question, we morphometrically quantified the distribution of normal distal airway epithelia and metaplasia in histological sections of distal lung from five additional donors lacking lung or systemic disease as well as from an additional 10 lungs of Stage 4 COPD transplant recipients (Table S3). Whereas metaplastic lesions in the normal lungs were rare, the end-stage COPD distal airways were replete with GCM (MUC5AC+) and SCM (IVL+) that, like normal distal airway epithelia, were subtended by basally positioned p63+ cells (Figure 3A). In quantitative terms, GCM occupied a mean of 32.7% of the distal airway epithelia (defined as that subtended by p63+ basal cells) of COPD lung versus 5.7% of the normal lungs, SCM occupied 26.8% of the COPD airways epithelia compared to less than 1% in normal lungs, and iSCM constituted approximately 21.6% of COPD airways and was not detected in normal lungs (Figure 3B). We also examined the distribution of marker genes associated with the p63+ basal cells of normal (AQP5+), iSCM (CXCL8+), and SCM or GCM (TRPC6+) airway epithelia in the same normal and Stage 4 COPD lungs (Figure 3C). Consistent with our morphometric analyses of lung metaplasia in COPD and control lung, CXCL8+ basal cells of iSCM comprised 19.3% of all p63+ distal airway basal cells of COPD lung, while these were not observed in normal lungs. Fully 52% of the basal cells in COPD lung expressed TRPC6, a marker of both GCM and SCM, while fewer than 2% of basal cells showed TRPC6 expression in the normal lungs (Figures 3D and S2). The close association of p63+ cells with the major forms of metaplasia in COPD is consistent with our finding that COPD lung possesses an array of p63+ clonogenic cells with absolute commitments to normal airway epithelia, GCM, or SCM. These findings are also in agreement with earlier studies that showed metaplasia in COPD and idiopathic pulmonary fibrosis (IPF) were subtended by p63+ cells (Araya et al., 2007; Chilosi et al., 2002; Plantier et al., 2011; Seibold et al., 2013; Smirnova et al., 2016).

Clonal Architecture of COPD and Control Libraries

We next asked if the widespread distribution of metaplastic lesions in the distal airways of end-stage COPD lung was reflected in the properties of the clonogenic cell libraries generated from our 19 COPD and 11 non-COPD cases. Single-cell RNA sequencing (scRNA-seq) (Satija et al., 2015) analyses of three COPD and three control libraries revealed four major clusters with gene expression profiles similar to those identified by single colony sampling as clusters 1–4 (Figures 3E and S3). In particular, the three COPD lungs showed major contributions to the clonal architecture of these libraries by clones committed to GCM, SCM, and iSCM represented by clusters 2, 3, and 4, respectively. The coherence between markers identified by scRNA-seq and by RNA-seq of representative clones of each cluster was high, suggesting that our sampling approach likely captured all major clone variants in the COPD patients (Figures 3E and S3A). This analysis also indicated that while control libraries were dominated by cluster 1 clones committed to distal airway epithelia, these libraries also harbored small percentages (6%–12%) of metaplastic variants (Figures 3E and S3B).

To develop a more simplified means of assessing the heterogeneity of clone libraries from COPD and control patients, we exploited the consensus markers identified by scRNA-seq and RNAs-eq of representative clones for quantitative flow cytometry

Figure 2. Commitment of Variant Clones to Metaplastic Fates

(A) From left, schematic of clonal expansion and differentiation in air-liquid interface (ALI) cultures assessed by immunofluorescence on histological sections. Cluster 1 clones differentiated to an epithelium characterized by expression of SCGB1A1, SFTPB, α-TUB, and AQP4 and the absence of MUC5AC. Cluster 2 clones differentiated into an epithelium characterized by SCGB1A1+, MUC5AC+, and AQP4- goblet cells. cluster 3 and cluster 4 clones differentiated into squamous epithelia that expressed involucrin (IVL) but not SCGB1A1, AQP4, or SFTPB. Scale bar, 100 μm.

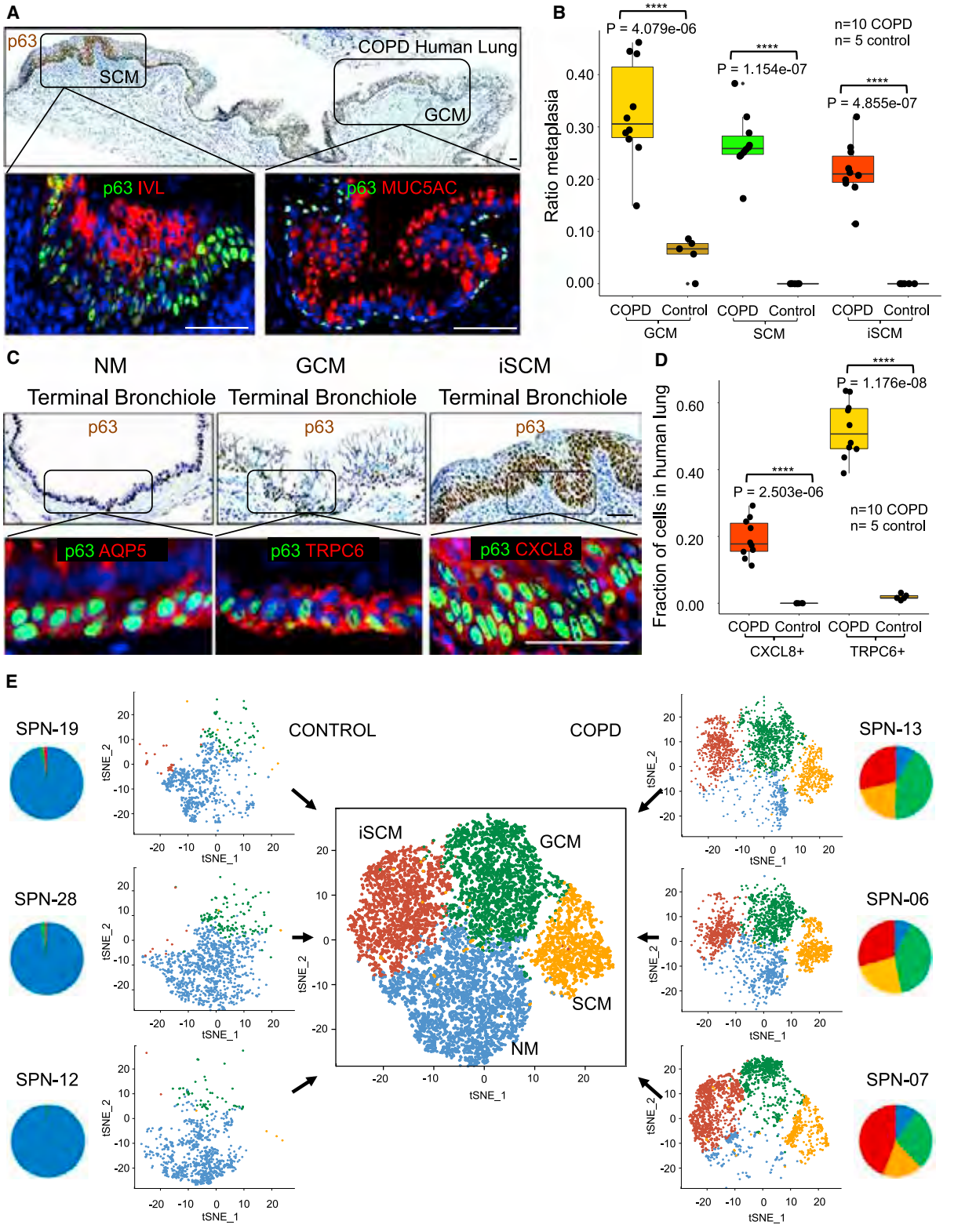
(B) Schematic of subcutaneous transplants of immature cells from clones or library of clones into immunodeficient mice. Nodules formed at 4 weeks were processed for histology and immunostaining and showed polarized epithelia that reacted with antibodies to the human-specific marker STEM121. Scale bar, 100 μm.

(C and D) *In vivo* differentiation following subcutaneous transplantation of cloned representatives of cluster 1 (SCGB1A1+, SFTPB+, and AQP4+), cluster 2 (MUC5AC+; GCM), and clusters 3 and 4 (IVL+; SCM). Scale bar, 100 μm.

(E) Xenografts of cluster 1–4 clones previously grown *in vitro* to P5 and P25 showing stability of fate differentiation and expression of cluster-specific markers. Scale bar, 100um.

(F) Copy number and single nucleotide variation analysis derived from whole exome sequencing of representative clones of clusters 1–4 from SPN-13 relative to patient blood. Copy number variation (CNV) events of larger than 10–20Kb were not detected in any of the clones. Venn diagram of all detected exonic single-nucleotide variants (SNVs) (synonymous, non-synonymous, indels) in each clone relative to all others. See also Figure S1; Tables S2 and S5.

Please cite this article in press as: Rao et al., Regenerative Metaplastic Clones in COPD Lung Drive Inflammation and Fibrosis, Cell (2020), https://doi.org/10.1016/j.cell.2020.03.047



(legend on next page)

(FACS) analysis. Antibodies to AQP5 were specific to cluster 1 cells, CXCL8 for cluster 4 cells, and TRPC6 antibodies for both clusters 2 and 3 (Figure 4A). This limited set of markers was used to quantify the relative distribution of clone variants across our 19 COPD and 11 control patients (Figures 4A and 4B; Table S1). Consistent with our analyses of scRNA-seq profiles, the quantification of clone types by flow cytometric analyses of markers showed that variants (TRPC6+ for clusters 2 and 3; CXCL8+ for cluster 4) comprised 77.7 ± 5% of all cells in the 19 COPD clone libraries, while in control specimens, 12.2 ± 6% of the p63+ clonogenic cells in the 11 control libraries fell within clusters 2–4 based on FACS analyses of markers TRPC6 and CXCL8 ($p < 2.2e-16$; Figures 4B and S4A; Table S2).

Xenografts of COPD Clone Libraries Drive Neutrophilic Inflammation

To assess the pathogenic potential of the COPD epithelial cells, we performed subcutaneous transplants of composite clone libraries of each of the 19 COPD patients and 11 control patients into immunodeficient mice. Over four weeks, clone libraries from control patients yielded epithelial cysts with appropriate basal-apical polarity around largely vacant spaces (Figures 4C and S4B; Table S2). In contrast, clone libraries generated from COPD patients produced cysts occupied by dense arrays of epithelial and non-epithelial cells (Figures 4D and S4C; Table S2). The majority of non-epithelial luminal cells were hematopoietic in origin as evidenced by anti-murine CD45 staining, and the majority of those were positive for antibodies to Ly6G, a marker of neutrophils (Figure 4D). Similar patterns of leukocyte transepithelial migration (TEM) (Brazil and Parkos, 2016) are present in COPD lung (Barnes et al., 2015; Butler et al., 2018; Quint and Wedzicha, 2007). Quantification of the extent of neutrophil infiltration at the level of individual epithelial cysts revealed that 36.4 ± 14% of these cysts scored "severe" (closest neutrophil packing) in the COPD clone library xenografts in contrast to only 0.3 ± 0.9% of the cysts in control library xenografts ($p = 1.2e-09$, Student's t test; Figures 4E and S4D).

Given the robust inflammatory response triggered by xenografts of COPD clone libraries, we asked if this inflammatory activity was a function of one or more of the constituent clone types. Using pathway enrichment analysis algorithms for the gene expression profiles of the four clone types, we found that cluster 4 clones, but not those of clusters 1, 2, or 3, displayed multiple inflammatory pathways including *Antigen Presentation*, *Interferon Signaling*, *Graft-versus-Host* responses, and *Dendritic Cell Maturation* (Figures 5A and S5A). We tested media conditioned by clones of clusters 1–4 for their ability to trigger phase I and II activation of human airway microvasculature endothelial cells, an essential step in leukocyte recruitment (Filippi, 2016). Endothelial cell activation was assessed by the expression of Vcam1 (CD106), a vascular adhesion protein that binds VLA-1 (alpha4beta1 integrin) on monocytes and lymphocytes, and it was found that cluster 1 clones from COPD patients showed no induction, whereas IL-13 challenge yielded a 30-fold induction of Vcam1 (Figure S5B). In this same assay, media conditioned by cluster 2 (GCM) or cluster 3 (SCM) clones, respectively, yielded 4- and 10-fold inductions of VCAM1, and media from cluster 4 (iSCM) clones induced Vcam1 by 60-fold (Figure S5B). These data provide functional support for the notion that individual clone variants can promote, at least *in vitro*, an early step in inflammatory responses.

A more detailed expression heatmap of the variant clones revealed that cluster 4 clones in particular displayed a constitutive expression of a broad array of chemokines, interleukins, and interferon genes compared to clones from cluster 1, 2, and 3 (Figures 5B and S5C). Among the large array of cluster 4-specific chemokines were key determinants of neutrophil responses including CXCL1, CXCL5, and CXCL8 (Barnes, 2016; Brazil and Parkos, 2016; Ponce-Gallegos et al., 2017; Traves et al., 2002), the lymphocyte and dendritic cell chemoattractant CCL20 (Demedts et al., 2007), and others such as CXCL10 and 11 implicated in Th1 responses (Tokunaga et al., 2018). In addition, cluster 4 clones expressed a broad array of interleukin genes, including IL1α, IL1β, IL6, IL17C, and IL33, known to interact with multiple cellular mediators of the innate and adaptive immune response (Barnes, 2016; Byers et al., 2013; Holtzman et al., 2014). Lastly, this analysis highlighted cluster 4 clones as a robust source of Type I and Type II interferon pathway genes typically induced by viral infection (Schneider et al., 2014). In fact, cluster 4 clones showed a constitutively high expression of genes implicated in the entire interferon-γ pathway, including those involved in recognition of pathogen-associated molecular patterns (PAMPs), such as TLR2, TLR3, and MYD88; transcription factors driving the interferon-response genes (IRF1, IRF6, IRF7, and IRF9); as well as genes in the JAK-STAT pathway that cooperate in driving the interferon response such as STAT1, STAT2, and

Figure 3. p63+ Cells in COPD Metaplasia and Clone Libraries

(A) Top: p63 immunohistochemistry of distal lung of GOLD Stage 4 COPD showing contiguous regions of SCM and GCM subtended by p63+ basal cells (brown). Scale bar, 200 μm. Bottom: immunofluorescence micrographs of expanded regions of SCM and GCM stained with antibodies to p63 (green), IVL (red) and MUC5AC (red). Scale bar, 100 μm.

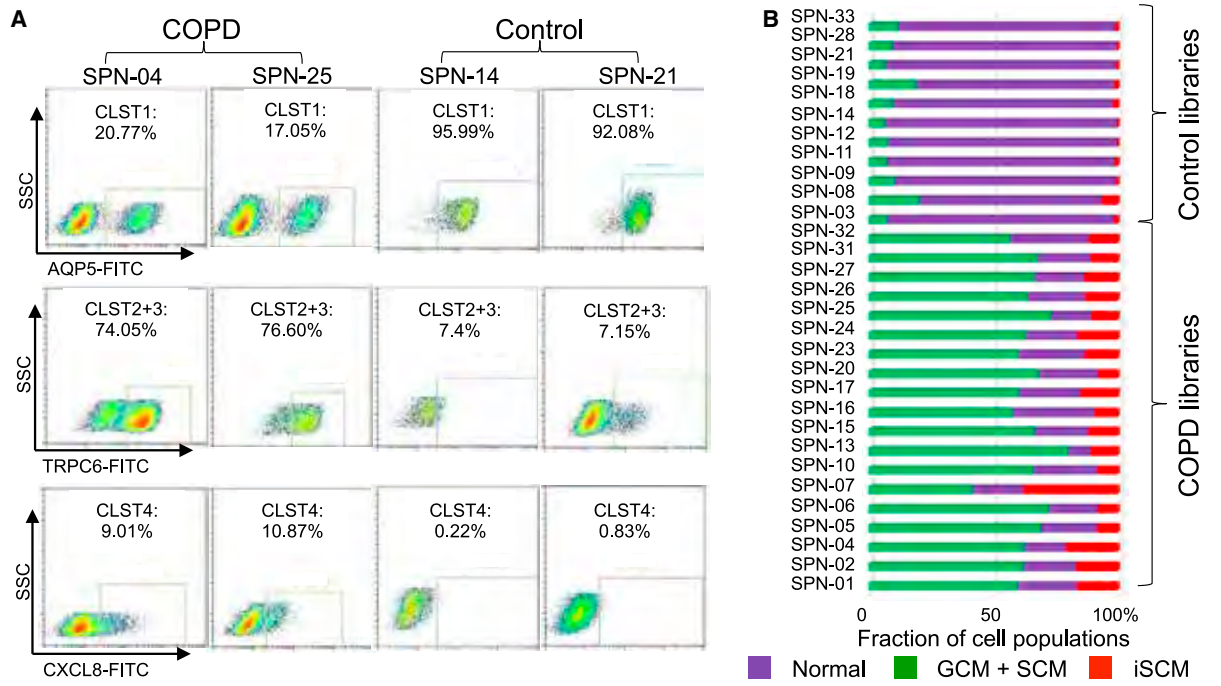
(B) Box-whisker plots for the linear occupancy of metaplastic lesions (GCM of $p = 4.1e-06$, SCM of $p = 1.2e-07$, and iSCM of $p = 4.9e-07$, Student's t test) across distal airways ten Stage 4 COPD lungs compared with five normal lungs without disease. Box-whisker plot indicates maximum, third quartile, median, first quartile, and minimum.

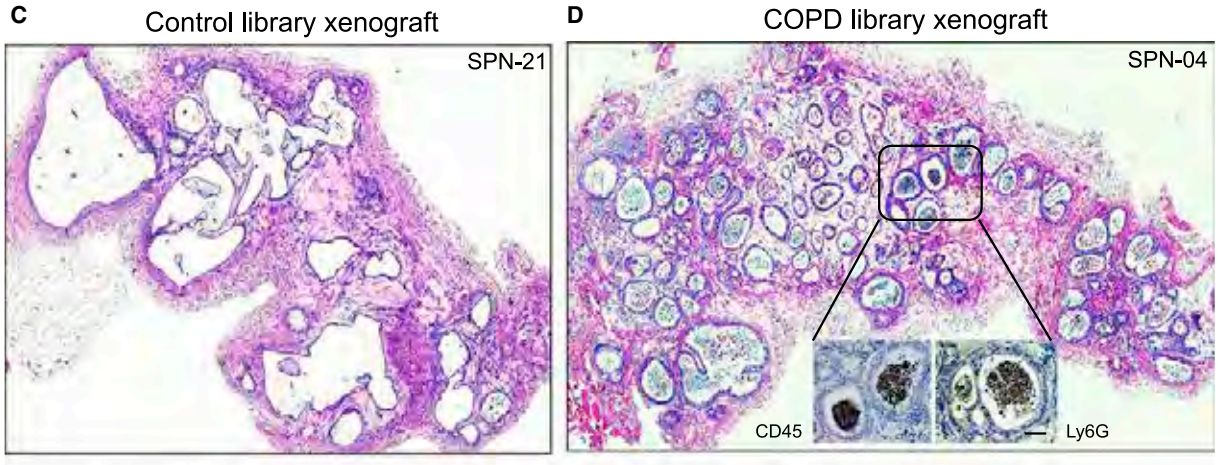
(C) Top: p63 immunohistochemistry micrographs of regions of COPD distal airways showing, from left, examples of terminal bronchiole, GCM, and SCM. Scale bar, 200 μm. Bottom: immunofluorescence micrographs of expanded regions of terminal bronchiole (p63+, Aqp5+), GCM (p63+, TRPC6+), and iSCM (p63+, CXCL8+). Scale bar, 100 μm.

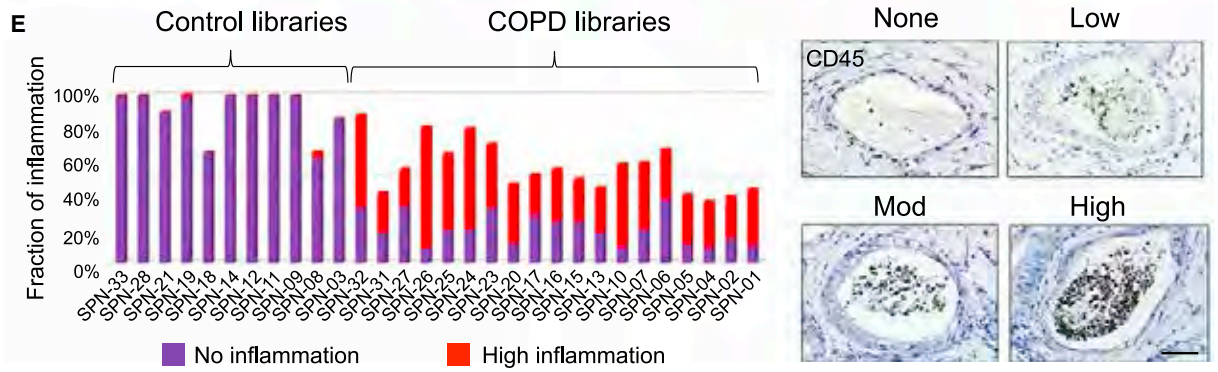
(D) Box-whisker plots of distribution of CXCL8+ ($p = 2.5e-06$, Student's t test) and TRPC6+ basal cells ($p = 1.2e-08$, Student's t test) in 10 cases of Stage 4 COPD distal lung compared with five normal lungs. Box-whisker plot indicates maximum, third quartile, median, first quartile, and minimum.

(E) Single and aggregate t-distributed stochastic neighbor embedding (tSNE) profiles of single cell RNA-seq data of three COPD and three control clone libraries. Pie charts indicate the fractional contributions of clones of clusters 1–4 to patient-specific clone libraries (NM, blue; GCM, green; SCM, orange; iSCM, red). See also Figures S2 and S3; Tables S3, S6, and S7.

Please cite this article in press as: Rao et al., Regenerative Metaplastic Clones in COPD Lung Drive Inflammation and Fibrosis, Cell (2020), https://doi.org/10.1016/j.cell.2020.03.047







(legend on next page)

JAK1 (Figures 5B and S5C). Together with the patterns of chemokine and interleukin gene expression, these data suggest the potential of cluster 4 clones to promote an inflammatory response involving diverse cells of the immune system.

To directly test the prediction that cluster 4 clones were primarily responsible for host neutrophil responses in whole COPD library transplants (*cf.* Figure 4D), we performed xenografts of the individual clone types in immunodeficient mice. Significantly, nodules formed by xenografts of cluster 4 clones showed robust leukocyte infiltration (Figure 5C). Consistent with their proinflammatory properties in xenografts, the epithelial cysts formed by cluster 4 clones were unique among the four clone types by showing high protein expression of multiple inflammatory mediators such as IL33, CXCL8, and IL1β (Figure 5D). Lastly, the leukocyte infiltration response to cluster 4 clones proved stable for eight months of continuous propagation *in vitro* (Figures 5E and 5F), suggesting that their proinflammatory activity is epigenetically maintained. Together, these data support the conclusion that cluster 4 clones play a major and likely autonomous role in promoting the observed host leukocyte responses observed in the COPD clone library transplants.

Clonogenic Variants Drive Fibrosis

Fibrosis of small airways and respiratory vasculature is an established feature of COPD (Araya and Nishimura, 2010; Aschner and Downey, 2016; Barnes, 2016; Hogg and Timens, 2009) and has been associated with TGFβ-induced activation of myofibroblasts (Black et al., 2019; Murphy-Ullrich and Suto, 2018). In this regard, we observed that many of the epithelial cysts in xenographs of clone libraries from all 19 COPD patients were surrounded by dense layers of fibroblast-like cells (Figure 4D). Antibodies to alpha smooth muscle actin (α-SMA), a key marker of activated myofibroblasts, labeled these submucosal assemblies along the majority (77.1 ± 7.2%) of the perimeter of the epithelial cysts in COPD xenografts, whereas only relatively few of these cysts in control xenografts showed these myofibroblast arrays (12.9 ± 8.1%; p = 7.044e-15, Student's t test; Figures 6A–6C, S6A, and S6B). Similar accumulations of submucosal myofibroblasts were observed in xenographs of single cluster 3 or cluster 4 clones but not in xenografts of clones of clusters 1 or 2 (Figure 6D). These data link the two SCMs produced by clusters 3 and 4 clones, but not GCM or normal airway epithelia, to the accumulation of myofibroblasts. Consistently, gene expression profiling of xenografts derived from clones of the respective clusters revealed differential expression of multiple, pro-fibrotic genes in xenografts of clones of cluster 3 and 4 that were not evident in xenografts of cluster 1 (Figure 6E). Among this large set of constitutively expressed genes implicated in the regulation of fibrosis were TGFβ3, GDF15, and TGFβR2; downstream genes including collagen isotypes (e.g., COL1A1); matrix metallopeptidases (MMP7, MMP13); and BACH1 (Dhakshinamoorthy et al., 2005), a transcriptional repressor of the Nrf2-activated antioxidant pathway known to suppress fibrosis in multiple tissues (Figure 6F). Finally, like the proinflammatory effect of cluster 4, the pro-fibrotic effects of clones of clusters 3 and 4 were stable to long-term propagation *in vitro* (Figure S6C).

Pre-existence of Variant Clone Types in Normal and Fetal Lungs

If the variant clones that dominate COPD lung indeed contribute to the disease process, their origin becomes a central question. These variant clones, all of which express p63, conceivably arise from an epigenetic "reprogramming" of normal, p63+ distal airway clones. Alternatively, these variant cells might already exist as distinct lineages in the normal distal airway epithelia, albeit at low ratios to the distal airway progenitor. In support of the pre-existence model, both scRNA-seq and FACS profiles of control lungs indicated an aggregate representation of variant clones of approximately 10% (Figures 3E and 4B), and direct cloning from control libraries showed that these variants possessed corresponding metaplastic fate commitment and pathological activity in xenografts (Figure S7A). Consistently, expression data of cluster 1–4 clones from control case SPN-14 showed significant overlap with those of COPD cases (Figures S3A and S7B; Table S8). However, we could not rule out the possibility that at least some of the control cases had "sub-clinical" disease reflected by these variant clones. To more definitively address this question, we examined the clonal architecture of libraries generated from 13- and 17-week fetal lungs (Figures 7A and S7C). Remarkably, scRNA-seq profiles of the clone libraries of these pseudoglandular fetal lungs (Schittny, 2017) revealed minor populations of clones similar to those of cluster 2, 3, and 4 variants (in aggregate, 17%–34%) among a majority of normal cluster 1 clones (Figure 7B, S7D, and S7E). The similarity of these four fetal clone types with those of clusters 1–4 from COPD cases was confirmed by their respective differentiation fate *in vitro* and upon xenografting, at the level of gene expression, and finally by their corresponding potential to drive mucus hypersecretion (GCM), fibrosis (SCM and iSCM), and neutrophilic inflammation (iSCM) (Figures 7C and 7D). The pre-existence of these variant clone types in both normal adult lung and in developing fetal lung favors some unknown, normal function of these variants in the lung as well as the notion that the evolution of COPD involves a pathological and irreversible expansion of these variant populations that, in turn, drives the disease process.

Figure 4. Library Composition and Proinflammatory Response in Xenografts

(A) FACS profiles of COPD and control clone libraries using markers established from library scRNA-seq and clonal RNA-seq including anti-AQP5 (cluster 1), anti-TRPC6 (clusters 2 and 3), and anti-CXCL8 (cluster 4).

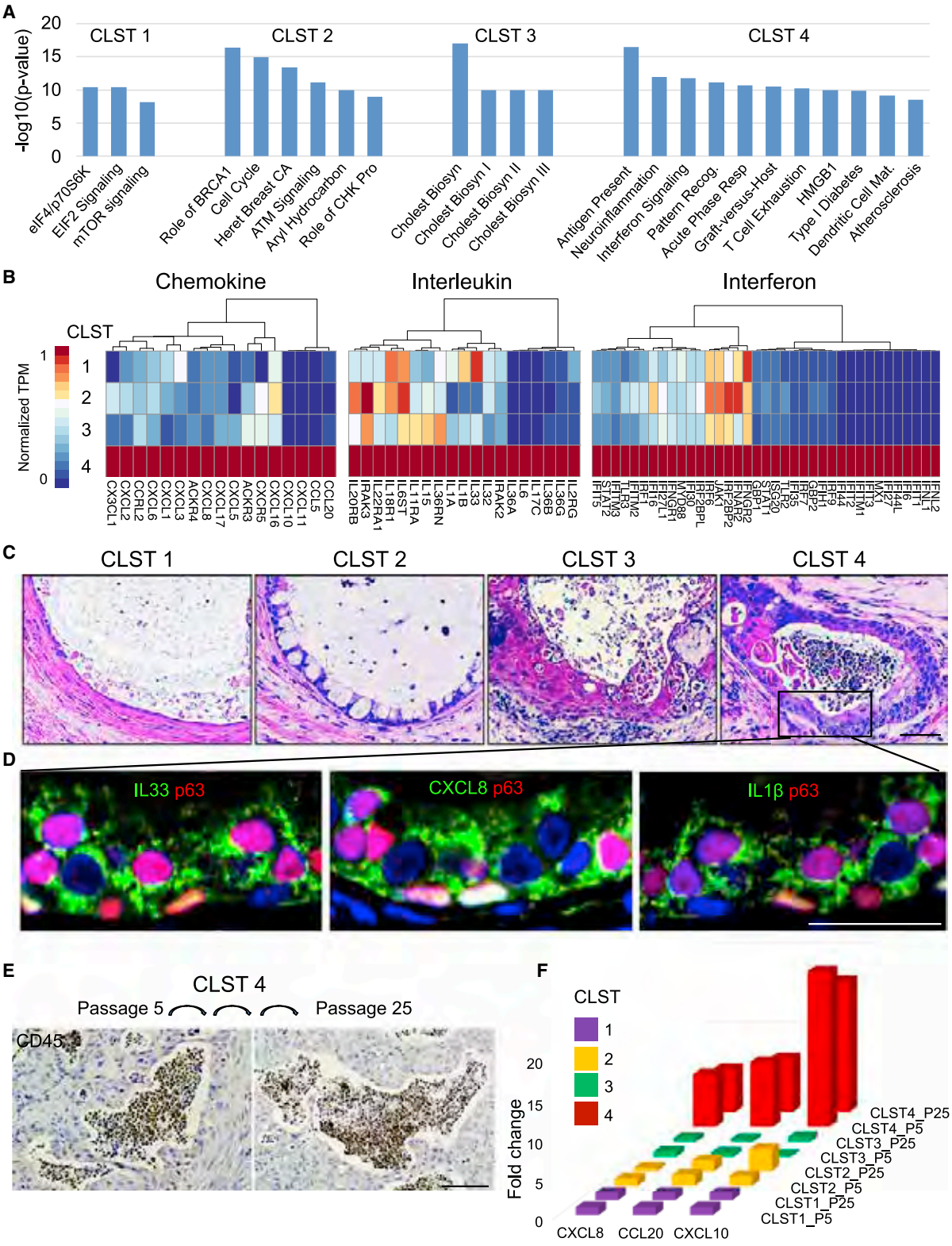
(B) Histogram compiling FACS quantification data on the relative clone composition of each patient library.

(C) Histological sections of four-week xenograft of clone libraries from control (SPN-21) showing epithelial cysts devoid of luminal cells.

(D) Histological sections of four-week xenograft of clone libraries from COPD case (SPN-04) showing epithelial cysts marked by abundant infiltration of CD45+/Ly6G+ leukocytes (insets).

(E) Histogram depicting the quantification of leukocyte infiltration in xenografts of clone libraries from 11 control and 19 COPD patients based on degree of CD45+ cells in cysts (right). Scale bar, 100 μm. See also Figure S4.

Please cite this article in press as: Rao et al., Regenerative Metaplastic Clones in COPD Lung Drive Inflammation and Fibrosis, Cell (2020), https://doi.org/10.1016/j.cell.2020.03.047



(legend on next page)

DISCUSSION

The abnormal clonogenic cell types in COPD lungs offer new insights into the natural history of COPD. The fates and biological properties of the three major clone types (GCM, SCM, and iSCM) in the COPD lung appear to be autonomously maintained and, in aggregate, they dominate the epithelia of moderate and end-stage COPD. There are two implications of this work. One is that these clonogenic variants are stem cells respectively committed to metaplastic lesions that, in turn, promote the fibrotic and inflammatory processes observed in COPD. The second is that these variant cells or the factors they secrete may represent important therapeutic targets in this disease.

The clonal analysis described here was instrumental in defining the heterogeneity of clonogenic epithelial cells in COPD. Unlike the normal cluster 1 clones committed to distal bronchiolar fates, the three variant types exhibited distinct pathologic phenotypes, with cluster 2 clones producing a GCM marked by the excess mucin secretion implicated in airway occlusion (Fahy and Dickey, 2010; Kesimer et al., 2017; Wedzicha, 2017), while SCM (cluster 3) clones induced an activation of airway endothelial cells *in vitro* and, in immunodeficient mice, a host myofibroblast response linked to fibrosis. cluster 4 clones not only activated endothelial cells *in vitro* but triggered both submucosal myofibroblast recruitment and leukocyte infiltration upon xenografting to immunodeficient mice. Given that the unparsed clone libraries from all 19 COPD patients induced leukocyte infiltration whereas only 1 of the 11 controls did so, as well as the major role of inflammation in this disease (Barnes, 2016; Brazil and Parkos, 2016; Butler et al., 2018), we predict that cluster 4 clones will figure prominently in the evolution of COPD.

It should be emphasized that the inflammatory genes expressed in proliferating clones isolated from COPD lung are constitutively activated for months even in a sterile, *in vitro* environment (Figure 5). The inflammatory pathways manifest in these cells are linked to the activation of a broad array of the innate and adaptive immune cell populations associated with COPD, including neutrophils, monocyte-derived macrophages and dendritic cells, as well as a host of T-helper subsets, natural killer cells, and other lineages such as innate lymphoid cells. Many of these immune cell types impact the development of fibrosis (Kasembeli et al., 2018; Lee and Kalluri, 2010). Notably, despite the broad range of the inflammatory pathways expressed in cluster 4 clones, only neutrophil responses were apparent in xenografts of these cells. At least some of this restricted host response can be attributed to strain of immunodeficient mice (NOD/scid/IL2rγ^{null}) used in these studies, which lacks mature B and T cells, natural killer cells, and shows defects in monocyte-derived macrophages and dendritic cells (Ito et al., 2012; Shultz et al., 2005; Shultz et al., 1995). Therefore, we were unable to assess whether other hematopoietic lineages associated with COPD (Barnes, 2016; Suzuki et al., 2017) might be impacted as well by the variant clones. Xenografts of these clones in immunodeficient strains having a greater complement of hematopoietic lineages may provide a more complete assessment of interactions between these clones and the immune system, as would syngeneic studies of homologous variant clones in genetically tractable model organisms.

This study raises important questions on the origin of the variant clones detected in COPD, how they become hegemonic, and what they mean to the etiology and progression of the disease. Taking just the cluster 4 clone (iSCM) that promotes host neutrophilic and fibrotic responses as an example, quantitative FACS profiling showed that it represents 13 ± 8% of all clonogenic cells across 19 COPD lungs but only 1.4 ± 1.6% of those in control lungs (Figure 7E). These numbers raise the possibility that the COPD phenotype becomes apparent at some percentage threshold of these clones. We tested this hypothesis in a tangential manner by asking what ratios of cluster 4 to cluster 1 clones in co-xenografts would elicit a host neutrophil response (Figure 7F). The resulting xenografts induced a minimal inflammatory response when cluster 4 clones comprised less than 5% of the total clones, whereas ratios between 10% and 20% of cluster 4 clones triggered a robust neutrophil response (Figure 7G). These findings support the notion that a threshold phenomenon, tied to the relative ratios of these variant cells, could be relevant to both the onset of clinical symptoms and the vectored progression of COPD. We anticipate that additional modeling of these variant clones singly or in combination will contribute to understanding their roles in COPD.

Given that similar variant stem cells preexist in control adult lungs as well as in lungs at multiple stages of fetal development, it is likely that these variants play some role in the normal lung, perhaps as sentinels for pathogen incursions. Understanding the responses of these variants in normal lung may provide insights into their intrinsic functions and how these cells might be suborned to disease. In this regard, key questions remain for how these minor variants become major variants in COPD. How do early-life pulmonary events or chronic smoking set in motion their numerical expansion, do genetic variations impact these expansion dynamics, does the disease process itself further alter these variants during the expansion process, and can this expansion be therapeutically preempted or reversed?

The overall findings here set the stage for more detailed studies of correlations between the abundance of such clones

Figure 5. Cluster 4 COPD Clones Are Constitutively Hyperinflammatory

(A) Histogram depicting most significant ($p < 1.0e-8$) pathways determined by Ingenuity Pathway Analysis of RNA-seq differentially expressed genes (FDR < 0.05) of patient-matched clones representative of clusters 1–4.

(B) Differential expression heatmaps of chemokine, interleukin, and interferon genes among RNA-seq DEGs (FDR < 0.05) of patient-matched clones representative of clusters 1–4 (SPN-13).

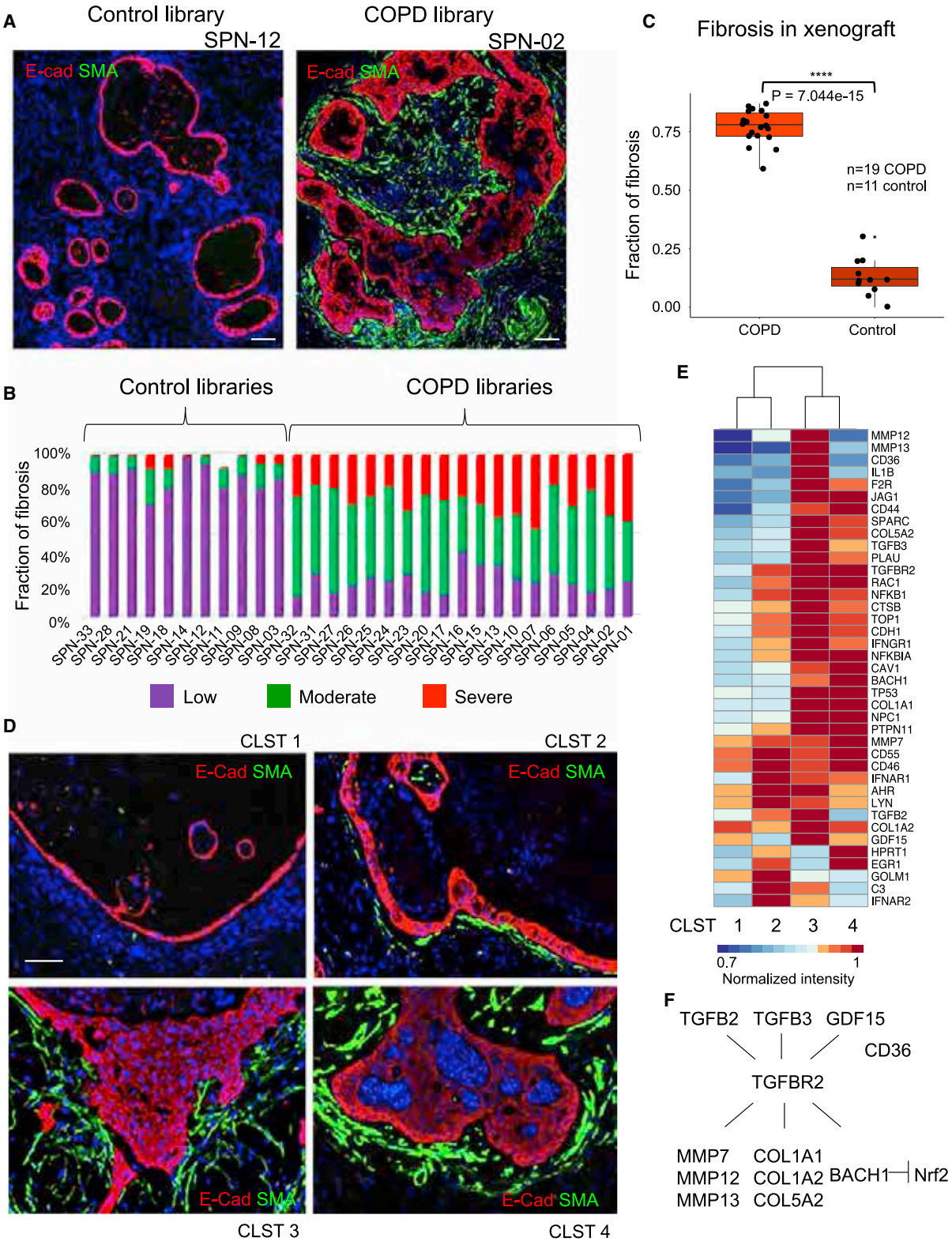
(C) Hematoxylin and eosin stain (H&E) on sections through four-week xenografts of patient-matched clones of clusters 1–4 showing that only cluster 4 clones are accompanied by abundant intraluminal leukocytes. Scale bar, 100 μm.

(D) Immunofluorescence micrographs of cluster 4 xenografts revealing high expression in epithelia of inflammatory mediators including IL33, CXCL8, and IL1B. Scale bar, 50 μm.

(E) CD45 immunohistochemistry of xenografts derived from cluster 4 clone grown *in vitro* to P5 and to P25. Scale bar, 200 μm.

(F) Histogram of CXCL8, CCL20, and CXCL10 gene expression in clonal representatives of clusters 1–4 at *in vitro* P5 and P25. See also Figure S5.

Please cite this article in press as: Rao et al., Regenerative Metaplastic Clones in COPD Lung Drive Inflammation and Fibrosis, Cell (2020), https://doi.org/10.1016/j.cell.2020.03.047



(legend on next page)

and COPD stage as well as their correlation with the known regional, intrapulmonary variations in COPD pathology (Nambu et al., 2016). We should note here that multiple studies have highlighted the possibility that alterations in epithelial cells in IPF, chronic rhinosinusitis, and COPD may contribute to the pathology of these conditions (Byers et al., 2013; Habiel et al., 2018; Ordovas-Montanes et al., 2018; Vieira Braga et al., 2019; Xu et al., 2016). While those studies did not examine clonogenic cells per se, their findings support the speculation that many if not all chronic lung conditions involve pathogenic clone variants of the sort described here.

If indeed these clones contribute to COPD, multiple opportunities become available to limit their impact on disease progression. These include neutralizing one or more of the pathogenically relevant chemokines or cytokines secreted by individual variants, targeting particular variants with cell surface-directed antibodies, or through the discovery of small molecules that selectively affect one or more of these clone types. This latter strategy could be predicated on the observation that COPD patients retain normal clones that would potentially compensate for the loss of their pathogenic counterparts.

STAR★METHODS

Detailed methods are provided in the online version of this paper and include the following:

- KEY RESOURCES TABLE
- LEAD CONTACT AND MATERIALS AVAILABILITY
- EXPERIMENTAL MODEL AND SUBJECT DETAILS
  - Human Subjects
  - Primary Cell Culture
  - Animals
  - Cell Lines
- METHOD DETAILS
  - *In vitro* culture of clonogenic cells from 19 COPD and 11 control lungs
  - Histology validation set of five control and 10 Stage-4 COPD lungs
  - Histology and immunostaining
  - *In vitro* differentiation
  - Xenografts in immunodeficient mice
  - RNA sample preparation
  - Flow cytometry analysis
  - Transcriptomic sequencing data analysis
  - Sequence alignment of single cell RNA sequencing
  - Single cell RNA sequencing
  - Expression microarray and bioinformatics
  - Whole genome exome sequencing data analysis
- QUANTIFICATION AND STATISTICAL ANALYSIS
- DATA AND CODE AVAILABILITY

SUPPLEMENTAL INFORMATION

Supplemental Information can be found online at https://doi.org/10.1016/j.cell.2020.03.047.

ACKNOWLEDGMENTS

This work was supported by grants from the Cancer Prevention Research Institute of Texas (CPRIT; RR150104 to W.X. and RR1550088 to F.D.M.), the National Institutes of Health (1R01DK115445-01A1 to W.X., 1R01CA241600-01 and U24CA228550 to F.D.M., R01 DK047967 to J.F.E., 5R01 HL138510 to H.K.-Q., P01 HL108808 and R01 HL136961 to R.C.B., R01 HL129795 to B.F.D., and 1R01 HL136370-01A1 to K.R.P.), the U.S. Department of Defense (W81XWH-17-1-0123 to W.X.), the American Gastroenterological Association Research and Development Pilot Award in Technology (to WX), and the Cystic Fibrosis Foundation (BOUCHE15R0 to R.C.B. and DICKEY18G0 to B.F.D.). W.X. and F.D.M. are CPRIT Scholars in Cancer Research. We thank all the members in the Xian-McKeon laboratory for helpful discussions and support. We thank H. Green for advice and support. Dedicated to Hazel and Richard T. and the valiant patients who have made this study possible.

AUTHOR CONTRIBUTIONS

Experimental design and conception were done by W.X., F.D.M., M.L.M., K.R.P., M.V., C.P.C., J.F.E., M.E.W., W.R., R.C.B., and B.F.D. Human airway cell cloning and analysis *in vitro* and in xenografts were performed by W.R., M.D., K.G., R.N., and S.N. W.R., A.-A.L., S.W., and J.X. coordinated molecular genetics analyses. S.W., R.M., W.R., and J.X. performed bioinformatics analyses. M.L.M., K.R.P., H.K.-Q., C.P.C., W.K.O., K.O., T.C.J.M., W.W., S.S.K.J., H.K., and O.I. acquired consented biopsy materials and lung tissues. W.X., M.L.M., and F.D.M. wrote the manuscript with input from all other authors. W.X. and F.D.M. supervised the research.

DECLARATION OF INTERESTS

W.X., F.D.M., W.R., S.W., J.X., M.D., and M.L have filed patents related to technologies used in the present work. M.L., F.D.M., and W.X. have financial interests in Lung Medical Systems, Houston, TX, USA and Tract Pharmaceuticals, Houston, TX, USA. Lung Medical Systems is a trade name of Tract Pharmaceuticals.

Received: July 26, 2019
Revised: November 26, 2019
Accepted: March 20, 2020
Published: April 15, 2020

Figure 6. Cluster 3 and 4 Clones Drive Host Myofibroblast Activation

(A) Immunofluorescence micrographs of xenografts derived from control case (SPN-12; left) and COPD case (SPN-02; right) clone libraries stained with antibodies to the myofibroblast marker α-SMA. Scale bar, 200 μm.

(B) Quantification of myofibroblast submucosal accumulation in xenografts based on general scale applied to cysts within 11 control and 19 COPD clone library transplants.

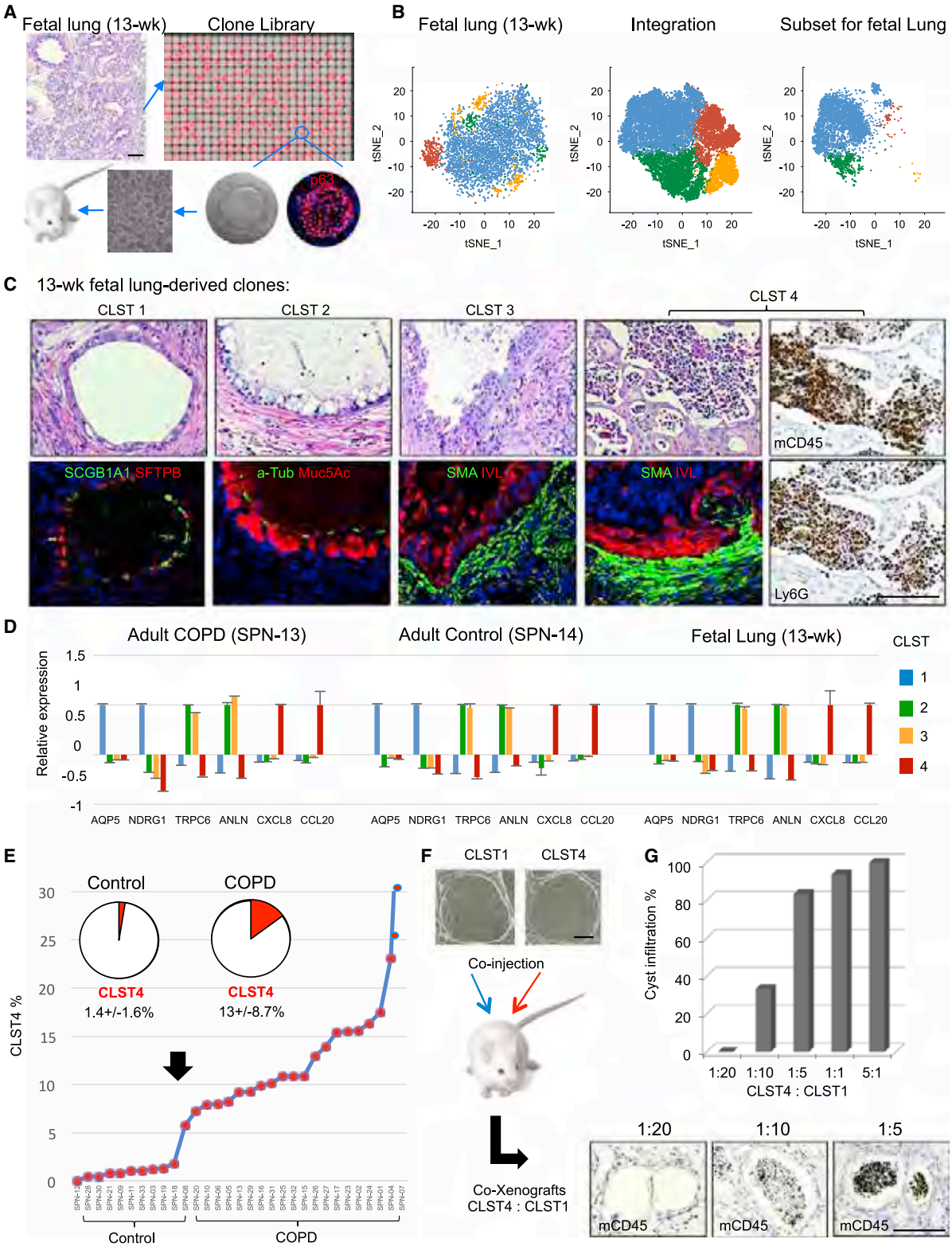
(C) Box-whisker plot representation of fibrosis accumulation about cysts in each of 19 COPD and 11 control library xenografts ($p = 7.0e-15$, Student's t test). Box-whisker plot indicates maximum, third quartile, median, first quartile, and minimum.

(D) Immunofluorescence micrographs of xenografts derived from patient-matched clones of clusters 1–4 using antibodies to E-cadherin (ECAD, red) and α-SMA, green. Scale bar, 100 μm.

(E) Differential expression heatmap of fibrosis-related genes (1.5-fold, $p < 0.05$) of xenografts derived from patient-matched clones representative of clusters 1–4.

(F) Schematic TGF-β pathway including genes differentially expressed in clones of clusters 3 and 4. See also Figure S6.

Please cite this article in press as: Rao et al., Regenerative Metaplastic Clones in COPD Lung Drive Inflammation and Fibrosis, Cell (2020), https://doi.org/10.1016/j.cell.2020.03.047



(legend on next page)

REFERENCES

Araya, J., and Nishimura, S.L. (2010). Fibrogenic reactions in lung disease. Annu. Rev. Pathol. *5*, 77–98.

Araya, J., Cambier, S., Markovics, J.A., Wolters, P., Jablons, D., Hill, A., Finkbeiner, W., Jones, K., Broaddus, V.C., Sheppard, D., et al. (2007). Squamous metaplasia amplifies pathologic epithelial-mesenchymal interactions in COPD patients. J. Clin. Invest. *117*, 3551–3562.

Aschner, Y., and Downey, G.P. (2016). Transforming Growth Factor-β: Master Regulator of the Respiratory System in Health and Disease. Am. J. Respir. Cell Mol. Biol. *54*, 647–655.

Barnes, P.J. (2016). Inflammatory mechanisms in patients with chronic obstructive pulmonary disease. J. Allergy Clin. Immunol. *138*, 16–27.

Barnes, P.J., Burney, P.G., Silverman, E.K., Celli, B.R., Vestbo, J., Wedzicha, J.A., and Wouters, E.F. (2015). Chronic obstructive pulmonary disease. Nat. Rev. Dis. Primers *1*, 15076.

Black, L.M., Lever, J.M., and Agarwal, A. (2019). Renal Inflammation and Fibrosis: A Double-edged Sword. J. Histochem. Cytochem. *67*, 663–681.

Bolger, A.M., Lohse, M., and Usadel, B. (2014). Trimmomatic: a flexible trimmer for Illumina sequence data. Bioinformatics *30*, 2114–2120.

Brazil, J.C., and Parkos, C.A. (2016). Pathobiology of neutrophil-epithelial interactions. Immunol. Rev. *273*, 94–111.

Busch, R., Hobbs, B.D., Zhou, J., Castaldi, P.J., McGeachie, M.J., Hardin, M.E., Hawrylkiewicz, I., Sliwinski, P., Yim, J.J., Kim, W.J., et al.; National Emphysema Treatment Trial Genetics; Evaluation of COPD Longitudinally to Identify Predictive Surrogate End-Points; International COPD Genetics Network; COPDGene Investigators (2017). Genetic Association and Risk Scores in a Chronic Obstructive Pulmonary Disease Meta-analysis of 16,707 Subjects. Am. J. Respir. Cell Mol. Biol. *57*, 35–46.

Butler, A., Walton, G.M., and Sapey, E. (2018). Neutrophilic Inflammation in the Pathogenesis of Chronic Obstructive Pulmonary Disease. COPD *15*, 392–404.

Byers, D.E., Alexander-Brett, J., Patel, A.C., Agapov, E., Dang-Vu, G., Jin, X., Wu, K., You, Y., Alevy, Y., Girard, J.P., et al. (2013). Long-term IL-33-producing epithelial progenitor cells in chronic obstructive lung disease. J. Clin. Invest. *123*, 3967–3982.

Chakravarty, D., Gao, J., Phillips, S.M., Kundra, R., Zhang, H., Wang, J., Rudolph, J.E., Yaeger, R., Soumerai, T., Nissan, M.H., et al. (2017). OncoKB: A Precision Oncology Knowledge Base. JCO Precis. Oncol. https://doi.org/10.1200/PO.17.00011.

Chen, E.Y., Tan, C.M., Kou, Y., Duan, Q., Wang, Z., Meirelles, G.V., Clark, N.R., and Ma'ayan, A. (2013). Enrichr: interactive and collaborative HTML5 gene list enrichment analysis tool. BMC Bioinformatics *14*, 128.

Chen, X., Schulz-Trieglaff, O., Shaw, R., Barnes, B., Schlesinger, F., Källberg, M., Cox, A.J., Kruglyak, S., and Saunders, C.T. (2016). Manta: rapid detection of structural variants and indels for germline and cancer sequencing applications. Bioinformatics *32*, 1220–1222.

Chilosi, M., Poletti, V., Murer, B., Lestani, M., Cancellieri, A., Montagna, L., Piccoli, P., Cangi, G., Semenzato, G., and Doglioni, C. (2002). Abnormal re-epithelialization and lung remodeling in idiopathic pulmonary fibrosis: the role of deltaN-p63. Lab. Invest. *82*, 1335–1345.

Conway, T., Wazny, J., Bromage, A., Tymms, M., Sooraj, D., Williams, E.D., and Beresford-Smith, B. (2012). Xenome–a tool for classifying reads from xenograft samples. Bioinformatics *28*, i172–i178.

Decramer, M., Janssens, W., and Miravitlles, M. (2012). Chronic obstructive pulmonary disease. Lancet *379*, 1341–1351.

Demedts, I.K., Bracke, K.R., Van Pottelberge, G., Testelmans, D., Verleden, G.M., Vermassen, F.E., Joos, G.F., and Brusselle, G.G. (2007). Accumulation of dendritic cells and increased CCL20 levels in the airways of patients with chronic obstructive pulmonary disease. Am. J. Respir. Crit. Care Med. *175*, 998–1005.

DePristo, M.A., Banks, E., Poplin, R., Garimella, K.V., Maguire, J.R., Hartl, C., Philippakis, A.A., del Angel, G., Rivas, M.A., Hanna, M., et al. (2011). A framework for variation discovery and genotyping using next-generation DNA sequencing data. Nat. Genet. *43*, 491–498.

Dhakshinamoorthy, S., Jain, A.K., Bloom, D.A., and Jaiswal, A.K. (2005). Bach1 competes with Nrf2 leading to negative regulation of the antioxidant response element (ARE)-mediated NAD(P)H:quinone oxidoreductase 1 gene expression and induction in response to antioxidants. J. Biol. Chem. *280*, 16891–16900.

Fahy, J.V., and Dickey, B.F. (2010). Airway mucus function and dysfunction. N. Engl. J. Med. *363*, 2233–2247.

Ferguson, A., and Chen, K. (2020). Analysis of Transcriptional Profiling of Immune Cells at the Single-Cell Level. Methods Mol. Biol. *2111*, 47–57.

Filippi, M.D. (2016). Mechanism of Diapedesis: Importance of the Transcellular Route. Adv. Immunol. *129*, 25–53.

Fletcher, C., and Peto, R. (1977). The natural history of chronic airflow obstruction. BMJ *1*, 1645–1648.

Gamble, E., Grootendorst, D.C., Hattotuwa, K., O'Shaughnessy, T., Ram, F.S., Qiu, Y., Zhu, J., Vignola, A.M., Kroegel, C., Morell, F., et al. (2007). Airway mucosal inflammation in COPD is similar in smokers and ex-smokers: a pooled analysis. Eur. Respir. J. *30*, 467–471.

Habiel, D.M., Espindola, M.S., Jones, I.C., Coelho, A.L., Stripp, B., and Hogaboam, C.M. (2018). CCR10+ epithelial cells from idiopathic pulmonary fibrosis lungs drive remodeling. JCI Insight *3*, 122211.

Hogg, J.C., and Timens, W. (2009). The pathology of chronic obstructive pulmonary disease. Annu. Rev. Pathol. *4*, 435–459.

Hogg, J.C., Chu, F., Utokaparch, S., Woods, R., Elliott, W.M., Buzatu, L., Cherniack, R.M., Rogers, R.M., Sciurba, F.C., Coxson, H.O., and Paré, P.D. (2004). The nature of small-airway obstruction in chronic obstructive pulmonary disease. N. Engl. J. Med. *350*, 2645–2653.

Holtzman, M.J., Byers, D.E., Brett, J.A., Patel, A.C., Agapov, E., Jin, X., and Wu, K. (2014). Linking acute infection to chronic lung disease. The role of IL-33-expressing epithelial progenitor cells. Ann. Am. Thorac. Soc. *11* (*Suppl 5*), S287–S291.

Ito, R., Katano, I., Ida-Tanaka, M., Kamisako, T., Kawai, K., Suemizu, H., Aiso, S., and Ito, M. (2012). Efficient xenoengraftment in severe immunodeficient NOD/Shi-scid IL2rγnull mice is attributed to a lack of CD11c+B220+CD122+ cells. J. Immunol. *189*, 4313–4320.

Karczewski, K.J., Francioli, L.C., Tiao, G., Cummings, B.B., Alföldi, J., Wang, Q., Collins, R.L., Laricchia, K.M., Ganna, A., Birnbaum, D.P., et al. (2019).

Figure 7. Identification of Variant Clone Types in Normal and Fetal Lung

(A) Schematic of clone library generation from pseudoglandular fetal lung and analysis by scRNA-seq and xenografting.

(B) scRNA-seq of clone library from 13-week fetal lung yielding tSNE profile (left), integration with three adult control and three COPD libraries (middle), and the fetal subset profile based on the integrated profile (right).

(C) Histology and indicated marker analysis of xenografts of 13-week fetal clones corresponding to clusters 1–4. Cluster 4 xenografts are further assessed by immunohistochemistry with antibodies to CD34 and Ly6G.

(D) Ratio of qPCR-determined marker expression across cluster 1–4 clones from COPD, control, and 13-week fetal lung. Data represented as mean ± SEM. Cluster 1 markers, AQP5 and NDRG1; clusters 2 and 3, TRPC6 and ANLN; cluster 4, CXCL8 and CCL20.

(E) Percentage composition of cluster 4 clones across 11 control and 19 COPD clone libraries.

(F) Schematic for generating xenografts from defined ratios of cluster 4 and cluster 1 cells.

(G) Histogram of quantification of host inflammatory response to co-xenografts of cluster 4 and cluster 1 clones based on CD45 and Ly6G monitoring of cystic infiltration by leukocytes. See also Figure S7 and Table S8.

Variation across 141,456 human exomes and genomes reveals the spectrum of loss-of-function intolerance across human protein-coding genes. bioRxiv. https://doi.org/10.1101/531210.

Kasembeli, M.M., Bharadwaj, U., Robinson, P., and Tweardy, D.J. (2018). Contribution of STAT3 to Inflammatory and Fibrotic Diseases and Prospects for its Targeting for Treatment. Int. J. Mol. Sci. *19*, E2299.

Kesimer, M., Ford, A.A., Ceppe, A., Radicioni, G., Cao, R., Davis, C.W., Doerschuk, C.M., Alexis, N.E., Anderson, W.H., Henderson, A.G., et al. (2017). Airway Mucin Concentration as a Marker of Chronic Bronchitis. N. Engl. J. Med. *377*, 911–922.

Kim, S., Scheffler, K., Halpern, A.L., Bekritsky, M.A., Noh, E., Källberg, M., Chen, X., Kim, Y., Beyter, D., Krusche, P., and Saunders, C.T. (2018). Strelka2: fast and accurate calling of germline and somatic variants. Nat. Methods *15*, 591–594.

Krämer, A., Green, J., Pollard, J., Jr., and Tugendreich, S. (2014). Causal analysis approaches in Ingenuity Pathway Analysis. Bioinformatics *30*, 523–530.

Kumar, P.A., Hu, Y., Yamamoto, Y., Hoe, N.B., Wei, T.S., Mu, D., Sun, Y., Joo, L.S., Dagher, R., Zielonka, E.M., et al. (2011). Distal airway stem cells yield alveoli in vitro and during lung regeneration following H1N1 influenza infection. Cell *147*, 525–538.

Lapperre, T.S., Sont, J.K., van Schadewijk, A., Gosman, M.M., Postma, D.S., Bajema, I.M., Timens, W., Mauad, T., Hiemstra, P.S., and Group, G.S.; GLUCOLD Study Group (2007). Smoking cessation and bronchial epithelial remodelling in COPD: a cross-sectional study. Respir. Res. *8*, 85.

Lee, S.B., and Kalluri, R. (2010). Mechanistic connection between inflammation and fibrosis. Kidney Int. Supplemental (119), S22–S26.

Lee-Six, H., Øbro, N.F., Shepherd, M.S., Grossmann, S., Dawson, K., Belmonte, M., Osborne, R.J., Huntly, B.J.P., Martincorena, I., Anderson, E., et al. (2018). Population dynamics of normal human blood inferred from somatic mutations. Nature *561*, 473–478.

Li, H., and Durbin, R. (2010). Fast and accurate long-read alignment with Burrows-Wheeler transform. Bioinformatics *26*, 589–595.

Li, G.M., Zhang, C.L., Rui, R.P., Sun, B., and Guo, W. (2018). Bioinformatics analysis of common differential genes of coronary artery disease and ischemic cardiomyopathy. Eur. Rev. Med. Pharmacol. Sci. *22*, 3553–3569.

Love, M.I., Huber, W., and Anders, S. (2014). Moderated estimation of fold change and dispersion for RNA-seq data with DESeq2. Genome Biol. *15*, 550.

Martin, M. (2011). Cutadapt removes adapter sequences from high-throughput sequencing reads. EMBnet J *17*, 10–12.

Martinez, F.D. (2016). Early-Life Origins of Chronic Obstructive Pulmonary Disease. N. Engl. J. Med. *375*, 871–878.

Martinez, F.J., Han, M.K., Allinson, J.P., Barr, R.G., Boucher, R.C., Calverley, P.M.A., Celli, B.R., Christenson, S.A., Crystal, R.G., Fagerås, M., et al. (2018). At the Root: Defining and Halting Progression of Early Chronic Obstructive Pulmonary Disease. Am. J. Respir. Crit. Care Med. *197*, 1540–1551.

McDonough, J.E., Yuan, R., Suzuki, M., Seyednejad, N., Elliott, W.M., Sanchez, P.G., Wright, A.C., Gefter, W.B., Litzky, L., Coxson, H.O., et al. (2011). Small-airway obstruction and emphysema in chronic obstructive pulmonary disease. N. Engl. J. Med. *365*, 1567–1575.

McGeachie, M.J., Yates, K.P., Zhou, X., Guo, F., Sternberg, A.L., Van Natta, M.L., Wise, R.A., Szefler, S.J., Sharma, S., Kho, A.T., et al. (2016). Patterns of Growth and Decline in Lung Function in Persistent Childhood Asthma. N. Engl. J. Med. *374*, 1842–1852.

McKenna, A., Hanna, M., Banks, E., Sivachenko, A., Cibulskis, K., Kernytsky, A., Garimella, K., Altshuler, D., Gabriel, S., Daly, M., and DePristo, M.A. (2010). The Genome Analysis Toolkit: a MapReduce framework for analyzing next-generation DNA sequencing data. Genome Res. *20*, 1297–1303.

Miller, M., Cho, J.Y., Pham, A., Friedman, P.J., Ramsdell, J., and Broide, D.H. (2011). Persistent airway inflammation and emphysema progression on CT scan in ex-smokers observed for 4 years. Chest *139*, 1380–1387.

Murphy-Ullrich, J.E., and Suto, M.J. (2018). Thrombospondin-1 regulation of latent TGF-β activation: A therapeutic target for fibrotic disease. Matrix Biol. *68-69*, 28–43.

Nambu, A., Zach, J., Schroeder, J., Jin, G., Kim, S.S., Kim, Y.I., Schnell, C., Bowler, R., and Lynch, D.A. (2016). Quantitative computed tomography measurements to evaluate airway disease in chronic obstructive pulmonary disease: Relationship to physiological measurements, clinical index and visual assessment of airway disease. Eur. J. Radiol. *85*, 2144–2151.

Nestorowa, S., Hamey, F.K., Pijuan Sala, B., Diamanti, E., Shepherd, M., Laurenti, E., Wilson, N.K., Kent, D.G., and Göttgens, B. (2016). A single-cell resolution map of mouse hematopoietic stem and progenitor cell differentiation. Blood *128*, e20–e31.

Okuda, K., Chen, G., Subramani, D.B., Wolf, M., Gilmore, R.C., Kato, T., Radicioni, G., Kesimer, M., Chua, M., Dang, H., et al. (2019). Localization of Secretory Mucins MUC5AC and MUC5B in Normal/Healthy Human Airways. Am. J. Respir. Crit. Care Med. *199*, 715–727.

Ordovas-Montanes, J., Dwyer, D.F., Nyquist, S.K., Buchheit, K.M., Vukovic, M., Deb, C., Wadsworth, M.H., 2nd, Hughes, T.K., Kazer, S.W., Yoshimoto, E., et al. (2018). Allergic inflammatory memory in human respiratory epithelial progenitor cells. Nature *560*, 649–654.

Patro, R., Duggal, G., Love, M.I., Irizarry, R.A., and Kingsford, C. (2017). Salmon provides fast and bias-aware quantification of transcript expression. Nat. Methods *14*, 417–419.

Plantier, L., Crestani, B., Wert, S.E., Dehoux, M., Zweytick, B., Guenther, A., and Whitsett, J.A. (2011). Ectopic respiratory epithelial cell differentiation in bronchiolised distal airspaces in idiopathic pulmonary fibrosis. Thorax *66*, 651–657.

Ponce-Gallegos, M.A., Ramírez-Venegas, A., and Falfán-Valencia, R. (2017). Th17 profile in COPD exacerbations. Int. J. Chron. Obstruct. Pulmon. Dis. *12*, 1857–1865.

Quaderi, S.A., and Hurst, J.R. (2018). The unmet global burden of COPD. Glob Health Epidemiol Genom *3*, e4.

Quint, J.K., and Wedzicha, J.A. (2007). The neutrophil in chronic obstructive pulmonary disease. J. Allergy Clin. Immunol. *119*, 1065–1071.

Raju, S.V., Kim, H., Byzek, S.A., Tang, L.P., Trombley, J.E., Jackson, P., Rasmussen, L., Wells, J.M., Libby, E.F., Dohm, E., et al. (2016). A ferret model of COPD-related chronic bronchitis. JCI Insight *1*, e87536.

Ray, S., Chiba, N., Yao, C., Guan, X., McConnell, A.M., Brockway, B., Que, L., McQualter, J.L., and Stripp, B.R. (2016). Rare SOX2^{+} Airway Progenitor Cells Generate KRT5^{+} Cells that Repopulate Damaged Alveolar Parenchyma following Influenza Virus Infection. Stem Cell Reports *7*, 817–825.

Risso, D., Ngai, J., Speed, T.P., and Dudoit, S. (2014). Normalization of RNA-seq data using factor analysis of control genes or samples. Nat. Biotechnol. *32*, 896–902.

Satija, R., Farrell, J.A., Gennert, D., Schier, A.F., and Regev, A. (2015). Spatial reconstruction of single-cell gene expression data. Nat. Biotechnol. *33*, 495–502.

Scanlon, P.D., Connett, J.E., Waller, L.A., Altose, M.D., Bailey, W.C., Buist, A.S., and Tashkin, D.P.; Lung Health Study Research Group (2000). Smoking cessation and lung function in mild-to-moderate chronic obstructive pulmonary disease. Am. J. Respir. Crit. Care Med. *161*, 381–390.

Schamberger, A.C., Staab-Weijnitz, C.A., Mise-Racek, N., and Eickelberg, O. (2015). Cigarette smoke alters primary human bronchial epithelial cell differentiation at the air-liquid interface. Sci. Rep. *5*, 8163.

Schittny, J.C. (2017). Development of the lung. Cell Tissue Res. *367*, 427–444.

Schneider, W.M., Chevillotte, M.D., and Rice, C.M. (2014). Interferon-stimulated genes: a complex web of host defenses. Annu. Rev. Immunol. *32*, 513–545.

Seibold, M.A., Smith, R.W., Urbanek, C., Groshong, S.D., Cosgrove, G.P., Brown, K.K., Schwarz, M.I., Schwartz, D.A., and Reynolds, S.D. (2013). The idiopathic pulmonary fibrosis honeycomb cyst contains a mucocilary pseudostratified epithelium. PLoS ONE *8*, e58658.

Shultz, L.D., Schweitzer, P.A., Christianson, S.W., Gott, B., Schweitzer, I.B., Tennent, B., McKenna, S., Mobraaten, L., Rajan, T.V., Greiner, D.L., et al. (1995). Multiple defects in innate and adaptive immunologic function in NOD/LtSz-scid mice. J. Immunol. *154*, 180–191.

Shultz, L.D., Lyons, B.L., Burzenski, L.M., Gott, B., Chen, X., Chaleff, S., Kotb, M., Gillies, S.D., King, M., Mangada, J., et al. (2005). Human lymphoid and myeloid cell development in NOD/LtSz-scid IL2R gamma null mice engrafted with mobilized human hemopoietic stem cells. J. Immunol. *174*, 6477–6489.

Singh, D., Agusti, A., Anzueto, A., Barnes, P.J., Bourbeau, J., Celli, B.R., Criner, G.J., Frith, P., Halpin, D.M.G., Han, M., et al. (2019). Global Strategy for the Diagnosis, Management, and Prevention of Chronic Obstructive Lung Disease: the GOLD science committee report 2019. Eur. Respir. J. *53*, 1900164.

Smirnova, N.F., Schamberger, A.C., Nayakanti, S., Hatz, R., Behr, J., and Eickelberg, O. (2016). Detection and quantification of epithelial progenitor cell populations in human healthy and IPF lungs. Respir. Res. *17*, 83.

Sudmant, P.H., Rausch, T., Gardner, E.J., Handsaker, R.E., Abyzov, A., Huddleston, J., Zhang, Y., Ye, K., Jun, G., Fritz, M.H., et al.; 1000 Genomes Project Consortium (2015). An integrated map of structural variation in 2,504 human genomes. Nature *526*, 75–81.

Suzuki, M., Sze, M.A., Campbell, J.D., Brothers, J.F., 2nd, Lenburg, M.E., McDonough, J.E., Elliott, W.M., Cooper, J.D., Spira, A., and Hogg, J.C. (2017). The cellular and molecular determinants of emphysematous destruction in COPD. Sci. Rep. *7*, 9562.

Tanaka, Y., Yamaguchi, M., Hirai, S., Sumi, T., Tada, M., Saito, A., Chiba, H., Kojima, T., Watanabe, A., Takahashi, H., and Sakuma, Y. (2018). Characterization of distal airway stem-like cells expressing N-terminally truncated p63 and thyroid transcription factor-1 in the human lung. Exp. Cell Res. *372*, 141–149.

Tokunaga, R., Zhang, W., Naseem, M., Puccini, A., Berger, M.D., Soni, S., McSkane, M., Baba, H., and Lenz, H.J. (2018). CXCL9, CXCL10, CXCL11/CXCR3 axis for immune activation - A target for novel cancer therapy. Cancer Treat. Rev. *63*, 40–47.

Traves, S.L., Culpitt, S.V., Russell, R.E., Barnes, P.J., and Donnelly, L.E. (2002). Increased levels of the chemokines GROalpha and MCP-1 in sputum samples from patients with COPD. Thorax *57*, 590–595.

Van der Auwera, G.A., Carneiro, M.O., Hartl, C., Poplin, R., Del Angel, G., Levy-Moonshine, A., Jordan, T., Shakir, K., Roazen, D., Thibault, J., et al. (2013). From FastQ data to high confidence variant calls: the Genome Analysis Toolkit best practices pipeline. Curr. Protoc. Bioinformatics *43*, 11.10.11–11.10.33.

Vaughan, A.E., Brumwell, A.N., Xi, Y., Gotts, J.E., Brownfield, D.G., Treutlein, B., Tan, K., Tan, V., Liu, F.C., Looney, M.R., et al. (2015). Lineage-negative progenitors mobilize to regenerate lung epithelium after major injury. Nature *517*, 621–625.

Vieira Braga, F.A., Kar, G., Berg, M., Carpaij, O.A., Polanski, K., Simon, L.M., Brouwer, S., Gomes, T., Hesse, L., Jiang, J., et al. (2019). A cellular census of human lungs identifies novel cell states in health and in asthma. Nat. Med. *25*, 1153–1163.

Wedzicha, J.A. (2017). Airway Mucins in Chronic Obstructive Pulmonary Disease. N. Engl. J. Med. *377*, 986–987.

Wen, Y., Reid, D.W., Zhang, D., Ward, C., Wood-Baker, R., and Walters, E.H. (2010). Assessment of airway inflammation using sputum, BAL, and endobronchial biopsies in current and ex-smokers with established COPD. Int. J. Chron. Obstruct. Pulmon. Dis. *5*, 327–334.

Wills-Karp, M., Luyimbazi, J., Xu, X., Schofield, B., Neben, T.Y., Karp, C.L., and Donaldson, D.D. (1998). Interleukin-13: central mediator of allergic asthma. Science *282*, 2258–2261.

Wodehouse, T., Demopoulos, M., Petty, R., Miraki-Moud, F., Belhaj, A., Husband, M., Fulton, L., Randive, N., Oksche, A., Mehta, V., et al. (2019). A randomized pilot study to investigate the effect of opioids on immunomarkers using gene expression profiling during surgery. Pain *160*, 2691–2698.

Xu, Y., Mizuno, T., Sridharan, A., Du, Y., Guo, M., Tang, J., Wikenheiser-Brokamp, K.A., Perl, A.T., Funari, V.A., Gokey, J.J., et al. (2016). Single-cell RNA sequencing identifies diverse roles of epithelial cells in idiopathic pulmonary fibrosis. JCI Insight *1*, e90558.

Yang, H., and Wang, K. (2015). Genomic variant annotation and prioritization with ANNOVAR and wANNOVAR. Nat. Protoc. *10*, 1556–1566.

Yang, Y., Riccio, P., Schotsaert, M., Mori, M., Lu, J., Lee, D.K., Garcia-Sastre, A., Xu, J., and Cardoso, W.V. (2018). Spatial-Temporal Lineage Restrictions of Embryonic p63(+) Progenitors Establish Distinct Stem Cell Pools in Adult Airways. Dev. Cell *44*, 752–761.e4.

Zhou-Suckow, Z., Duerr, J., Hagner, M., Agrawal, R., and Mall, M.A. (2017). Airway mucus, inflammation and remodeling: emerging links in the pathogenesis of chronic lung diseases. Cell Tissue Res. *367*, 537–550.

Zuo, W., Zhang, T., Wu, D.Z., Guan, S.P., Liew, A.A., Yamamoto, Y., Wang, X., Lim, S.J., Vincent, M., Lessard, M., et al. (2015). p63(+)Krt5(+) distal airway stem cells are essential for lung regeneration. Nature *517*, 616–620.

nature protocols

PROTOCOL

https://doi.org/10.1038/s41596-020-0298-4

Check for updates

Cloning of ground-state intestinal stem cells from endoscopic biopsy samples

Marcin Duleba[1,10], Yusuke Yamamoto[2,10], Rahul Neupane[1], Wei Rao[1], Jingzhong Xie[1], Yutao Qi[1], Audrey-Ann Liew[1], Suchan Niroula[1], Yanting Zhang[1], Rajasekaran Mahalingam[1], Shan Wang[1], Kristina Goller[1], Jaffer A. Ajani[3], Matthew Vincent[4], Khek Yu Ho[5], Jason K. Hou[6], Jeffrey S. Hyams[7], Francisco A. Sylvester[8], Christopher P. Crum[9], Frank McKeon[1]✉ and Wa Xian[1]✉

'Adult' or 'somatic' stem cells harbor an intrinsic ability to regenerate tissues. Heterogeneity of such stem cells along the gastrointestinal tract yields the known segmental specificity of this organ and may contribute to the pathology of certain enteric conditions. Here we detail technology for the generation of 'libraries' of clonogenic cells from 1-mm-diamter endoscopic biopsy samples from the human gastrointestinal tract. Each of the 150–300 independent clones in a typical stem cell library can be clonally expanded to billions of cells in a few weeks while maintaining genomic stability and the ability to undergo multipotent differentiation to the specific epithelia from which the sample originated. The key to this methodology is the intrinsic immortality of normal intestinal stem cells (ISCs) and culture systems that maintain them as highly immature, ground-state ISCs marked by a single-cell clonogenicity of 70% and a corresponding 250-fold proliferative advantage over spheroid technologies. Clonal approaches such as this enhance the resolution of molecular genetics, make genome editing easier, and may be useful in regenerative medicine, unravelling heterogeneity in disease, and facilitating drug discovery.

Introduction

Adult stem cell–based drug discovery and regenerative medicine may lead to treatments and cures for numerous diseases and conditions that have defied conventional therapeutic approaches. Pluripotent stem cells, including embryonic stem cells (ESCs) and induced pluripotent stem cells (iPSCs), currently dominate stem cell research and clinical trials in regenerative medicine[1]. The drawbacks of these remarkable cells include teratoma formation, complicated and inefficient processes for directed commitment to desired lineages, and lack of regenerative capacity in derived lineages[2–7]. By contrast, 'adult' or 'somatic' stem cells harbor an intrinsic ability to regenerate tissues. Green and colleagues pioneered a system dependent on 3T3-J2 feeder cells for capturing p63+ epidermal stem cells[6] in their most immature and clonogenic form and showed that these cells can be differentiated, at will, to yield a stratified squamous epithelium. Subsequently, the Green protocol was successfully adapted for the cloning and expansion of p63+ stem cells from other stratified epithelia, including those of the thymus, cornea, and lung[7–9], and has become the basis of successful autologous stem cell transplants in thousands of patients with severe burns, blindness resulting from industrial accidents, and genetic blistering conditions[6,8,10]. However, the Green protocol does not support the cloning and expansion of the stem cells of the gastrointestinal tract.

Leveraging the remarkable success of Green's system of cloning stem cells of stratified epithelia, we developed a parallel system that enables the cloning of highly undifferentiated stem cells from 1-mm-diameter endoscopic biopsy samples from the human gastrointestinal tract[11–13] (Fig. 1). We demonstrated that these ground-state intestinal stem cells (gISCs) can be propagated to enormous

[1]Stem Cell Center, Department of Biology and Biochemistry, University of Houston, Houston, Texas, USA. [2]Division of Cellular Signaling, National Cancer Center Research Institute, Tokyo, Japan. [3]Department of Gastrointestinal Medical Oncology, Division of Cancer Medicine, University of Texas MD Anderson Cancer Center, Houston, Texas, USA. [4]Tract Pharmaceuticals, Inc., Marlborough, Massachusetts, USA. [5]Departments of Medicine and Pathology, National University of Singapore, Singapore, Singapore. [6]Division of Gastroenterology, Baylor College of Medicine, Houston, Texas, USA. [7]Division of Digestive Diseases, Hepatology, and Nutrition, Connecticut Children's Medical Center, Hartford, Connecticut, USA. [8]Division of Gastroenterology, Department of Pediatrics, University of North Carolina at Chapel Hill, Chapel Hill, North Carolina, USA. [9]Department of Pathology, Harvard Medical School and Brigham and Women's Hospital, Boston, Massachusetts, USA. [10]These authors contributed equally: Marcin Duleba, Yusuke Yamamoto. ✉e-mail: fdmckeon@uh.edu; wxian@uh.edu

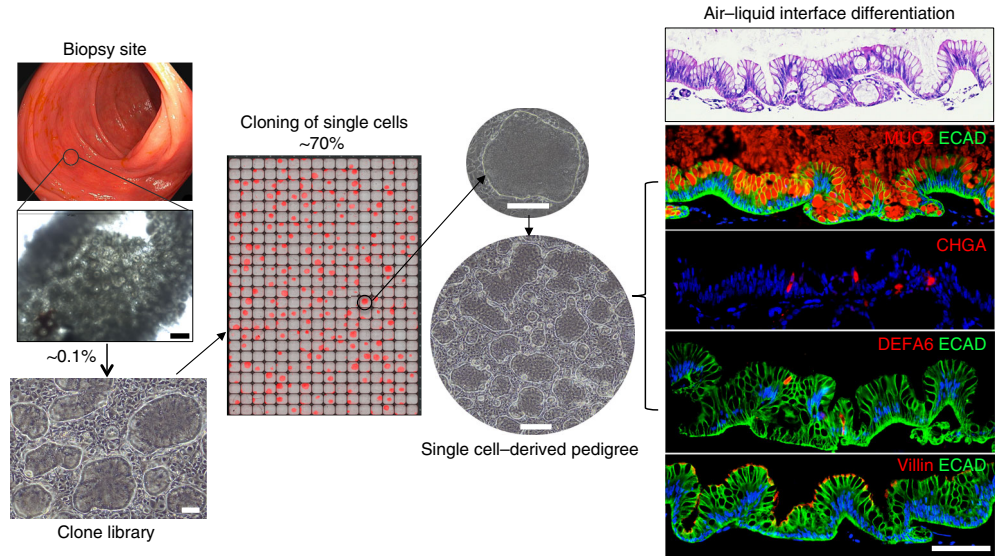


Fig. 1 | Schematic of cloning of gISCs from endoscopic biopsy samples. Left, endoscopic biopsy sample (1-mm diameter) from gastrointestinal mucosa is processed to yield a 'library' of clonogenic cells representing <0.1% of all epithelial cells. Scale bars, 100 μm. Center, libraries are further single-cell-sorted into 384-well plates and, right, clones are sampled for expansion as immature cells or differentiated to 3D epithelial-containing goblet cells (MUC2$^+$; red), endocrine cells (CHGA$^+$; red), Paneth cells (DEFA6$^+$; red), or enterocytes (Villin$^+$; red). See Table 1 for details of antibodies. Scale bar, 100 μm. ECAD, E-cadherin antibody. Adapted with permission from ref. [13], Elsevier.

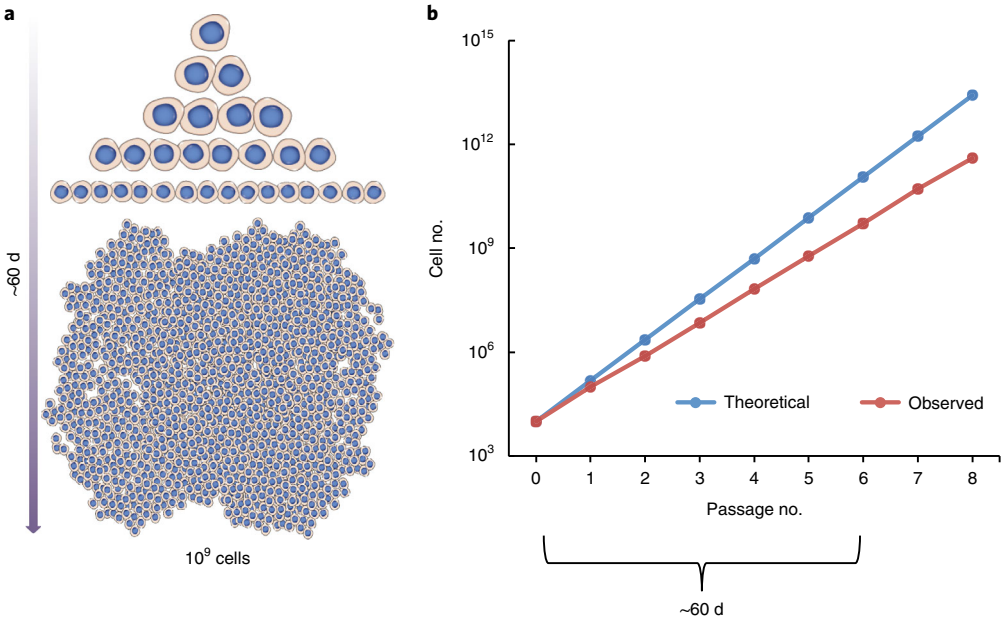


Fig. 2 | High clonogenicity facilitates the expansion of single cell–derived clones. a, High proliferation and symmetric division enable the expansion of a single gISC to 1 billion cells in 6 weeks. **b**, Theoretical expansion of a clone undergoing uniform proliferation over time compared with the representative expansion of a gISC clone (representative data; 6 clones were analyzed in total), reflecting only minor deviations. **a** adapted with permission from ref. [13], Elsevier.

numbers (Fig. 2) while maintaining genomic integrity (Fig. 3), epigenetically enforced fate commitment, and high clonogenicity. Our findings support the potential of gISCs in disease modeling and regenerative medicine. Herein, we present a detailed experimental protocol for the generation of gISCs from endoscopic biopsy samples.

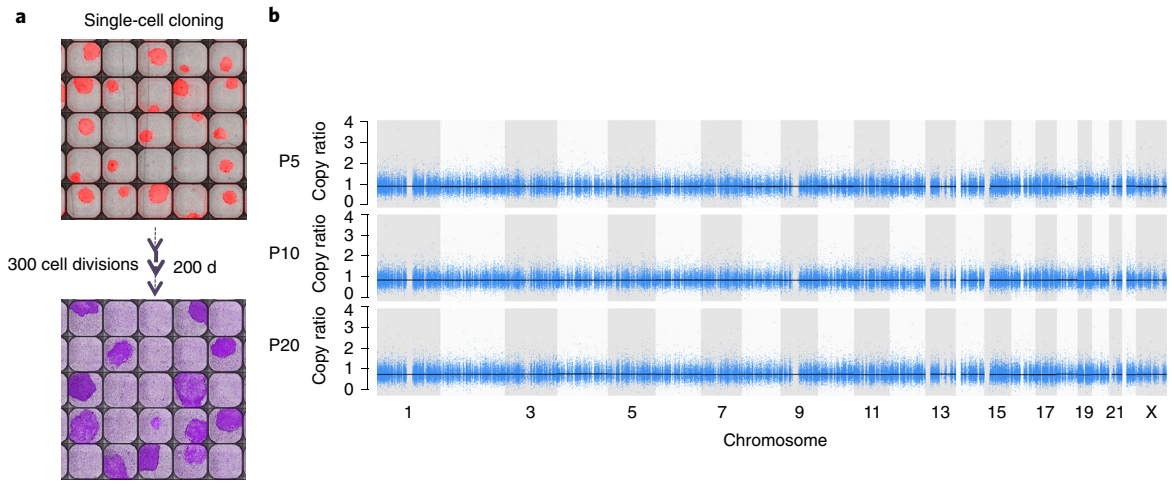


Fig. 3 | Conservation of high clonogenicity of gISCs over proliferative time. a, Clonogenicity assay based on FACS sorting into 384-well plates of passage 5 cells (P5; top) and passage 20 cells (P20; bottom), yielding similar results. **b**, Copy ratio of gISC clone, determined by whole-exome sequencing, showing absence of CNV events over continuous passaging. Chr, chromosome.

Development and applications of the protocol

The system developed by Green and colleagues for propagating epidermal stem cells[6,14–17] used a custom medium containing growth factors such as EGF and, importantly, an irradiated feeder cell layer of Swiss 3T3-J2 murine embryonic fibroblasts. About 1 in every 1,000 cells of a single-cell suspension of an epidermal biopsy sample forms 2D, circular colonies termed 'holoclones', which are composed of immature cells having a clonogenicity approaching 95% in subsequent passages. Expanded holoclones form a stratified epithelium upon transplant to abraded skin of immunodeficient mice or upon exposure to an air–liquid interface (ALI) in vitro, and have been the basis of autologous transplants for regenerative medicine treatments of damaged or mutant epithelia.

As adult stem cells residing in stratified epithelium and columnar epithelium require distinct signaling pathways for the maintenance of stemness, the medium devised by Green was not able to support adult stem cells in columnar epithelium. To overcome this obstacle, we developed and continue to improve media containing novel combinations of growth factors and regulators of an array of signaling pathways such as the TGF-β, Wnt/β-catenin, EGF, IGF, and Notch pathways[12,13] that support ISC cloning and maintenance in their most undifferentiated, ground state (referred to herein as "gISCs"). This new feeder-dependent system maintains gISCs as highly proliferative and clonogenic cells in culture so that they can quickly reach numbers necessary for downstream applications in a timely manner. Owing to their high clonogenicity and attending proliferation, a single gISC will yield >1 billion stem cells within 60–80 d in this system[18] (Fig. 2). Importantly, the apparent unlimited proliferative potential or 'immortality' of gISCs is evident in the absence of mutations or copy-number variation (CNV) events in pRB, CDKN2A, p53, or any of a host of tumor suppressor or proto-oncogenes[11] (Fig. 3). Furthermore, gISCs in this system retain their multipotent, region-specific differentiation capacity despite continuous cultivation for >1 year[11]. This cell-autonomous, region-specific commitment of stem cells along the intestinal tract suggests a developmentally established spectrum of stem cells that preserves the histological and functional properties that define these segments. Because there is not a unitary 'intestinal stem cell' or even one for each of the histologically recognized segments, we believe that this technology for cloning regionally committed gISCs offers real hope to permanently address both short-bowel syndrome (SBS) and non-SBS conditions using autologous regenerative medicine. Judging from lessons learned from the pioneering transplants of corneal epithelial stem cells for caustic eye burns[8], the high clonogenicity of gISCs will favor their use in regenerative therapies.

Comparing gISC cloning technology with organoids

For almost half a century, researchers have grown mammalian cells in collagen and laminin-rich, 3D hydrogels as 'organoids'[19–23], and this technology has facilitated fundamental advances in stem cell and developmental biology research. That being said, multiple studies have shown that the vast

majority of cells in an organoid are not stem cells, and those that are account for <1% of all organoid cells[13,23,24]. It is unclear at present how this low stem cell content will affect the utility of organoids for regenerative medicine, but the key indicator of success in corneal regeneration therapy was the ratio of stem cells in the transplant itself[8]. Apart from this potential concern, gISCs provide multiple practical advantages over the widely used organoids that largely stem from their high clonogenicity and the clonal platform this enables. For instance, the maintenance of gISCs with a >70% clonogenicity underlies the 250-fold proliferative advantage of gISCs over organoids that speeds the production of high-quality stem cells for downstream molecular analyses, transplant studies, genomic manipulation and drug screening. Moreover, gISCs naturally accommodate clonal approaches and the precision of these downstream studies, whereas clonal analyses with organoids are complex, labor intensive and largely confined to proof-of-concept experiments. The advantages of gISCs can be summarized by listing six routine processes with gISCs that are not practical with organoids: (i) generation of libraries of 100–300 independent ISC clones from a single 1-mm-diameter endoscopic biopsy sample of gastrointestinal mucosa; (ii) expansion of single gISCs to 1 billion highly clonogenic cells in 60 d; (iii) clonal determination of genomic profiles ahead of regenerative medicine applications; (iv) demonstration and validation of stable epigenetic commitment to region-specific differentiation of gISCs; (v) generation of accurate mucosal facsimiles with appropriate and accessible apical–basal polarity for drug and biologics testing; and (vi) rapid parsing of genome-edited populations for clonal analysis of variants.

Limitations of the protocol

We have successfully derived and cultured gISCs of human gastrointestinal epithelia from a large number of donors and have observed similar efficiency of cloning and long-term culture independent of donor age[11–13] (Supplementary Table 1). The condition of the 3T3-J2 feeder layer can play a defining role in the success of human ISC derivation, and this condition is ultimately dependent on adherence to rigid parameters of 3T3-J2 growth and expansion as defined below (Fig. 4). Not every investigator in the laboratory can or will work within these parameters. Another important limitation of this method is the tendency of gISCs to spontaneously differentiate if colonies are allowed to merge to confluence. Thus, to maintain the stemness of gISCs, the seeding density and confluency of the cultures need to be strictly monitored. In addition, gISCs tend to differentiate if they are seeded as clusters instead of single cells during passaging. Thus, thorough trypsinization and single-cell filtration or flow-sorting before seeding will be essential to maintaining the potential of these cells. Finally, it is critical to ensure the quality of gISCs before seeding them on Transwell membranes for ALI differentiation, transplanting them as xenografts, or subjecting them to genome-editing protocols.

Experimental design considerations

Herein, we present a step-by-step description of the whole process, including acquisition and processing of biopsy samples, gISC propagation and pedigree establishment, and purification of stem cells.

Acquisition and processing of endoscopic biopsy samples

It is critical to recognize that collection of biopsy samples must be compliant with institutional review board (IRB) regulations and guidelines, as well as requiring patient consent. The biopsy samples used for the experiments described here were obtained under informed consent as de-identified material under approved IRB protocols at the Connecticut Children's Medical Center (IRB approval no. HSC-MS-16-0330), the University of North Carolina (IRB approval no. 15-2813), the Baylor College of Medicine (IRB approval no. H-38746) or the National University of Singapore (IRB approval no. NHG DSRB ref.: 2014/00836). Under IRB-approved protocols, biopsy samples were collected with one pass of the biopsy forceps through a colonoscope. Captura disposable biopsy forceps (2.4 mm; Cook Medical), disposable jumbo biopsy forceps (2.8 mm; Boston Scientific) or equivalents were used, depending on the endoscopist's preferences. The biopsy samples weighed 8 mg on average. The biopsy samples should be immediately deposited in sterile, 15-ml conical tubes containing ice-cold wash buffer and transferred to the investigator's laboratory after de-identification and coding. Long-distance shipment under optimal conditions is feasible, and we routinely obtain samples in Houston from other cities in the United States or Asia; these are shipped on wet ice and take up to 7 d to reach us. A decline of clonogenicity might be expected with time, but we have not directly assessed this

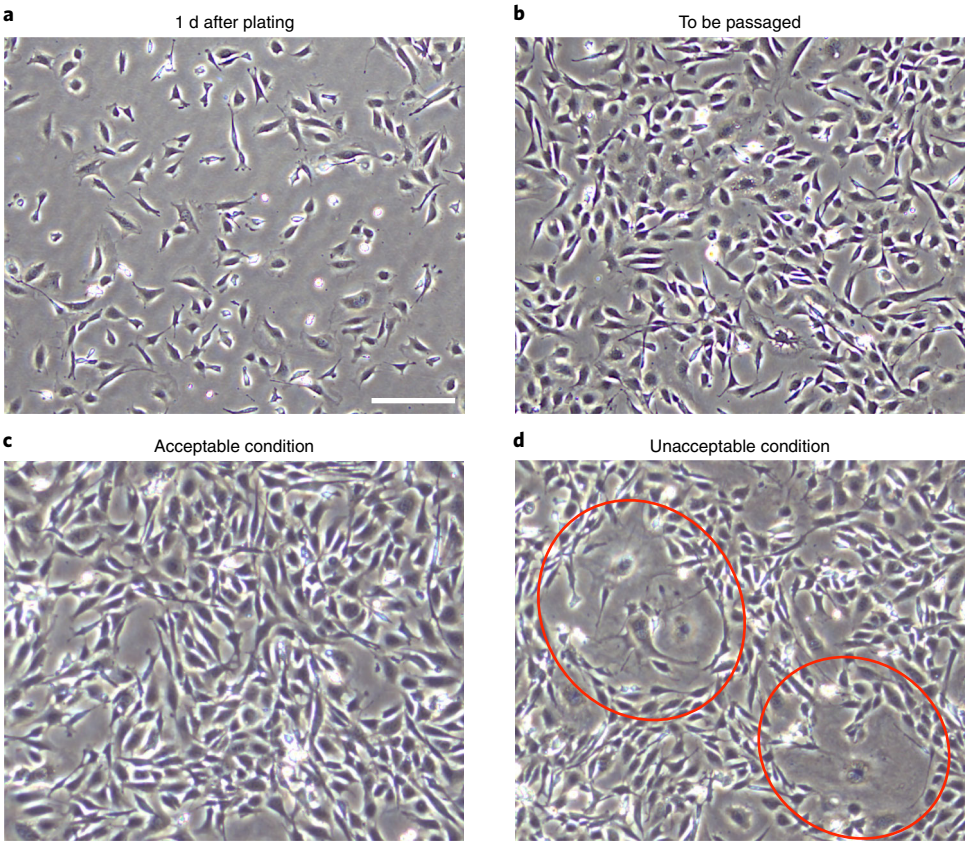


Fig. 4 | Representative images of 3T3-J2 cells. a, One day after seeding, the 3T3-J2 cells attach, spread and start proliferating. **b**, The 3T3-J2 cells should be passaged when the cells reach 80–90% confluence, with space apparent between cells. **c**, For irradiation, 3T3-J2 cells can proliferate to 95% confluence before harvest. The space between cells should still be visible in some regions. The cells should appear uniform and show contact inhibition. **d**, Giant 3T3-J2 cells with extensive cytoplasmic domains indicate an unhealthy condition (red circles); in this case, the culture should be discarded. Scale bar, 100 μm.

issue. Before receiving biopsy samples, 3T3-J2 feeder cells should be prepared according to the protocol below. Preferably, the biopsy samples would be processed immediately upon arriving at the laboratory. We have processed hundreds of biopsy samples from human small intestine and colon and demonstrated a success rate of at least 95% independent of age and sex[13] (Supplementary Table 1). Processing of biopsy samples from ascending, transverse and descending colon is uniformly successful, whereas that of samples from small intestine is somewhat more variable but still >90%.

Expanding gISCs and setting up single cell-derived clones

The gISC colonies appear 7–10 d after seeding, and generally 100–300 independent colonies form from a typical 1-mm-diameter biopsy sample that harbors 300.000–900,000 epithelial cells at all stages of differentiation (Fig. 1). The cells should be passaged within 10 d, before the 3T3 J2 feeder cell lawn ages. Immature gISC colonies are compact and composed of highly proliferative cells with high nucleus/cytoplasm ratio. These gISCs are highly clonogenic (>70%) and consequently proliferate to >1 billion cells in 6–8 weeks. Inappropriate handling, such as use of aged or non-optimal 3T3 J2 feeders, will lead to a differentiation of gISCs marked by an increased cytoplasm/nucleus ratio and expression of differentiation markers, as well as a loss of clonogenicity and proliferation potential. As long as the protocols that we provide here are followed, the establishment of gISC clones is highly efficient. For cloning of gISCs from libraries of gISC colonies, we favor FACS-aided sorting from single-cell suspensions into 384-well plates previously seeded with 3T3-J2 feeder cells (Fig. 1; Supplementary Video 1). In 7–14 d, single cell–derived colonies can be observed and can be sampled and expanded to discrete lines for all downstream applications. We suggest freezing each passage of an gISC clone in liquid nitrogen until needed.

Table 1 | Antibodies used for immunofluorescence

Target	Cat. no.	Species	Dilution	Vendor	RRID no.
Primary antibodies					
Villin	ab52102	Rabbit	1:300	Abcam	AB_883445
E-Cadherin	AF648	Goat	1:400	R&D Systems	AB_355504
Mucin2	sc-515032	Mouse	1:400	Santa Cruz Biotechnology	AB_2815005
Chromogranin A	ab15160	Rabbit	1:350	Abcam	AB_301704
Defensin alpha 6	HPA019462	Rabbit	1:350	Sigma-Aldrich	AB_1847595
Secondary antibodies					
Alexa Fluor 488 donkey anti-goat IgG	A11055	Donkey	1:500	Invitrogen	AB_2534102
Alexa Fluor 594 donkey anti-mouse IgG	A21203	Donkey	1:500	Invitrogen	AB_141633
Alexa Fluor 594 donkey anti-rabbit IgG	A21207	Donkey	1:500	Invitrogen	AB_141637

Functional characterization of gISCs

We find that gISCs harbor intrinsic immortality, indicated by unlimited self-renewal ability and conditional, multipotent differentiation. To examine clonogenicity of gISC clones, single-cell suspensions can be FACS-sorted to single cells in 384-well plates, which typically yield a 70% rate of colony formation in wells for stem cells from the gastrointestinal tract (Fig. 1). Owing to the remarkably consistent clonogenicity across numerous passages, gISCs can achieve a proliferative expansion that is close to the theoretical limit (Fig. 2, Supplementary Video 2). Single clones selected from these 384-well plates can be expanded as clonal populations and validated by in vitro differentiation in ALI cultures that recapitulate intestinal epithelia comprising $Muc2^+$ goblet cells, $CHGA^+$ endocrine cells, $DEFA6^+$ Paneth cells and $Villin^+$ enterocytes (Fig. 1, Table 1). We note that these ALI cultures yield 3D epithelia whose histology is remarkably similar to the in situ histology of the corresponding regions of the gastrointestinal tract. From histology alone, the ALI cultures of gISCs appear to yield facsimiles of the gastrointestinal mucosa superior to those reported for organoids (Fig. 1). Alternatively, gISC clones can be readily adapted to organoid cultures by seeding into Matrigel and growth in established organoid media (Fig. 5). Using validated ISC clones, we also note that seeding 2,000 single cells in parallel into either ground-state or organoid cultures yields 1,500 colonies in the 2D, gISC cultures, and ~1,000 spheroids in organoid cultures. Subsequent passaging showed that although the gISCs maintain their 70% clonogenicity, cells from organoids showed a marked decline of clonogenicity, suggesting gISC culture comprises a uniform population of stem cell cells, whereas organoid culture comprises a majority of differentiated cells or transit-amplifying cells[23].

We previously demonstrated that gISCs display remarkable genomic stability during long-term culture[11]. For instance, when we examined copy-number and single-nucleotide variation in gISC clones across extended periods of continuous proliferation to 1 billion cells (6–8 passages of 10 d each), we found no chromosomal aneuploidy, no CNV events >10 kb, and very few single-nucleotide variations, none of which impacted known proto-oncogenes or tumor suppressor genes[11]. After 20 passages, this situation changed in some clones, and this should be borne in mind. Ample numbers of cells for downstream applications can be generated before this point. We collected DNA from single cell–derived gISC clones at P5 (50 d in culture), P10 (100 d in culture) and P20, and subjected the DNA for whole-exome sequencing. On the basis of the somatic allelic CNVs called by the best-practices pipeline of GATK v.4.0.4 (https://gatk.broadinstitute.org/hc/en-us), we did not observe any chromosomal aneuploidies during the passaging of selected clones (Fig. 3).

Separation of gISC from 3T3-J2 feeder cells

Some downstream applications require the elimination of feeder cells from gISCs, which can be achieved by several routes. gISCs can be labeled with GFP, using retroviral or lentiviral transduction, and then readily separated by FACS sorting from feeder cells. As shown in Fig. 6, live-cell sorting based on green fluorescence can efficiently separate GFP-labeled gISC from mouse feeder cells.

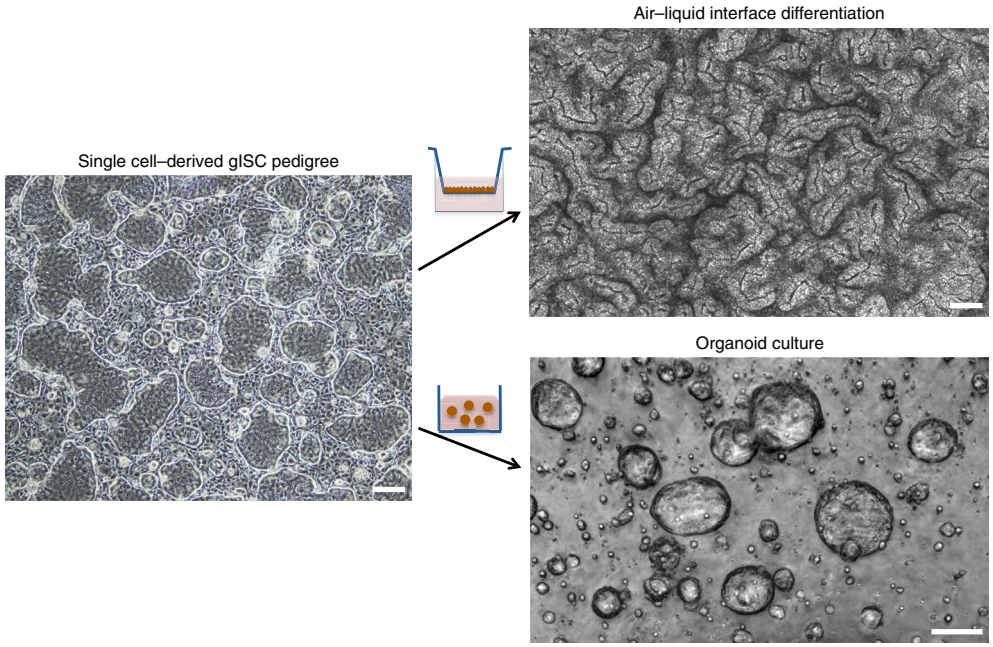


Fig. 5 | Adaptation of gISC clone to ALI differentiation or organoid culture format. Left, 2D colonies of a single gISC clone 10 d after seeding. Right, 3D intestinal mucosal resulting from 10-d ALI differentiation of an gISC clone (top) and 3D organoids 10 d after gISC seeding into Matrigel in organoid culture medium. Scale bars, 200 μm.

Alternatively, murine 3T3-J2 feeder cells can be depleted from co-cultures with gISCs by using Feeder Removal MicroBeads (Miltenyi Biotec), LS columns, and a MidiMACS separator, with human-specific PCR primers indicating a 99% purity of gISCs (Table 2). In unpurified samples, we can detect 25–40% of mouse DNA. By contrast, after purification, we observed <1% of mouse DNA (Supplementary Methods). This level of purity ensures the integrity of DNA and RNA from these gISCs in the analyses of clonal heterogeneity, genome stability and genome editing.

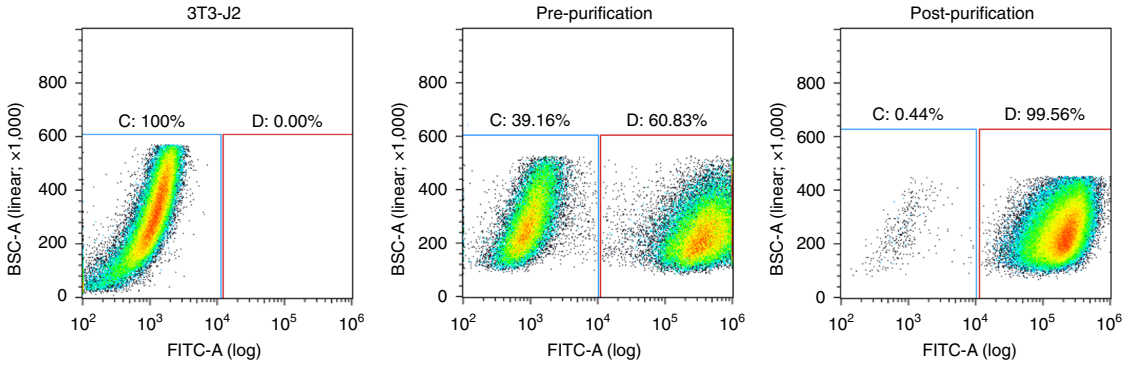
Materials

Biological materials

- Endoscopic biopsy samples from human gastrointestinal mucosa **! CAUTION** Ethical approval is required for acquisition and use of human-derived samples; collection must conform to relevant institutional and national regulations, and patient consent is required. Our biopsy samples were collected under IRB approval from Connecticut Children's Medical Center (IRB approval no. HSC-MS-16-0330), the University of North Carolina (IRB approval no. 15-2813), the Baylor College of Medicine (IRB approval no. H-38746) and the National University of Singapore (National Healthcare Group (NHG) Domain Specific Review Board (DSRB) IRB approval no. 2014/00836).
- Resected human intestine tissue collected as surgical waste **! CAUTION** Ethical approval is required for acquisition and use of human-derived samples; collection must conform to relevant institutional and national regulations, and patient consent is required. Our biopsy samples were collected under IRB approval from the MD Anderson Cancer Center (IRB approval no. LAB06-0893).
- 3T3-J2 fibroblasts. The 3T3-J2 fibroblast cell line[25] was generously provided by H. Green. 3T3-J2 cells can also be purchased commercially (https://web.expasy.org/cellosaurus/CVCL_W667; https://www.biocompare.com/11023-Cells-Strains/8563571-3T3-J2-Cell-Line/) **▲ CRITICAL** The cell lines used in your research should be regularly checked to ensure that they are authentic using short tendem repeat (STR) profiling and that they are not infected with mycoplasma.

Reagents

- DMEM without L-glutamine, without sodium pyruvate (DMEM$^-$; 4.5 g/liter glucose; Invitrogen, cat. no. 11960-044)
- F12 (Gibco, Life Technologies, cat. no. 11765-054)
- HEPES (Gibco, Life Technologies, cat. no. 15630-080)
- Gentamycin (Gibco, Life Technologies, cat. no. 15710-064)



	3T3-J2		Pre-purification		Post-purification	
Name	Events	Parent%	Events	Parent%	Events	Parent%
C	49,800	100	27,452	39.15785	365	0.436619
D	0	0	42,643	60.82646	83,226	99.5562

Fig. 6 | FACS profiling of GFP-labeled gISCs for monitoring of purification. Top, from left to right, FACS profile of 3T3-J2 cells, FACS profile of co-culture of 3T3-J2 cells and gISCs, and FACS profile of co-cultured cells following removal of feeder cells. Bottom, quantification of 3T3-J2 in FACS gate C in 3T3-J2 cultures (left), in co-cultures with gISCs (in FACS gate D), and following removal of 3T3-J2 cells. See Supplementary Figs. 1–4 for gating strategy and numerical data. BSC-A, back scatter area.

Table 2 | Primers used for assessment of DNA purity

Primer	Species	Forward sequence	Reverse sequence
MHC1	Human	ATC ATG ACT CTC ACC CTC CA	TCA ACC CTT TTG CTT ACC TG
MICA1	Mouse	AGG GTC TGT GAG ATC CAT GA	CTG CAT GCA TAG CGT GAT AG

- Fungizone (Gibco, Life Technologies, cat. no. 15290018)
- Bovine calf serum (BCS) (HyClone, cat. no. SH130072.03)
- Fetal bovine serum (FBS) (HyClone, cat. no. SH30396.03)
- Penicillin–streptomycin (Invitrogen, cat. no. 15140-122) **! CAUTION** Penicillin–streptomycin is a health hazard if swallowed. It should be disposed of by appropriate routes. Consult safety and hazard sheets provided by the seller.
- L-glutamine (Invitrogen, cat. no. 25030-081)
- 0.05% Trypsin–EDTA (Invitrogen, cat. no. 25300-062)
- TrypLE Express enzyme (1×; Gibco, Invitrogen, cat. no. 12605-010)
- DPBS, no calcium, no magnesium ($DPBS^{-}$; 1 ×; Invitrogen, cat. no. 14190-144)
- Dimethyl sulfoxide (DMSO; Sigma-Aldrich, cat. no. 41640-500ml)
- Trypan blue solution (0.4% (wt/vol) in $DPBS^{-}$, pH 7.5 ± 0.5; Corning, cat. no. 25-900-CI) **! CAUTION** Trypan blue solution is acutely toxic if swallowed and is a health hazard. Consult safety and hazard sheets provided by the seller.
- Collagenase, type IV (1g; Life Technologies 17104-019)
- Expansion medium (StemECHO202; Tract Pharmaceuticals, cat. no. 044102)
- Bullet enhancer (StemECHObullet002; Tract Pharmaceuticals, cat. no. 044002)
- Differentiation medium (StemECHO204; Tract Pharmaceuticals, cat. no. 044104)
- Neutralization medium (StemECHO200; Tract Pharmaceuticals, cat. no. 044100)
- Growth-factor-reduced Matrigel (Corning, cat. no. 354230)

Equipment

- Inverted microscope (Nikon, model no. Eclipse Ts2)
- CO_2 incubator (Eppendorf/New Brunswick Galaxy 48R incubator; Eppendorf, cat. no. CO48R230 or Panasonic, cat. no. KM-CC17RU2)
- Tissue culture biological safety cabinet (class II; LabGard ES; NuAire, cat. no. NU-437)

- pH meter (Five Easy FE20; Mettler Toledo, cat. no. 10385343)
- Fine forceps (student Dumont no. 5 forceps; Interfocus, cat. no. 91150-20)
- Fine scissors (straight/large loop; Interfocus, cat. no. 14040-10)
- Pasteur pipettes (Scientific Laboratory Supplies, cat. no. PIP4172)
- Sterile disposable scalpels (Dynarex, cat. no. 4122)
- Tissue culture–grade plates (Corning, cat. no. CLS3506)
- Nalgene rapid-flow sterile disposable filter units with PES membrane (1,000 ml, 0.2μm; Fisher Scientific, cat. no. 09-741-03)
- Steriflip filtration units (50 ml; Millipore, cat. no. C3238)
- Cell strainer (40 μm; Corning, cat. no. 07-201-430)
- Cell strainer (30 μm; Miltenyi Biotec, 130-041-407)
- QuadroMACS Starting Kit (LS) (Miltenyi Biotec, cat. no. 130-091-051)
- Transwell multiple-well plate with 0.4-μm-pore polyester membrane inserts (Fisher Scientific, cat. no. 07-200-154)
- Tissue culture–treated microplates (96 wells, flat, clear, polystyrene; Fisher Scientific, cat. no. 07-200-90)
- Cell sorter (Sony, cat. no. SH800S)
- X-ray irradiation machine (RadSource, model no. RS1800, cat. no. 1087)
- Mini shaking incubator (WISBiomed, cat. no. BS-ICH1)
- Centrifuge (Eppendorf, model no. 5810 R)
- Hemocytometer with cover glass (Daigger, cat. no. EF16034F)
- CoolCell freezing container (Corning, cat. no. 432008)
- Freezer (−80 °C; VWR, cat. no. 76307-942)
- Liquid nitrogen tank (VWR, cat. no. 10027-532)
- Tissue culture dishes (Corning, 6-well plates, cat. no. 08-772-1B; 12-well plates, cat. no. 08-772-29; 24-well plates, cat. no. 08-772-1; 48-well plates, cat. no. 07-200-86; 100-mm dish, cat. no. 08-772-22; 60-mm dish, cat. no. 430589; 150-mm plates, Corning 08-772-24; 24-well Transwell inserts, cat. no. 3470)
- Plates (96 well; Greiner Bio-One, cat. no. 65500)
- Filters (0.22 μm; Corning 09-741-08)
- Pipette tips
- Feather scalpels
- Nylon mesh strainer (100 μm)
- Cell sorter

Reagent setup

3T3-J2 culture medium

To 440 ml of DMEM$^-$, add 50 ml of BCS, 5 ml of penicillin–streptomycin and 5 ml of L-glutamine. Filter the medium with a 0.22-μm filter. The culture medium can be stored at 4 °C for up to 1 month.

! CAUTION Be sure to use BCS for the 3T3-J2 culture medium. Do not use FBS.

3T3-J2 freezing medium

To 700 ml of DMEM$^-$, add 200 ml of BCS and 100 ml of DMSO. Pass the medium through a 0.22-μm filter. Make aliquots and store at −80 °C for up to a year.

Wash buffer

To 950 ml of F12 medium, add 50 ml of FBS, 10 ml of penicillin–streptomycin, 10 ml of gentamycin and 1 ml of Fungizone. Filter the medium with 0.22 μm filter. The wash buffer can be stored at 4 °C for up to 1 month.

Digestion buffer

Dissolve 1 mg of collagenase in 10 ml of wash buffer in a 37 °C water bath for 30 min. Filter the medium with a 0.22-μm filter. Prepare fresh digestion buffer each time. Use approximately 2–3 ml of digestion buffer for each biopsy sample.

gISC growth medium

To prepare gISC growth medium (complete expansion medium; StemECHO202 + StemECHObullet002), add 0.25 ml of StemECHObullet002 to 250 ml of StemECHO202. Mix thoroughly and store at 4 °C for up to 1 month.

gISC freezing medium
To prepare 100 ml of ISC freezing medium, add 10 ml of DMSO and 10 ml of FBS to 80 ml of gISC growth medium. Filter the medium using a 0.22-μm filter. Make aliquots and store at −80 °C for up to 1 year.

Diluted Matrigel
Thaw one aliquot of Matrigel at 4 °C overnight packed in ice. Pipette 2 ml of Matrigel into 8 ml of cold (4 °C) 3T3-J2 culture medium. Swirl the tube to mix the contents completely, store at 4 °C and use within 1 week.

Equipment setup

Humidified incubator
Set to 37 °C, 7.5% CO_2.

Matrigel-coated plates
Chill tissue culture plates and pipette tips at 4 °C overnight. Add diluted Matrigel to the wells of a tissue culture plate in a biological safety cabinet. Incubate for a minimum of 30 min at 37 °C. Plates should be used immediately to plate feeder cells.

Procedure

! CAUTION All procedures should be undertaken in class II biological safety cabinets to ensure sterility.
! CAUTION All procedures used for handling human tissues should assume potential contamination of tissue with human pathogens (e.g., HBV, HCV, HIV, *Clostridium difficile*) and should be in compliance with IRB-approved protocols.

Reviving 3T3-J2 cells from frozen stock ● Timing 3 d

1 Clean the hood with 70% ethanol and turn on a UV light for 15 min before the cell culture experiment.
! CAUTION This should be repeated before and after each cell culture session.
2 Warm 3T3-J2 culture medium in a water bath (37 °C) for 30 min before thawing the vial.
3 Retrieve a cryovial of 3T3-J2 cells from frozen cell storage and thaw the vial (each vial should contain 10^6 cells) in water bath.
4 Gently transfer cells with a 1,000-μl pipette to a 50-ml Falcon tube and add 30 ml of 3T3-J2 culture medium drop by drop while swirling the tube slowly.
▲ **CRITICAL STEP** Thaw the cells quickly in the water bath and swab the vial with 70% ethanol before bringing it into the hood. Dilute freezing medium slowly, drop by drop. Do not pipette the cells up and down.
5 After resuspension, seed the cells into a 15-cm tissue culture plate.
▲ **CRITICAL STEP** Do not centrifuge to wash away the freezing medium.
6 Gently shake the plates with cells in the hood to evenly distribute the cells.
▲ **CRITICAL STEP** Flow the medium left and right five times and let it sit for 5 s or until the medium is stabile. Then flow toward the back and front five times in the hood.
7 Repeat Step 6 three times in the incubator.
▲ **CRITICAL STEP** Do not change the location once the plates are placed in the incubator. This step is very important to evenly distributing the cells in the plate.
8 Change the medium the day after thawing the frozen vial. After that, change medium every 2 or 3 d.
▲ **CRITICAL STEP** It is important to change the medium the day after thawing the vial because the freezing medium contains DMSO, which is harmful to cells.
9 Proceed to the next step to passage the cells when they become 80% confluent. Generally 80% confluency will be reached 3 d after seeding, however, monitoring is required.
▲ **CRITICAL STEP** Do not continue culturing if 3T3-J2 cells grown past confluence. Abandon them and thaw a new vial.
? TROUBLESHOOTING

Passaging 3T3-J2 cells for expansion ● Timing variable

10 Warm 3T3-J2 culture medium and 0.05% Trypsin–EDTA in a water bath (37 °C) for 30 min before use.

11 Remove the plates from the incubator, check the 3T3-J2 cells under a microscope and gently put the plates into a cleaned hood.

12 Remove the medium, add 30 ml of $DPBS^{-}$ to thoroughly wash away the serum, and add 5 ml of warmed 0.05% Trypsin–EDTA.
▲ **CRITICAL STEP** It is important to evenly spread the Trypsin–EDTA in the plates.

13 Incubate the cells with Trypsin–EDTA in incubator at 37 °C for 5 min.
▲ **CRITICAL STEP** Do not leave the cells in Trypsin–EDTA for >10 min.

14 Add 10 ml of warmed 3T3-J2 culture medium to the plate to neutralize the Trypsin–EDTA following 5 min of incubation. Pipette up and down five times to obtain a single cell solution.

15 Collect the cells into a 50-ml Falcon tube and spin down at 300*g* for 5 min at 4 °C.

16 Remove the supernatant carefully and resuspend the cell pellet with a fresh 5 ml of 3T3-J2 growth medium.

17 Count the cells using hemocytometer by mixing 10 µl of cells with 10 µl trypan blue, and using a hemocytometer to count the cells.
▲ **CRITICAL STEP** If you are working on a number of tubes, all should be combined in one container and mixed gently by swirling before counting.

18 Calculate the number of cells using the following equations:

$$\text{Avg. cell counts of the four corner squares} \times 10^4\text{, corrected for dilution factor} = \text{cells/mL}\quad \text{Total Cells} = \text{cells/ml} \times \text{amount of total volume of medium in mL}$$

19 Determine the number of 15-cm plates to seed with 500,000 cells per plate and reserve medium as necessary.

20 Seed 500,000 cells per plate and shake the plates in the incubator.
▲ **CRITICAL STEP** Add 30 ml of warmed growth medium to the required number of plates and then add 500 µl of cell suspension into the plates. Shake the tube continuously to ensure the cells do not accumulate at the bottom. Shake the plate left and right five times and let it sit for 5 s or until the medium is stabile, and then shake back and forth five times in the hood. Repeat the process of shaking three times in the incubator.
? TROUBLESHOOTING

21 When the cells are 80% confluent, passage them for further expansion by repeating Steps 10–20. When you have sufficient cells, proceed to the next stage to irradiate and freeze the cells.
? TROUBLESHOOTING

Irradiating and freezing irradiated 3T3-J2 cells ● Timing 1 d

▲ **CRITICAL** Freeze as many early-passage 3T3-J2 cells as you will need for your experiments. We freeze ~10^6 cells per vial, but as many as 4×10^6 and as few as 5×10^5 can be frozen in one vial.

22 When the confluency of 3T3-J2 cells reaches 90–95%, change the medium.

23 The next day, repeat Steps 10–16 to passage cells and place the cells in a 50-ml Falcon tube on ice.
▲ **CRITICAL STEP** Move immediately to the next step of irradiation.

24 Irradiate the 3T3-J2 cells at 2,000 rad.
▲ **CRITICAL STEP** The duration required to administer 2,000 rad (20 Gy) must be calculated each time according to the facility records.

25 Following the irradiation, put the container back on the ice and immediately count the number of viable cells using a hemocytometer and trypan blue (as described in Steps 17 and 18).

26 Spin down cells at 300*g* for 5 min at 4 °C.

27 Resuspend cells in freezing medium very gently to freeze 6×10^6 cells/vial. Use 0.5 ml of freezing medium per vial.
▲ **CRITICAL STEP** 3T3-J2 cells are extremely fragile after irradiation and need to be handled with extreme care. Do not pipette the cells up and down to mix the cells. Swirl the container of cells very gently for mixing.

28 Put the cells in the CoolCell freezer box at −80 °C overnight for gradual freezing.

29 Transfer the cryovials with cells to a liquid nitrogen tank or deep freezer the next day for long-term storage.
■ **PAUSE POINT** 3T3-J2 cells can be stored indefinitely at −80 °C.
? TROUBLESHOOTING

Table 3 | The seeding density of 3T3-J2 cells and gISCs in different tissue culture dishes

Plates	6-well	12-well	24-well	48-well	96-well	100 × 20 mm	60 × 15 mm	24-Transwellwell plate
Surface area (cm^2)	9.6	3.8	2	1.1	0.32	58.95	19.5	0.3
No. of feeder cells	1.5M–1.8M	600k–720k	300k–400k	120k–150k	50k–60k	9M–11M	3M–3.6M	300k–400k
No. of ISCs	50k–100k	15k–30k	8k–15k	5k–7k	1k–3k	0.4M–0.6M	0.1M–0.6M	250k–300k

k, thousand; M, million.

Preparing feeders for ISCs ● Timing 2 d

30 Thaw growth-factor-reduced Matrigel on ice and dilute in cold 3T3-J2 growth medium at a concentration of 25%.
▲ CRITICAL STEP Be sure to use pre-cooled tips to add Matrigel to the cold growth medium in order to prevent the solidification of the Matrigel during this process.

31 Precool the tissue culture plates at −20 °C for 15 min.

32 Add diluted Matrigel to the cold plate, swirl the plate to evenly distribute the diluted Matrigel and pipette out the extra Matrigel.

33 Place the plates in a 37 °C incubator for 30 min to allow the Matrigel layer to solidify.

34 Seed irradiated 3T3-J2 cells in the presence of 3T3-J2 culture medium and shake the plates with cells in a 37 °C incubator to evenly distribute the cells (see Table 3 for recommended cell numbers). We recommend using these 3T3-J2-seeded plates 24 h after seeding and within 72 h of seeding.

35 Change the 3T3-J2 medium each day after seeding.

gISC derivation from a 1-mm-diameter biopsy sample ● Timing 11 d

36 Wash the human intestinal biopsy sample (transferred from the hospital in cold wash buffer on ice) with 5 ml of cold wash buffer in a 15-ml Falcon tube, centrifuge at 300*g* for 7 min at 4 °C, and then remove the medium carefully without disturbing the biopsy sample. Repeat the washing procedure three times.
▲ CRITICAL STEP Washing the biopsy sample thoroughly can help to avoid potential contamination. However, it is critical not to lose the biopsy sample during washing steps, so pay particular attention to the step of aspirating the medium.

37 Pipette the biopsy sample into a tissue culture Petri dish and mince the tissue between two Feather scalpels. Mince until the tissue resembles a paste.
▲ CRITICAL STEP This mincing step is imperative and will determine cloning efficiency.

38 Digest tissue in digestion buffer (1.5 ml of digestion buffer per biopsy sample) for ~30 min on a 37 °C rocker set to 100 r.p.m. Every 10 min, pipette the mixture up and down to break up any aggregated clumps.
▲ CRITICAL STEP At the end of digestion, you should not observe any undigested pieces. Any remaining, undigested tissue fragments can be removed by passing the minced tissue through a 100-μm Nylon mesh strainer.

39 At the end of digestion, add 10 ml of cold wash buffer to each tube containing digested tissue. Mix the contents by inverting the tubes ten times.

40 Centrifuge the digested tissue at 300*g* for 7 min at 4 °C, remove the wash buffer carefully and repeat the washing step five times.
▲ CRITICAL STEP The pellet of the biopsy sample is very small, so the wash buffer should be saved and rechecked prior to discarding.

41 After the last wash with wash buffer, spin down the digested biopsy sample at 300*g* for 7 min at 4 °C and wash one more time with 10 ml of cold StemECHO neutralization medium.
▲ CRITICAL STEP Do not skip this step. It is critical to removing all residual wash buffer.

42 Following centrifugation at 300*g* for 7 min at 4 °C, resuspend the pellet in 1 ml of gISC growth medium completely by pipetting up and down ten times.

43 Seed the suspension of each biopsy sample in one well of a 24-well tissue culture dish pre-coated with 20% growth-factor reduced Matrigel and irradiated 3T2 J2 feeder cells (from Step 35). Return the plates to incubator.
? TROUBLESHOOTING

44 Change the gISC growth medium every 2 d.

45 When the ISC colonies are visible (in about 1 week), wash the culture with DPBS^{-} twice, add 500 µl of TrypLE, and incubate the cells with TrypLE in the incubator at 37 °C for 15 min.
? TROUBLESHOOTING

46 Pipette the cells gently up and down five times to dissociate them into single cells. If the cells still look clumpy under a microscope, put the plate back into the incubator for another 15 min.

47 Add 5 ml of warmed StemECHO neutralization medium *quickly* to the well-trypsinized cells and pipette up and down ten times.
▲ **CRITICAL STEP** Do not add neutralization medium dropwise because it will lead to the re-aggregation of stem cells.

48 Centrifuge the cells at 300*g* for 7 min at 4 °C, and completely resuspend the pellet in 1 ml of gISC growth medium by pipetting up and down ten times. Pass the cell solution through a 40-µm cell strainer and seed as single cells into one well of a 24 well plate pre-coated with growth factor-reduced Matrigel and irradiated 3T3-J2 feeder cells (from Step 35).
▲ **CRITICAL STEP** We always recommend freezing half of the stem cells at this step (as described in Step 50).

49 Change the medium every 2 d. Three days later, individual ISC clones should be observable. In about 10 d, the stem cell culture should be ready for the next step (passaging, freezing, or generation of single cell–derived pedigrees).

Downstream assays

50 Follow option A to freeze cells, option B to establish a gISC pedigree, and option C to differentiate cells at an ALI.

(A) **Freezing of ISC clones** ● **Timing 4 h**

(i) Trypsinize ISC clones as described in Steps 45–47 and count the cells using a hemocytometer. We recommend freezing 100,000 cells per vial in 500 µl of freezing medium, which will be sufficient for recovery in 1 well of a 6-well plate.
▲ **CRITICAL STEP** It is critical to count the ISCs and record the cell number on the freezing vial. Seeding too few or too many cells after thawing will negatively affect the quality of stem cell culture.

(B) **Establishment of a gISC pedigree** ● **Timing 14 d**

(i) When the ISC culture reaches ~60% confluency (<100 cells in each colony), trypsinize the ISC clones by following Steps 45–47.

(ii) Gently pipette up and down to achieve a single-cell suspension and pass the cells through a 30-µm cell strainer.

(iii) Remove mouse feeder cells using a QuadroMACS Starting Kit (LS) according to the manufacturer's instructions. Briefly, cells are trypsinized to a single-cell suspension, incubated with antibody-coated microbeads for 15 min at 4 °C, and then run through an LS column to collect the stem cell–containing flow-through.

(iv) Use a cell sorter to sort single cells into individual wells of a 96-well plate previously coated with 30% growth factor-reduced Matrigel and seeded with the feeder cells.

(v) Monitor the cells daily. It generally takes ~5 d to observe colony formation in the 96-well plates.

(vi) In ~7–10 d, before the colonies become confluent and within the 2-week period of optimal 3T3-J2 lawn integrity, wash the culture with DPBS^{-} twice, add 30 µl of TrypLE, and incubate the cells with TrypLE in the incubator at 37 °C for 15 min.
▲ **CRITICAL STEP** Do not add >30 µl of TrypLE.

(vii) Gently pipette the cells up and down ten times to dissociate them into single cells. If the cells still look microscopically clumpy, put the plate back into the incubator for another 15 min.

(viii) Add 100 µl of warmed gISC growth medium quickly to the well-trypsinized cells and pipette up and down ten times.
▲ **CRITICAL STEP** Pipette carefully to avoid cross-contamination.

(ix) Transfer the resuspended cells to 1 well of a 24-well plate that has been coated with Matrigel and seeded with feeder cells.
▲ **CRITICAL STEP** Make sure the colony is trypsinized to single cells before reseeding.

(x) Expand these single cell–derived ISCs to billions of cells within a few weeks.
▲ **CRITICAL STEP** Freeze early-passage ISCs as described in Step 50(A).
? TROUBLESHOOTING

(C) **Differentiating gISCs in ALI culture** ● Timing **10 d**

(i) Prepare the Transwell inserts in a 24-well plate by coating the inserts with 30 µl of 30% growth-factor-reduced Matrigel. Gently shake the plate to make sure that the Matrigel solution evenly covers the surface of the inserts. Remove excess Matrigel solution, and incubate the plate at 37 °C for 30 min.

(ii) Add 700 µl of 3T3-J2 growth medium to each well of the 24-well plate, and then place the Matrigel-coated inserts into the wells.

(iii) Prepare 200,000 irradiated 3T3-J2 cells in 200 µl of growth medium (from Step 29) and seed onto each insert.

(iv) Incubate the plate at 37 °C overnight in the incubator.

(v) The next day, aspirate the gISC growth medium from the ISC plate and rinse with $DPBS^{-}$ thoroughly.

(vi) Trypsinize with TrypLE Express enzyme (1×) for 10–20 min.

(vii) Gently pipette up and down to achieve a single-cell suspension. Add StemECHO neutralization medium to neutralize the trypsin and pass the cells through a 30-µm cell strainer.

(viii) Remove the mouse feeder cells using a QuadroMACS Starting Kit, as described in Step 50B(iii).

(ix) Determine the cell number as described in Step 18.

(x) To start an ALI culture, remove the medium from a Transwell plate and change to gISC growth medium.

(xi) Prepare 200,000–300,000 ISCs in 200 µl of gISC growth medium and seed each insert.

(xii) Incubate Transwell inserts in a 37 °C incubator.

(xiii) Change the gISC growth medium every day.

(xiv) In 3–4 d, the ISCs in the insert should reach confluency. Remove the gISC growth medium from the inserts by careful pipetting to create ALI culture. Change the medium in the Transwell plate to StemECHO differentiation medium and incubate in a 37 °C incubator.

(xv) Change the medium every day and continue the cultures for an additional 10–12 d to induce differentiation.

? TROUBLESHOOTING

Troubleshooting

Troubleshooting advice can be found in Table 4.

Table 4 | Troubleshooting table

Step	Problem	Possible reason	Solution
9, 20, 21	3T3-J2 cells lose contact inhibition	Cells might spontaneously transform	Contact inhibition is a unique feature of 3T3-J2 cells and it is an essential characteristic indicating the suitability of these cells as feeders for adult stem cells. 3T3-J2 cells that have lost this feature should not be used any longer. Start from a new vial of early-passage 3T3-J2 cells
29	Significant rise in the saturation density of 3T3-J2 cells	Continuous passaging of 3T3-J2 cells from over-confluent flasks	It is normal to notice a slight rise in the saturation density of the flask as you increase passage number, but the maximum number of cells you should get from a just-confluent 15-cm plate^2 is ~8×10^6 to 10×10^6. If you are getting on the order of 15×10^6 to 20×10^6 cells, then your feeders are not being passaged properly. This can affect the quality of your ISC cultures Therefore, immediately switch to a new vial of 3T3-J2 cells These guidelines should be strictly adhered to
43	Poor feeder cell condition	Feeder cell death after irradiation	Shake the tube containing irradiated 3T3-J2 cells regularly and gently so that cells do not become concentrated at the bottom of the tube while adding cells to the freezing vials
		Inaccurate cell counting	Use one vial of freshly irradiated cells to check the cell condition and density each time after irradiation
		Insufficient Matrigel coating	Use fresh Matrigel and be sure to coat for >30 min
45, 50B	gISCs lose clonogenicity	Cells differentiate	You should not observe a decline of clonogenicity during long-term culture. Loss of clonogenicity indicates a loss of stemness of the culture. If this occurs, you then should start a new culture from early-passage ISCs
50C	Leakage in the ALI	gISCs are not in optimal condition before seeding or the structure was damaged during medium changes	Five days following removal of the medium from the insert, you should observe intestine-like structures. If leakage is observed, you need to restart the experiment

Timing

Steps 1–9, reviving 3T3-J2 cells from frozen stock: 3 d
Steps 10–21, passaging 3T3-J2 cells for expansion: variable
Steps 22–29, irradiating and freezing irradiated 3T3-J2 cells: 1 d
Steps 30–35, preparing feeders for ISCs: 2 d
Steps 36–49, deriving ISCs from a 1-mm-diameter biopsy sample: 11 d
Step 50A, freezing of ISC clones: 4 h
Step 50B, establishment of a single cell–derived pedigree: 14 d
Step 50C, inducing gISCs to differentiate in an ALI culture: 10 d

Anticipated results

Herein, we provide a protocol that details how to derive and expand cells from standard human endoscopic biopsy samples. This 2D culture system enables the generation of libraries of 100–300 independent gISC clones from clinically standard, 1-mm-diameter biopsy samples of human intestinal mucosa. We anticipate that this culture medium system will support the expansion of gISC clones in a highly undifferentiated and clonogenic state to practically unlimited numbers in vitro and specifically 1 billion cells in ~60 d (Fig. 2). Importantly, the gISC culture medium system described here confers a host of advantages over either induced pluripotent stem cells or the organoid approach, both of which yield relatively few stem cells among many differentiated cells. Moreover, these single cell–derived clones can be induced to differentiate into mucosa-like structures, including all appropriate cell lineages, such as enterocytes, goblet cells, enteroendocrine cells and Paneth cells (Fig. 1). The high clonogenicity of gISCs confers a uniquely high rate of 'expandability' for experimental manipulation, regenerative medicine, and drug discovery. Taken together, this is a remarkably simple culture system for generating unlimited numbers of genetically stable and regionally committed gISCs from any patient for analysis via multiple technologies.

Reporting Summary

Further information on research design is available in the Nature Research Reporting Summary linked to this article.

Data availability

The corresponding authors will provide all data presented in the article and address technical questions upon reasonable request.

References

1. Karagiannis, P. et al. Induced pluripotent stem cells and their use in human models of disease and development. *Physiol. Rev.* **99**, 79–114 (2019).
2. Müller, A. M. & Dzierzak, E. A. ES cells have only a limited lymphopoietic potential after adoptive transfer into mouse recipients. *Development* **118**, 1343–1351 (1993).
3. Helgason, C. D., Sauvageau, G., Lawrence, H. J., Largman, C. & Humphries, R. K. Overexpression of HOXB4 enhances the hematopoietic potential of embryonic stem cells differentiated in vitro. *Blood* **87**, 2740–2749 (1996).
4. Amabile, G. et al. In vivo generation of transplantable human hematopoietic cells from induced pluripotent stem cells. *Blood* **121**, 1255–1264 (2013).
5. Suzuki, N. et al. Generation of engraftable hematopoietic stem cells from induced pluripotent stem cells by way of teratoma formation. *Mol. Ther.* **21**, 1424–1431 (2013).
6. Green, H. The birth of therapy with cultured cells. *BioEssays* **30**, 897–903 (2008).
7. Senoo, M., Pinto, F., Crum, C. P. & McKeon, F. p63 is essential for the proliferative potential of stem cells in stratified epithelia. *Cell* **129**, 523–536 (2007).
8. Rama, P. et al. Limbal stem-cell therapy and long-term corneal regeneration. *N. Engl. J. Med.* **363**, 147–155 (2010).
9. Kumar, P. A. et al. Distal airway stem cells yield alveoli in vitro and during lung regeneration following H1N1 influenza infection. *Cell* **147**, 525–538 (2011).
10. Hirsch, T. et al. Regeneration of the entire human epidermis using transgenic stem cells. *Nature* **551**, 327–332 (2017).
11. Wang, X. et al. Cloning and variation of ground state intestinal stem cells. *Nature* **522**, 173–178 (2015).
12. Yamamoto, Y. et al. Mutational spectrum of Barrett's stem cells suggests paths to initiation of a precancerous lesion. *Nat. Commun.* **7**, 10380 (2016).

13. Duleba, M. *et al.* An efficient method for cloning gastrointestinal stem cells from patients via endoscopic biopsies. *Gastroenterology* **156**, 20–23 (2018).
14. Rheinwald, J. G. & Green, H. Serial cultivation of strains of human epidermal keratinocytes: the formation of keratinizing colonies from single cells. *Cell* **6**, 331–343 (1975).
15. Rheinwald, J. G. & Green, H. Formation of a keratinizing epithelium in culture by a cloned cell line derived from a teratoma. *Cell* **6**, 317–330 (1975).
16. Barrandon, Y. & Green, H. Cell migration is essential for sustained growth of keratinocyte colonies: the roles of transforming growth factor-α and epidermal growth factor. *Cell* **50**, 1131–1137 (1987).
17. Barrandon, Y. & Green, H. Cell size as a determinant of the clone-forming ability of human keratinocytes. *Proc. Natl Acad. Sci. USA* **82**, 5390–5394 (1985).
18. Xian, W., Duleba, M., Yamamoto, Y., Vincent, M. & McKeon, F. Biobanking organoids or ground-state stem cells? *J. Clin. Med.* **7**, 555 (2018).
19. Yin, X. et al. Niche-independent high-purity cultures of Lgr5+ intestinal stem cells and their progeny. *Nat. Methods* **11**, 106–112 (2014).
20. Hong, S. N., Dunn, J. C. Y., Stelzner, M. & Martín, M. G. Concise review: the potential use of intestinal stem cells to treat patients with intestinal failure. *Stem Cells Transl. Med.* **6**, 666–676 (2017).
21. Fukuda, M. et al. Small intestinal stem cell identity is maintained with functional Paneth cells in heterotopically grafted epithelium onto the colon. *Genes Dev.* **28**, 1752–1757 (2014).
22. Simian, M. & Bissell, M. J. Organoids: a historical perspective of thinking in three dimensions. *J. Cell Biol* **216**, 31–40 (2017).
23. Sato, T. et al. Single Lgr5 stem cells build crypt-villus structures in vitro without a mesenchymal niche. *Nature* **459**, 262–265 (2009).
24. Wang, F. et al. Isolation and characterization of intestinal stem cells based on surface marker combinations and colony-formation assay. *Gastroenterology* **145**, 383–395.e21 (2013).
25. Todaro, G. J. & Green, H. Quantitative studies of the growth of mouse embryo cells in culture and their development into established lines. *J. Cell Biol.* **17**, 299–313 (1963).

Acknowledgements

This work was supported by grants from the Cancer Prevention Research Institute of Texas (CPRIT; RR15014 to W.X. and RR15088 to F.M.), the National Institutes of Health (1R01DK115445-01A1 to W.X.; U24CA228550 and 1R01CA241600-01 to F.M.), the US Dept. of Defense (W81XWH-17-1-0123 to W.X.; W81XWH-19-1-0127 to C.P.C.), the Singapore National Medical Research Council (to K.Y.H. and F.M.), a University of Texas Presidential Award (to W.X.) and an American Gastroenterology Association Research and Development Pilot Award in Technology (to W.X.). W.X. and F.M. are CPRIT Scholars for Cancer Research. We thank all the members of the Xian–McKeon laboratory for helpful discussions and support. We thank H. Green and J. Rosen for advice and support. We thank H. Green for the generous gift of the 3T3-J2 fibroblast cell line.

Author contributions

W.X., Y.Y., M.D. and F.M. wrote the manuscript with input from all other authors. J.A.A., K.Y.H., J.K.H., J.S.H., F.A.S. and C.P.C. provided biopsy material; M.D., Y.Y., Y.Z. and R.N. cloned gISCs; J.X., S.W. and R.M. performed informatics analyses; A-A.L., Y.Q. and K.G. performed xenografts and ALI cultures; W.R. and R.N. performed the FACS analyses; and all authors collaborated on the concepts of this work.

Competing interests

W.X., F.M., M.D. and M.V. have filed patents related to the technology used in the present work. W.X., M.V. and F.M. have financial interests in Tract Pharmaceuticals, Inc.

Additional information

Supplementary information is available for this paper at https://doi.org/10.1038/s41596-020-0298-4.

Correspondence and requests for materials should be addressed to F.MK. or W.X.

Reprints and permissions information is available at www.nature.com/reprints.

Publisher's note Springer Nature remains neutral with regard to jurisdictional claims in published maps and institutional affiliations.

Received: 30 September 2019; Accepted: 16 January 2020;
Published online: 01 April 2020

Related links
Key references using this protocol
Wang, X. et al. *Nature* **522**, 173–178 (2015): https://doi.org/10.1038/nature14484
Duleba, M. et al. *Gastroenterology* **156**, 20–23 (2019): https://doi.org/10.1053/j.gastro.2018.08.062
Yamamoto, Y. et al. *Nat. Commun.* **7**, 10380 (2016): https://doi.org/10.1038/ncomms10380

nature research

Corresponding author(s): Karen Duff, Hongjun Fu, Michele Vendruscolo

Reporting Summary

Nature Research wishes to improve the reproducibility of the work that we publish. This form provides structure for consistency and transparency in reporting. For further information on Nature Research policies, see Authors & Referees and the Editorial Policy Checklist.

Statistical parameters

When statistical analyses are reported, confirm that the following items are present in the relevant location (e.g. figure legend, table legend, main text, or Methods section).

n/a	Confirmed	
☐	☒	The exact sample size (*n*) for each experimental group/condition, given as a discrete number and unit of measurement
☐	☒	An indication of whether measurements were taken from distinct samples or whether the same sample was measured repeatedly
☐	☒	The statistical test(s) used AND whether they are one- or two-sided *Only common tests should be described solely by name; describe more complex techniques in the Methods section.*
☐	☒	A description of all covariates tested
☐	☒	A description of any assumptions or corrections, such as tests of normality and adjustment for multiple comparisons
☐	☒	A full description of the statistics including central tendency (e.g. means) or other basic estimates (e.g. regression coefficient) AND variation (e.g. standard deviation) or associated estimates of uncertainty (e.g. confidence intervals)
☐	☒	For null hypothesis testing, the test statistic (e.g. *F*, *t*, *r*) with confidence intervals, effect sizes, degrees of freedom and *P* value noted *Give P values as exact values whenever suitable.*
☒	☐	For Bayesian analysis, information on the choice of priors and Markov chain Monte Carlo settings
☒	☐	For hierarchical and complex designs, identification of the appropriate level for tests and full reporting of outcomes
☐	☒	Estimates of effect sizes (e.g. Cohen's *d*, Pearson's *r*), indicating how they were calculated
☐	☒	Clearly defined error bars *State explicitly what error bars represent (e.g. SD, SE, CI)*

Our web collection on statistics for biologists may be useful.

Software and code

Policy information about availability of computer code

Data collection	No software was used.
Data analysis	Excel, ImageJ, ZEN 2 (blue edition), Python2.7 and Graphpad Prism 5.0 softwares were used.

For manuscripts utilizing custom algorithms or software that are central to the research but not yet described in published literature, software must be made available to editors/reviewers upon request. We strongly encourage code deposition in a community repository (e.g. GitHub). See the Nature Research guidelines for submitting code & software for further information.

Data

Policy information about availability of data

All manuscripts must include a data availability statement. This statement should provide the following information, where applicable:

- Accession codes, unique identifiers, or web links for publicly available datasets
- A list of figures that have associated raw data
- A description of any restrictions on data availability

All the datasets we used are publicly available datasets generated by other groups with accession codes indicated in the paper. All the raw data associated with all the figures and supplementary figures are available upon request. There is no restrictions on data availability.

Field-specific reporting

Please select the best fit for your research. If you are not sure, read the appropriate sections before making your selection.

☒ Life sciences ☐ Behavioural & social sciences ☐ Ecological, evolutionary & environmental sciences

For a reference copy of the document with all sections, see nature.com/authors/policies/ReportingSummary-flat.pdf

Life sciences study design

All studies must disclose on these points even when the disclosure is negative.

Sample size	Sample size was reported in the 'Statistical analysis' section of the Methods and figure legends. The sample size for quantifying the number of neurons and single-mRNA molecules was based on previous publications for biological experiments as well as the property of our data, i.e. clear separation between excitatory neurons and inhibitory neurons. For single-nucleu RNA-seq datasets, there are 3227 single nuclei and 19,550 single nuclei in each dataset, which are enough based on previous single-nucleus RNA-seq analysis.
Data exclusions	In order to avoid biases in the analysis and reduce the amount of noise, the bottom 5% low quality samples (samples with less reads across the transcriptome) in DroNc-Seq dataset were discarded as they were considered to have been damaged during the experimental procedure.
Replication	In order to ensure our experimental findings can be reliably reproduced, we include appropriate number of animals, sections, and neurons as listed in the figure legends. Further, three independent experiments were repeated with similar results. Also, the staining has been repeated by three persons in the lab independently. In order to ensure our experimental findings can be reliably reproduced, we include appropriate number of animals, sections, and neurons as listed in the figure legends. Further, three independent experiments were repeated with similar results. Also, the staining has been repeated by three persons in the lab independently.
Randomization	The experimental groups were allocated by the animal genotype, human case information, and the treatment. The covariants of age, gender, culture days, and vehicle were controlled as the same between experimental groups. Further, the sections, coverslips and neurons within each group were selected randomly. 10 images per sm-FISH stained section was randomly taken from the superficial layers of the entorhinal cortex or BA9 region. 60 excitatory and 60 inhibitory neurons from 3 human non-AD and AD sections were randomly selected for comparing the mean intensity of BAG3. Also, 5 excitatory and 5 inhibitory neurons from each coverslip (n = 11 coverslips each group) were randomly taken for comparing the endogenous 12E8 tau+ punta in neurites. Additionally, 20 images per coverslip at 1,024 × 1,024 resolution were taken randomly from all the orientations of the coverslip for the tau seeding experiment. The number of TBR1+ EX and GAD1+ IN neurons with tau inclusions were quantified blindly.
Blinding	The experimenter was blind to the experimental groups when they performed the immunostaining and sm-FISH as well as the counting of neurons and the single-mRNA molecules, and the comparison of the mean intensity of BAG3.

Reporting for specific materials, systems and methods

Materials & experimental systems

n/a	Involved in the study
☐	☒ Unique biological materials
☐	☒ Antibodies
☒	☐ Eukaryotic cell lines
☒	☐ Palaeontology
☐	☒ Animals and other organisms
☒	☐ Human research participants

Methods

n/a	Involved in the study
☒	☐ ChIP-seq
☒	☐ Flow cytometry
☒	☐ MRI-based neuroimaging

Unique biological materials

Policy information about availability of materials

Obtaining unique materials	The Tau RD-P301S-YFP lentivirus and DS9 clone cell lines were provided by Dr. Marc Diamond. The BAG3 shRNA and the shRNA-resistant BAG3 were provided by Dr. Gail Johnson. All the brain tissue were provided by New York Brain Bank and Banner Sun Health Research Institute Brain and Body Donation Program.

Antibodies

Antibodies used

Human conformation-dependent tau (MC1, 1:750) and human/murine phospho-tau pSer396/ Ser404 (PHF1, 1:500) monoclonal antibodies were provided by Dr. Peter Davies. Mouse anti-phosphorylated tau Ser262 and/or Ser356 (12E8, 1:2000) antibody is a kind gift from Dr. Philip Dolan. Human/murine phospho-tau pSer202/Thr205 (AT8, Cat# MN1020, 1:500) and pThr212/Ser214 (AT100, Cat# MN1060, 1:500) monoclonal antibodies, rabbit anti-phospho-tau pSer422 (pS422, Cat# 44-764G, 1:250) and parvalbumin (PVALB, Cat# PA5-18389, 1:1000) polyclonal antibodies, Alexa Fluor dye-labeled cross-absorbed goat and donkey secondary antibodies (Cat# A-11029, A-11037, A-11007, A-11058, and A-21202, 1:1000) were purchased from Thermo Fisher Scientific. Rabbit anti-TBR1 (Cat# ab31940, 1:250) and SATB2 (Cat# ab92446, 1:250) polyclonal antibodies were purchased from Abcam. Rat anti-somatostatin (SST) (Cat# MAB354, 1:100) and mouse anti-NeuN (Cat# MAB377, 1:250) monoclonal antibody and goat anti-GAD1 (Cat# AF2086, 1:100) polyclonal antibody were purchased from Millipore and R&D Systems, respectively. Rabbit anti-calretinin (CALB2) (Cat# 7697, 1:1000), IBA-1 (Cat# 019-19741, 1:500), and GFAP (Cat# G9269, 1:2500) polyclonal antibodies were purchased from Swant, Wako and Sigma-Aldrich, respectively. Rabbit anti-TBR1 (Cat# 20932-1-AP, 1:250) and rabbit anti-BAG3 (Cat# 10599-1-AP, 1:100) polyclonal antibody were purchased from Proteintech Group.

Validation

All of them have been used in previous publications and validated by the manufacturers or research scientists.
MC1: validated in Neurobiol Aging. 2000 Sep-Oct;21(5):719-27; https://www.alzforum.org/antibodies/tau-mc1
PHF1: validated in https://www.alzforum.org/antibodies/tau-phos-ser396ser404-phf-1
12E8: validated in https://www.alzforum.org/antibodies/tau-12e8
AT8: validated in https://www.thermofisher.com/antibody/product/Phospho-Tau-Ser202-Thr205-Antibody-clone-AT8-Monoclonal/MN1020
AT100: validated in https://www.thermofisher.com/antibody/product/Phospho-Tau-Thr212-Ser214-Antibody-clone-AT100-Monoclonal/MN1060
pS422: validated in https://www.thermofisher.com/antibody/product/Phospho-Tau-Ser422-Antibody-Polyclonal/44-764G
PVALB: validated in https://www.thermofisher.com/antibody/product/Parvalbumin-Antibody-Polyclonal/PA5-18389
TBR1: validated in http://www.ptglab.com/Products/TBR1-Antibody-20932-1-AP.htm#validation
SATB2: validated in https://www.abcam.com/satb2-antibody-epncir130a-ab92446.html
SST: validated in http://www.emdmillipore.com/US/en/product/Anti-Somatostatin-Antibody-clone-YC7,MM_NF-MAB354#overview
NeuN: validated in http://www.emdmillipore.com/US/en/product/Anti-NeuN-Antibody-clone-A60,MM_NF-MAB377
GAD1: validated in https://www.rndsystems.com/products/human-mouse-rat-gad1-gad67-antibody_af2086
calretinin : validated in https://www.swant.com/?p=products&c=1.2
IBA-1: validated in http://www.wako-chem.co.jp/english/labchem/product/life/Antilba1/index.htm
GFAP: validated in https://www.sigmaaldrich.com/catalog/product/sigma/g9269?lang=en&region=US
BAG3: validated in https://www.ptglab.com/products/BAG3-Antibody-10599-1-AP.htm#validation

Animals and other organisms

Policy information about studies involving animals; ARRIVE guidelines recommended for reporting animal research

Laboratory animals

The species, strain, sex and age of the laboratory animals used in this study have been clearly written in the paper. The F1 mouse offspring (both males and females at 22 and 30+ months old, strain FVB/N:C57BL/6) were used as experimental animals. All animals were maintained on a 12 hr light/dark cycle with food and water provided ad libitum. All animal experiments were performed in accordance with national guidelines (National Institutes of Health) and approved by the Institutional Animal Care and Use Committee of Columbia University. Primary cortical neuron culture were prepared from and embryonic day 16-18 embryos from C57BL/6 mice.

Wild animals

This study does not include wild animals.

Field-collected samples

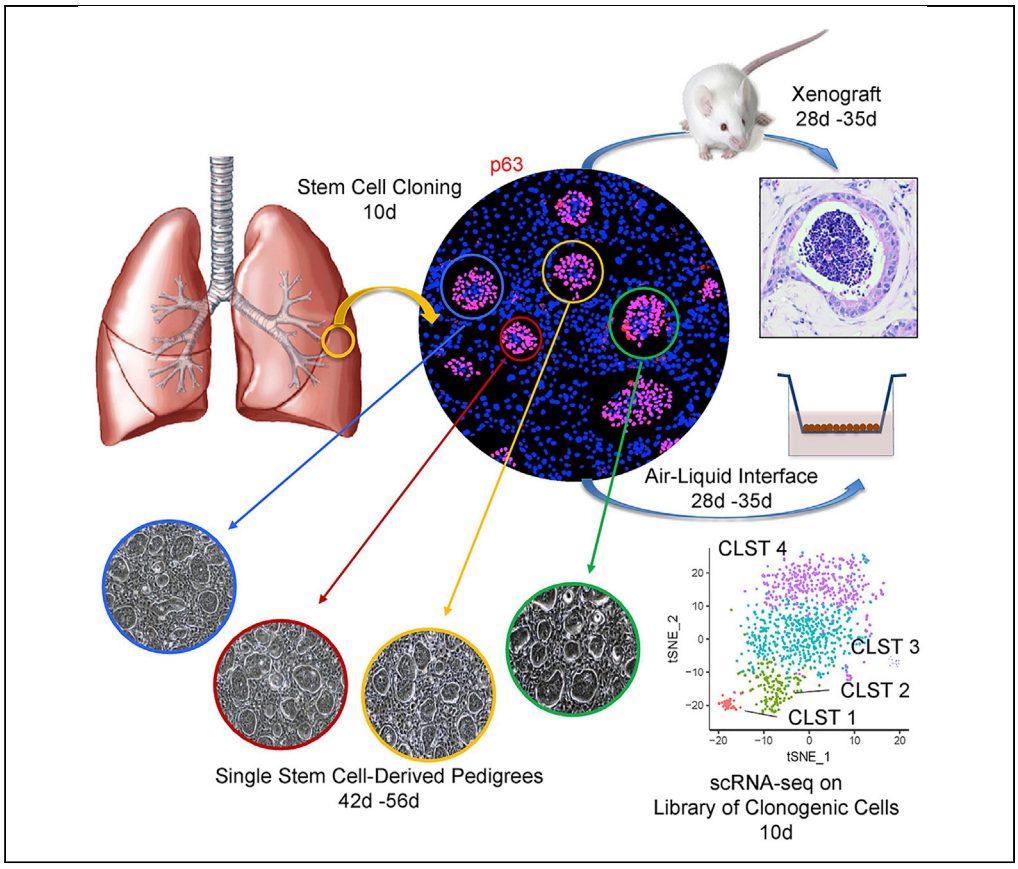
This study does not include the samples collected from the field.

STAR Protocols

CellPress
OPEN ACCESS

Protocol

Protocol for Cloning Epithelial Stem Cell Variants from Human Lung



The plurality of clonogenic cells derived from human lung includes a spectrum of diverse p63+ stem cells responsible for the regeneration of normal epithelial tissue and disease-associated metaplastic lesions. Here, we detail protocols for the cloning, expansion, and characterization of these stem cell variants, which in general assist in analyses of lung stem cell heterogeneity, genome editing, drug screening, and regenerative medicine.

Wei Rao, Suchan Niroula, Shan Wang, Matthew Vincent, Frank McKeon, Wa Xian

fdmckeon@uh.edu (F.M.)
wxian@uh.edu (W.X.)

HIGHLIGHTS

Protocol for generating libraries of p63+ clonogenic epithelial cells from lung

Normal lung dominated by type 1 clone, COPD lung by type 2, 3, and 4 clones

Type 2, 3, and 4 clones committed to discrete and pathogenic metaplasia

Protocol enables insights into disease, drug discovery, and regenerative medicine

Rao et al., STAR Protocols 1, 100063
September 18, 2020 © 2020 The Author(s).
https://doi.org/10.1016/j.xpro.2020.100063

Please cite this article in press as: Rao et al., Protocol for Cloning Epithelial Stem Cell Variants from Human Lung, STAR Protocols (2020), https://doi.org/10.1016/j.xpro.2020.100063

STAR Protocols

CellPress
OPEN ACCESS

Protocol

Protocol for Cloning Epithelial Stem Cell Variants from Human Lung

Wei Rao,[1,3] Suchan Niroula,[1] Shan Wang,[1] Matthew Vincent,[2] Frank McKeon,[1,*] and Wa Xian[1,4,*]

[1]Stem Cell Center, Department of Biology and Biochemistry, University of Houston, Houston, TX 77204, USA

[2]Nüwa Medical Systems, Inc., Houston, TX 77479, USA

[3]Technical Contact

[4]Lead Contact

*Correspondence: fdmckeon@uh.edu (F.M.), wxian@uh.edu (W.X.)
https://doi.org/10.1016/j.xpro.2020.100063

SUMMARY

The plurality of clonogenic cells derived from human lung includes a spectrum of diverse p63+ stem cells responsible for the regeneration of normal epithelial tissue and disease-associated metaplastic lesions. Here, we report protocols for the cloning, expansion, and characterization of these stem cell variants, which in general assist in analyses of stem cell heterogeneity, genome editing, drug screening, and regenerative medicine.

For complete details on the use and execution of this protocol, please refer to Kumar et al. (2011), Zuo et al. (2015), and Rao et al. (2020).

BEFORE YOU BEGIN

The epithelial tissue regeneration relies on the intrinsic ability of adult stem cells to self-renew and differentiate to various cell types appropriate for respective tissues. Several decades ago, Howard Green and colleagues pioneered adult stem cell-based regenerative medicine. They established a culture system dependent on Swiss 3T3-J2 murine fibroblast feeder cells for capturing p63+ epidermal stem cells and demonstrated these cells can be maintained in their most immature and clonogenic form *in vitro* and yield a stratified squamous epithelium upon engraftment (Rheinwald and Green, 1975; Green, 2008; Hirsch et al., 2017). We have leveraged the success of Green's system and established a new system that employs a custom media and 3T3-J2 feeder cells for the cloning and expansion of single stem cells from human lung.

⚠ CRITICAL: Human lung tissues must be obtained in compliance with institutional review board regulations and guidelines. All procedures used for handling human tissues should assume potential contamination of tissue with human pathogens (HBV, HCV, HIV, *C. difficile*, etc.).

General Laboratory Preparations

Timing: 60–90 min

1. Prepare media and solutions. Refer to "Materials and Equipment" for more details
2. Set water bath to 37°C
3. Warm media to 37°C

This is an open access article under the CC BY-NC-ND license (http://creativecommons.org/licenses/by-nc-nd/4.0/).

KEY RESOURCES TABLE

REAGENT or RESOURCE	SOURCE	IDENTIFIER
Antibodies		
Mouse monoclonal CC10 Dilution factor: 1:100	Santa Cruz	Cat# sc-130411; RRID: AB_2183388
Rabbit polyclonal SFTPC Dilution factor: 1:100	Santa Cruz	Cat# sc-13979; RRID: AB_2185502
Rabbit polyclonal MUC5AC Dilution factor: 1:100	Santa Cruz	Cat# sc-20118; RRID: AB_2146854
Rabbit polyclonal AQP4 Dilution factor: 1:200	Sigma-Aldrich	Cat# HPA014784; RRID: AB_1844967
Rabbit polyclonal SFTPB Dilution factor: 1:200	Atlas Antibodies	Cat# HPA034820; RRID: AB_2674347
Mouse monoclonal acetylated tubulin Dilution factor: 1:500	Sigma-Aldrich	Cat# T7451; RRID: AB_609894
Mouse monoclonal p63 Dilution factor: 1:200	Abcam	Cat# ab735; RRID: AB_305870
Biological Samples		
Human Lung samples	UCONN Health; UTHSC; UIHC	NA
Chemicals, Peptides, and Recombinant Proteins		
DMEM without L-glutamine, without sodium pyruvate	Invitrogen	Cat# 11960-044
F12	Life Technologies	Cat# 11765-054
HEPES	Life Technologies	Cat# 15630-080
Gentamycin	Life Technologies	Cat# 15710-064
Fungizone	Life Technologies	Cat# 15290018
Bovine Calf Serum (BCS)	HyClone	Cat# SH130072.03
Fetal Bovine Serum (FBS)	HyClone	Cat# SH30396.03
Penicillin-streptomycin	Invitrogen	Cat# 15140-122
L-glutamine	Invitrogen	Cat# 25030-081
0.05% Trypsin-EDTA	Invitrogen	Cat# 25300-062
DPBS, no calcium, no magnesium	Invitrogen	Cat# 14190-144
Dimethyl sulfoxide (DMSO)	Sigma-Aldrich	Cat# 41640
Feeder removal beads	Miltenyi Biotec	Cat#130-095-531
TrypLE™ Express Enzyme (1×), phenol red	Thermo Fisher	Cat#12605036
Trypan blue solution	Corning	Cat# 25-900-CI
Corning™ Matrigel™ GFR Membrane Matrix	Fisher Scienitific	Cat# CB-40230
Collagenase Type IV	Life Technologies	Cat# 17104-019
StemECHO100	Nüwa Medical Systems, Inc.	http://www.stemecho.com
StemECHO™PU Expansion medium	Nüwa Medical Systems, Inc.	http://www.stemecho.com
PneumaCult-ALI Medium	STEMCELL Technologies	Cat# 05001

(*Continued on next page*)

Continued

REAGENT or RESOURCE	SOURCE	IDENTIFIER
Experimental Models: Cell Lines		
3T3-J2	Kerafast	Cat# EF3003
Experimental Models: Organisms/Strains		
Mouse: NOD.Cg-*Prkdc*^{scid} *Il2rg*^{tm1Wjl}/SzJ	The Jackson Laboratory	Stock No:005557 | NSG
Software and Algorithms		
SH800S Cell Sorter Software version 2.1	SH800S Cell Sorter	https://www.sonybiotechnology.com/us/instruments/sh800s-cell-sorter/software/
Other		
Inverted microscope	Nikon	Eclipse Ts2
CO_2 incubator	Panasonic	Cat# KM-CC17RU2
Tissue culture biological safety cabinet	NuAire LabGard ES	Cat# NU-437
Student Dumont no. 5 forceps	Interfocus	Cat# 91150-20
Fine scissors straight large loops 10 cm	Interfocus	Cat# 14040-10
Pasteur pipettes	Scientific Laboratory Supplies	Cat# PIP4172
Sterile disposable scalpels	Dynarex	Cat# 4122
6 Well Falcon™ Polystyrene Microplates	Fisher Scientific	Cat# 08-772-1B
12 Well Falcon™ Polystyrene Microplates	Fisher Scientific	Cat# 08-772-29
24 Well Falcon™ Polystyrene Microplates	Fisher Scientific	Cat# 08-772-1
Nunc™ 384-Well, Nunclon Delta-Treated, Flat-Bottom Microplate	Fisher Scientific	Cat# 12-565-342
Nalgene™ Rapid-Flow™ Sterile Disposable Filter Units with PES Membrane	Fisher Scientific	Cat# 09-741-03
Steriflip 50 mL filtration units	Millipore	Cat# C3238
100 µm cell strainer	Falcon	Cat# 08-771-19
Pre-separation filters (30 µm)	Miltenyi Biotec	Cat# 130-041-407
QuadroMACS Starting Kit (LS)	Miltenyi Biotec	Cat# 130-091-051
Transwell with 0.4um pore polyester membrane insert	Fisher Scientific	Cat# 07-200-154
Cell Sorter	Sony	Cat# SH800S
X-ray irradiation machine	RadSource	Cat# RS1800
Mini shaking incubator	WISBiomed	Cat# BS-ICH1
Centrifuge	Eppendorf	Cat# 5810 R
Hemocytometer	Daigger	Cat# EF16034F
Cool Cell Freezing Container	Corning	Cat# 432008
-80°C freezer	VWR	Cat# 76307-942
Liquid nitrogen tank	VWR	Cat# 10027-532

MATERIALS AND EQUIPMENT

Preparation of Media and Buffers

⚠ CRITICAL: The preparation needs to be performed in a Class II biological hood with standard aseptic technique.

Murine 3T3-J2 Embryonic Fibroblast Culture Medium

Reagent	Amount	Final Concentration
DMEM	440 mL	n/a
BCS	50 mL	10%
Penicillin-streptomycin	5 mL	1%
L-glutamine	5 mL	1%

Filter the medium with a 0.22 μm filter. The culture medium can be stored at 4°C for up to 1 month.

3T3-J2 Freezing Medium

Reagent	Amount	Final Concentration
DMEM	700 mL	n/a
BCS	200 mL	20%
DMSO	100 mL	10%

Filter the medium using a 0.22 μm filter. Aliquot and store at −80°C for up to a year.

Tissue Processing Buffer

Reagent	Amount	Final Concentration
F12	914 mL	n/a
FBS	50 mL	5%
Penicillin-streptomycin	10 mL	1%
Gentamycin	10 mL	1%
HEPES	15 mL	1.5%
Fungizone	1 mL	0.1%

Filter the medium with a 0.22 μm filter. The buffer can be stored at 4°C for up to 1 month.

Digestion Buffer

Measure and dissolve 1 mg collagenase in 1 mL tissue processing buffer. Filter the medium with a 0.22 μm filter. Prepare fresh digestion buffer each time.

Neutralizing Medium

StemECHO100 is a ready-to-use neutralizing medium. The culture medium can be stored at 4°C for up to 1 month.

Stem Cell Growth Medium

To prepare complete growth medium, StemECHO^{TM}PU Expansion Medium, add 0.25 mL StemECHObullet003 to 250 mL StemECHO103. Mix thoroughly and store at 4°C for up to 1 month.

Stem Cell Freezing Medium

Reagent	Amount	Final Concentration
StemECHO^{TM}PU Expansion Medium	70 mL	n/a
FBS	20 mL	20%
DMSO	10 mL	10%

Filter the medium using a 0.22 μm filter. Aliquot and store at −80°C for up to a year.

Please cite this article in press as: Rao et al., Protocol for Cloning Epithelial Stem Cell Variants from Human Lung, STAR Protocols (2020), https://doi.org/10.1016/j.xpro.2020.100063

PneumaCult-ALI Media

Prepare the PneumaCult-ALI Media following the product instructions (StemCell Technologies).

STEP-BY-STEP METHOD DETAILS

The procedures described in this protocol can be conducted in a typical Class II biological hood using standard aseptic technique. Given their high clonogenicity and rapid proliferation, a single stem cell will yield more than 1 billion stem cells with 60–80 days in this system, which enables downstream applications in a timely manner (Figure 1). Importantly, the intrinsic "immortality" of lung stem cell variants that renders their unlimited proliferative potential is not due to mutations of pRB, CDKN2A, p53, or any of a host of tumor suppressor or proto-oncogenes. Moreover, lung stem cell variants in this system retain their capacity of multipotent, lineage-specified differentiation despite continuous cultivation of more than one year.

Reviving 3T3-J2 Cells from Frozen Stock

Timing: 4–5 days

1. Retrieve cryovials from cell storage deep freezer and thaw the vial containing 10^6 cells/1 mL in 37°C water bath.
2. Gently transfer cells with 1 mL pipette into a 50 mL Falcon tube and add 30 mL culture medium drop by drop while swirling the tube slowly.
3. After re-suspension, seed cells into a 150 mm tissue culture plate.
4. Gently shake the plates with cells in the hood to evenly distribute the cells and transfer the cells in an incubator at 37°C with 7.5% CO_2.
5. Change the medium the next day after thawing the frozen vial and then change medium every 2 days. In general, cells will be ready for passaging and expansion 3 days after thawing.

⚠ CRITICAL: Do not centrifuge to wash away DMSO. Change the medium the day after thawing the vial because the freezing medium contains DMSO that is harmful to cells. Passage the cells when they become 70∼80% confluent. If 3T3-J2 cells have grown past confluence, abandon them and thaw a new vial.

Expanding 3T3-J2 Cells

Timing: 1 day

6. Transfer plates from the incubator and check the confluency and morphology of the 3T3-J2 cells under a microscope.

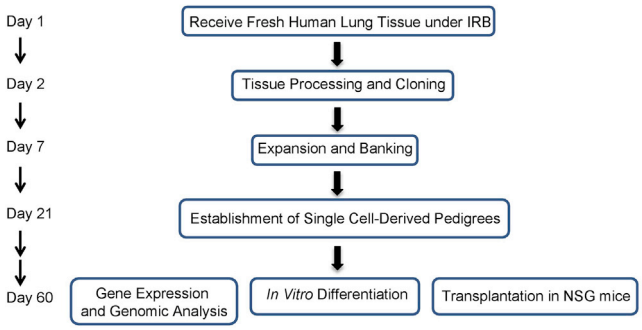


Figure 1. Workflow of Lung Stem Cell Isolation and Characterization Protocol

7. Move the plate gently into a cleaned hood, remove the medium, wash the plate with 20 mL of DPBS to remove any serum, and add evenly 5 mL of pre-warmed 0.05% Trypsin-EDTA to the plate.
8. Incubate the cells with trypsin in an incubator at 37°C with 7.5% CO_2 for 5–6 min.
9. Add 10 mL of warmed 3T3-J2 culture medium to neutralize the trypsin. Pipette up and down 10 times to make a single-cell suspension.
10. Spin down the cells at 300 g for 5 min, remove the supernatant carefully and resuspend the pellet into 5 mL of fresh 3T3-J2 culture medium. Count the cells using a hemocytometer and Trypan blue.
11. Seed 600,000–800,000 cells per plate in the amount of 20 mL 3T3-J2 culture medium, shake the plates to distribute the cells evenly and transfer the plates in the incubator at 37°C with 7.5% CO_2.

⚠ CRITICAL: It is important to strictly follow the seeding cell numbers recommended here; either higher or lower seeding density will affect the quality of the 3T3-J2 cells.

12. Every 2–3 days after passaging change the medium by removing the medium from the plate and adding 20 mL of fresh, pre-warmed medium.

Irradiating and Freezing Down 3T3-J2 Feeder Cells

Timing: 1 day

13. Repeat cell passaging procedure steps based on the need of cell number. Collect the cell pellets, resuspend the cells in 50 mL Falcon tubes containing 40 mL 3T3-J2 culture medium at the density less than 10^7 cells/mL and leave on ice before irradiation.
14. Irradiate 3T3-J2 cells at 2,000 rad. We use X-ray irradiation machine (RadSource, RS1800, Cat No. 1087). 2,000 rad is calculated based on the irradiation standard to the machine.

⚠ CRITICAL: Although the irradiation and mitomycin-C (MC) treatment seem to be qualitatively equivalent, some studies suggest that irradiation is more suitable and efficient than MC treatment for the preparation of nonreplicating feeder cells. (Roy et al., 2001; Fleischmann et al., 2009; Llames et al., 2015). However, we have not directly compared these treatments in our laboratory so it remains unclear whether MC treatment is suitable to prepare feeder cells for lung stem cell cloning.

15. After irradiation, put the container on the ice and immediately count viable cell numbers with a hemocytometer and Trypan blue.
16. Spin down cells at 300 g for 5 min at 4°C and resuspend in freezing medium very gently to freeze down 1×10^7 cells/vial. Use 0.6 mL freezing medium per vial.

⚠ CRITICAL: 3T3-J2 cells are extremely fragile after irradiation. Thus, cells need to be handled with extreme care. Do not pipet up and down to mix the cells. Swirl the container of cells very gently for mixing.

17. Put the cells in a Cool Cell Freezer box at −80°C for at least 24 hrs for gradual freezing. Transfer the frozen vials to a liquid nitrogen tank or deep freezer next day for long-term storage.

Preparing Feeder for Stem Cell Culturing

Timing: 1 day

Table 1. The Seeding Density of Feeder Cells and Lung Stem Cells in Different Cell Culture Vessels

Cell Culture Vessel	Approx. Growth Area (cm^2)	Recommended Culture Volume (mL)	Recommended No. of Feeder Cells	Recommended Seeding Density of Stem Cells
6 well	9.5	2	1,500,000–1,800,000	50,000–100,000
12 well	3.8	1	600,000–720,000	15,000–30,000
24 well	1.9	0.5	300,000–400,000	8,000–15,000
48 well	0.95	0.25	120,000–150,000	5,000–7,000
96 well	0.32	0.125	50,000–60,000	1,000–3,000
384 well	0.056	0.05	10,000–15,000	500–1,000
100 mm dish	55	12	9,000,000–11,000,000	500,000–1,000,000
150 mm dish	152	30	25,000,000–30,000,000	1,200,000–2,500,000
12 well Transwell	1.12	well 1.5, insert 0.5	800,000–1,000,000	400–600,000
24 well Transwell	0.33	well 0.7, insert 0.2	300,000–400,000	200–300,000

18. Revive and seed irradiated 3T3-J2 cells in the presence of 3T3 culture medium and shake the plates with cells to evenly distribute the cells (see Table 1 for recommended cell numbers and culture medium volume) and transfer the plates in an incubator at 37°C with 7.5% CO_2.

19. Change with 3T3-J2 culture medium next day.

Cloning Stem Cell Variants from Human Lung

Timing: 10 days

⚠ CRITICAL: Fresh human normal or diseased lung tissue should be preserved in cold tissue processing buffer for short-term storage or shipping and be processed within 48 hrs for optimal yield. If lung tissues are properly minced and frozen in the presence of stem cell freezing medium, the lung stem cells can be derived from these frozen tissues at a later time. We have successfully derived cells from tissues that have been frozen for 2 years. There is no obvious difference in the yield of clonogenic cells among different sections of the lung. In this protocol we used distal lung tissue, but this protocol is also applicable to proximal lung tissue. The improper storage or insufficient digestion will lead to unsatisfying yield of healthy and clonogenic human cells in this system.

20. Wash 1 cm^3 of distal lung tissue with 30 mL cold tissue processing buffer in 50 mL Falcon tube, centrifuge at 300 g for 10 min at 4°C, and then carefully remove the medium without disturbing the tissue. Repeat the washing procedure three times.
21. Carefully remove the tissue and put it into a 150 mm tissue culture dish. Mince the tissue between two feather scalpels until the tissue resembles a paste. The whole cutting process takes about 10–15 min.

⚠ CRITICAL: This mincing step is critical and will determine cloning efficiency. Thus, try to mince the tissue as thoroughly as possible. To keep the tissue from drying, add a few drops of tissue processing buffer during the process.

22. Digest minced tissue in digestion buffer (10 mL digestion buffer per 1 cm^3 lung tissue) for approximately 60 - 90 min in a 37°C rocker set to 150 rpm. Every 10 min, pipette the mixture up and down to break up any aggregated clumps.

Table 2. The Seeding Density of Primary Lung Cells on 3T3-J2 Feeder Cells

Culture Plate Format	6 Well	12 Well	24 Well
No. of cells	1,000,000–2,000,000	500,000–1,000,000	200,000–400,000
Volume of medium	2 mL	1 mL	0.5 mL

23. After digestion, add 20 mL cold tissue processing buffer to the tubes containing digested tissue. Then mix the contents by inverting the tubes ten times.
24. After mixing, pipet the solutions through a 100 μm cell strainer and collect the pass-through suspension in a new 50 mL Falcon tube.
25. Add tissue processing buffer to this filtered cell suspension until the total volume is 45 mL, centrifuge at 300 g for 20 min at 4°C, remove the buffer carefully and repeat washing steps 6 more times at 300 g for 10 min.
26. After the final wash, lyse the erythrocytes in the cell pellets by adding 5 mL ACK lysing buffer and incubating for 5 min at 20–22°C. Add 35 mL of tissue processing buffer and spin down at 300 g for 10 min at 4°C. Wash one more time with 10 mL cold neutralization medium.
27. Following the last centrifugation, resuspend the cell pellet in 1 mL of stem cell growth medium completely by pipetting up and down for ten times. Count the primary cells using hemocytometer. Seed the cells into the tissue culture dish pre-seeded with irradiated 3T3-J2 feeder cells (see Table 2 for the seeding density of primary cells).

28. Change stem cell growth medium every 2 days.

⚠ CRITICAL: Plates seeded with irradiated 3T3-J2 feeder cells need to be used within 5 days. Using the aged feeder plates will lead to the loss of stemness in these lung stem cell variants.

Passaging Human Lung Stem Cell Variants

Timing: 2–4 h

29. When small and round lung stem cell colonies with relatively large nucleus and high nucleus/cytoplasm ratio are visible under the microscope (takes about 7–10 days, Figure 2), wash the plate with DPBS twice, add 1 mL TrypLE and incubate at 37°C in the incubator with 7.5% CO_2 for 15 min. Check the cells once or twice and, if they are not totally dissociated, incubate another 5–10 min until cells are fully detached from the plate.

30. Pipet the cells gently up and down 5–10 times to further dissociate them into single cells.
31. Add 2 mL warmed neutralizing medium quickly into the well-trypsinized cells and pipet up and down 20 times. Pipet the cells through a 30 μm pre-separation filter, centrifuge them at 300 g for 6 min at 4°C and then discard the supernatant.

⚠ CRITICAL: Do not add neutralization medium dropwise as cells will aggregate. Pipet vigorously to break down cell clusters into single cells.

32. Resuspend the cell pellets into 6 mL stem cell growth medium, count the cells, and seed them onto a plate that was pre-seeded with irradiated 3T3-J2 feeder cells (see Table 1 for recommended seeding density).
33. Change the medium every 2 days. In about 2–3 days, individual lung stem cell colonies will be observed. In about 4–6 days, the stem cell culture plate should be ready for passaging, freezing down, single-cell cloning or single-cell RNA sequencing.

Please cite this article in press as: Rao et al., Protocol for Cloning Epithelial Stem Cell Variants from Human Lung, STAR Protocols (2020), https://doi.org/10.1016/j.xpro.2020.100063

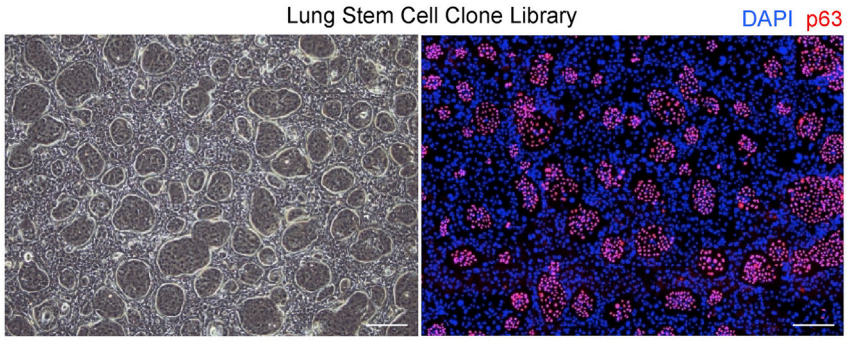


Figure 2. Cloned Lung Stem Cells Are p63 Positive

Left: A representative bright field image of the lung stem cell clones generated from resected human distal lung tissue. The image was taken 7 days after dissociated lung epithelial cells were plated on 3T3-J2 feeder cells before being passaged, and p63+ stem cells were selectively formed colonies in this culture system. Scale bar, 100 μm. Right: A representative immunofluorescence image of the lung stem cell libraries stained with antibody to p63 showing uniform nuclear staining within each p63+ stem cell colony. These are dissociated lung epithelial stem cells after 7 days growth before being passaged. Scale bar, 100 μm. The p63 negative cells are the 3T3-J2 feeder cells.

⚠ CRITICAL: This system can support lung stem cell immaturity for at least 25 passages (250 days continuous propagation). We recommend performing single-cell cloning and single-cell RNA sequencing as early as possible, preferably at passage 2.

Establishing Single Stem Cell-Derived Pedigrees

Timing: 6–8 weeks

34. After 2 days post seeding at a density of 100,000 cells per well of 6-well plate, the stem cell clone library culture is approximately 60% confluent and each colony has about 50 cells. Trypsinize the stem cell clones following steps mentioned above, pipette the neutralized cells up and down to achieve a single-cell suspension, and pass them through a 30 μm pre-separation filter.
35. Centrifuge at 300 g for 5 min and remove the 3T3-J2 feeder cells using QuadroMACS Starting Kit (LS) following manufacturer's protocol. Resuspend the cell pellet in 1 mL stem cell growth medium.
36. Use a cell sorter to sort single cells to individual wells of a 384-well plate previously seeded with feeder cells (Figure 3).

37. Change medium every 3–5 days. It will take around 7–10 days to observe colonies in many wells of the plate.
38. Two weeks after plating, gently wash the wells having colonies with 75 μL DPBS twice, add 30 μL TrypLE, incubate for 15 min or even longer in the incubator at 37°C with 7.5% CO_2.

⚠ CRITICAL: Check each well during trypsinization and make sure that all colonies are completely dissociated before neutralizing.

39. Gently pipet up and down 5 times for each well. Neutralize the TrypLE by adding 50 μL warmed stem cell growth medium quickly into each well and pipet up and down another 10 times to dissociate colonies.

⚠ CRITICAL: Change tips for each well and pipet carefully to avoid aerosols and cross-contamination.

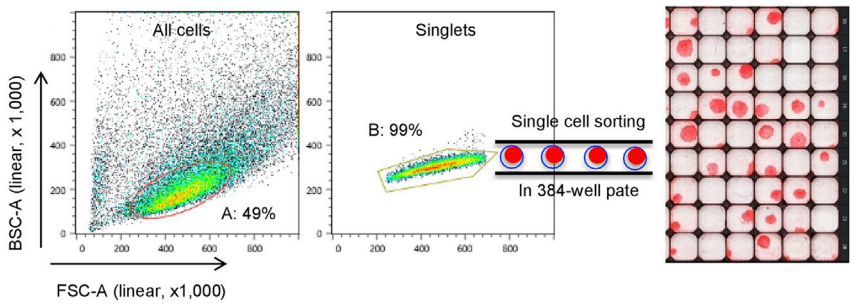


Figure 3. Schematic of Generating Single-Cell-Derived Pedigrees of Lung Stem Cells
Single cells are sorted into each well of 384-well plate and majority of them can be expanded to unique pedigrees.

40. For each well of dissociated cells, transfer the cell suspension into one well of 24-well plate each that has been seeded with feeder cells. Each well will be marked as a single-cell-derived clone and can be expanded into billions of cells in a few weeks.

Characterization of Individual Clones *In Vitro*

Timing: 4–5 weeks

Expansion of individual stem cell clones for molecular genetics and functional analyses *in vitro* (air-liquid interface, ALI) and *in vivo* (xenografts) is essential to deconstruct the heterogeneity among the epithelial stem cells of the lung and airways. Growing individual clones at ALI allows assessment of the *in vitro* differentiation potential of each clone.

41. Expand individual clones in one well of a 6-well plate pre-seeded with feeder cells. Aspirate the culture medium, rinse with DPBS thoroughly, and add 1 mL TrypLE™ Express Enzyme (1×) for 10–20 min in the incubator at 37°C with 7.5% CO_2.
42. Pipette up and down 5–10 times. Neutralize with 2 mL stem cell neutralizing medium, vigorously pipette up and down and pass through a 30 μm pre-separation filter to achieve a single-cell suspension. Remove mouse feeder cells using QuadroMACS Starting Kit.
43. Count the cells and seed 200,000–300,000 cells in 200 μL complete Stem Cell growth medium per well of a 24-well Transwell insert. Add 700 μL complete stem cell growth medium into the lower chamber of the insert.
44. Incubate the Transwell insert in a 37°C incubator with 7.5% CO_2 for 3–4 days until confluency, and change medium of both upper and lower chambers every other day.
45. At confluency, remove the medium of the upper chamber of the insert by carefully pipetting to create ALI culture. Change the medium of the lower chamber into PneumaCult-ALI Media, and keep for an additional 21 days in the incubator at 37°C with 7.5% CO_2 to induce complete differentiation.

Characterization of Individual Clones *In Vivo*

Timing: 4–5 weeks

To assess the pathogenic potential of the lung epithelial clones, such as neutrophilic inflammation and fibrosis, subcutaneous transplantation of them into highly immunodeficient NSG (NODscidIL2-ranull) is performed (Figure 4 and Video S1). A detailed phenotypic and molecular characterization of the stem cell variants in chronic obstructive pulmonary disease (COPD), for instance, has been presented (Rao et al., 2020).

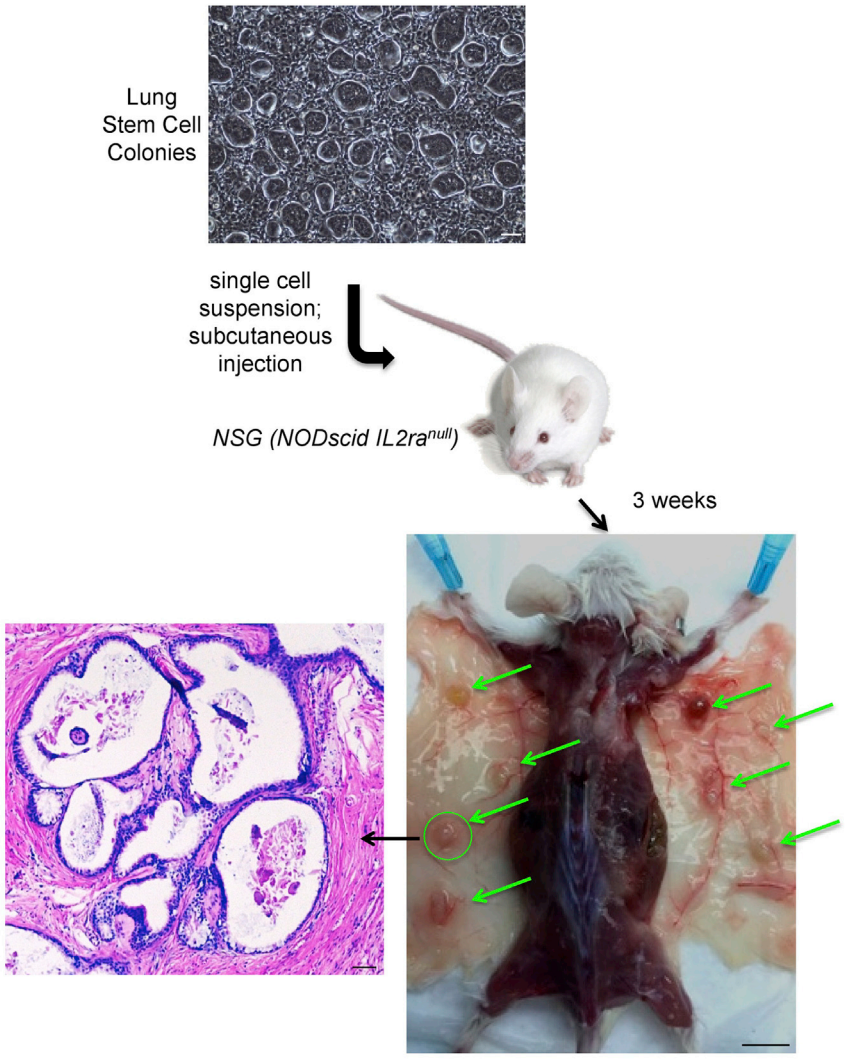


Figure 4. Work Flow of Subcutaneous Transplantation of Lung Stem Cells in NSG Mice

Lung stem cells in colonies (scale bar, 100 μm) are trypsinized to single cells, mixed with Matrigel and subcutaneously transplanted into appropriately anesthetized 8-week-old male or female NSG mice. At 3 weeks post-transplant, mice are euthanized by CO_2 and the xenograft nodules harvested (scale bar, 1 cm), embedded, and analyzed by H&E staining (scale bar, 100 μm).

46. Expand individual clone in three wells of a 6-well plate pre-seeded with feeder cells.
47. At 4 to 5 days post seeding, the stem cells in each well should reach 90% confluency in a 6-well plate. Trypsinize and collect the cell pellets following the same procedure as described above.
48. Resuspend the cell pellets in 50 μL serum-free F12 medium and keep the suspension on ice.
49. Mix approximately 1×10^6 lung stem cells with 50 μL (1:1) growth factor-reduced Matrigel, and subcutaneously inject the cells into the back of 8- to 10-week-old NSG mice of either sex following inhalation anesthetic using isoflurane gas (Video S1).

⚠ CRITICAL: In this step, both cell suspensions and GFR Matrigel should be kept on ice before injection. It is absolutely essential to use growth factor-reduced Matrigel as non-reduced contains factors that might affect complete differentiation of the cells. The differentiation fates of these clones in xenografts have been proved to be

remarkably stable to 250 days of continuous propagation *in vitro*, suggesting that the passages of these clones will unlikely affect the outcome of the xenograft experiment.

50. Clearly label the exact spots where cells were injected with a permanent marker.
51. 3 weeks after the injection, euthanize the mice, collect nodules, and fix them in 4% PFA for 24 hrs at 4°C (Figure 4).
52. Process the nodules as a small tissue sample in a tissue processor, embed in paraffin blocks, cut sections, and characterize the histology using recommended antibodies.

⚠ CRITICAL: It is important to keep the xenografts in the mice for at least 3 weeks before collecting to allow the stem cells to differentiate properly.

EXPECTED OUTCOMES

Using this protocol, libraries of epithelial stem cell variants from human normal lung or COPD lung have been established. This library comprises multiple types of p63+ stem cells that are committed to distinct lineages (e.g. Clusters 1–4; Rao et al., 2020). Single stem cell-derived pedigrees can be established and further characterized *in vitro* (molecular genetics, air-liquid interface assays, etc.) and *in vivo* (mouse xenograft assay). These established pedigrees are also suitable for the applications including RNA or DNA sequencing, genome editing, drug screening and stem cell-based regenerative medicine.

QUANTIFICATION AND STATISTICAL ANALYSIS

We provide the seeding density of irradiated 3T3-J2 cells in various types of tissue culture dishes in order to generate the highest quality of feeder seeded plates (Table 1). In addition, we provide the seeding density of lung stem cells for the optimal culture condition of maintaining stemness of these cells (Table 2).

LIMITATIONS

We have successfully derived and cultured stem cell variants from lungs of a large number of donors and observed very similar efficiency of cloning and long-term culturing independent of donor sex and age. The condition of the 3T3-J2 feeder layer can play a defining role in the success of human lung stem cell derivation, and this condition is ultimately dependent on adhering to rigid parameters of 3T3-J2 growth and expansion as defined in this protocol. Not every investigator in the laboratory can or will work within these parameters. Another important limitation of this method is the tendency of lung stem cells to spontaneously differentiate if colonies are allowed to merge to confluence. Thus, to maintain the stemness of lung stem cells, the seeding density and confluency of the cultures need to be strictly monitored. In addition, lung stem cells tend to differentiate if they are seeded as clusters of cells instead of single cells during passaging. Thus, thorough trypsinization and filtration or flow-sorting before seeding is essential to maintain the potential of these cells. While we have endeavored to control the culture conditions, we note that these media require fetal bovine serum, a variable whose impact is difficult to estimate but lot numbers should be monitored. Finally, it is critical to ensure the quality of lung stem cells prior to seeding them on *Transwell* membranes for ALI differentiation, transplanting them as xenografts, or subjecting them to genome editing protocols.

An important consideration in employing this technology is that the initial "libraries" of clonogenic cells from the lungs are complex and comprised of heterogeneous stem cells with respect to their fate commitment. Thus from COPD lungs, four major clone types were identified, all of which expressed high levels of the p63 transcription factor, a master regulator of all stratified epithelial stem cells (Senoo et al., 2007). Apart from this similarity, the four major classes of stem cells show distinct and absolute fate commitments (Cluster 1: distal airway: Club cells, type I and II pneumocytes; Cluster 2: goblet cell metaplasia; Cluster 3: squamous cell metaplasia; Cluster 4; inflammatory

Please cite this article in press as: Rao et al., Protocol for Cloning Epithelial Stem Cell Variants from Human Lung, STAR Protocols (2020), https://doi.org/10.1016/j.xpro.2020.100063

cell metaplasia; Rao et al., 2020). Given this complexity, and the possibility that one clone type might display proliferation advantages over another, it is likely that long-term expansion of the libraries could alter the clone distribution. We therefore recommend that analyses such as single-cell RNA sequencing or the generation of single-cell-derived clones be performed at early-passage stages, preferably at passage 2 or 3 of the library.

TROUBLESHOOTING

Problem

3T3-J2 cells lose contact inhibition and continue to proliferate at high density resulting in a loss of lawn quality.

Potential Solution

Contact inhibition is a feature of the 3T3-J2 line that makes these cells suitable to use as feeder layers for cloning stem cells. Growth at high densities will select for those that have lost this property. If this happens, it is better to discard the cells and start over with a new, early-passage vial of 3T3-J2.

Problem

Increased saturation density of 3T3-J2 cells

Potential Solution

Typically, 150 mm dish of 3T3-J2 cells yields 8–10 million cells. If you get around 15–20 million cells, your 3T3-J2 cells have been grown improperly and, as detailed above, have lost contact inhibition. This will adversely affect your stem cell culture. In this case, it is highly recommended that you thaw a new vial of 3T3-J2 cells.

Problem

Poor health of feeder cells

Potential Solution

The condition of feeder cells strongly depends on the quality of the 3T3-J2 culture. Ensure irradiation is performed on the collected 3T3-J2 cells as soon as possible. The cell suspension should be placed on ice at all times. After irradiation, the freezing medium must be added dropwise to the cells and gently mixed.

Problem

Stem cells lose clonogenicity.

Potential Solution

Loss of clonogenicity indicates a loss of stemness. This happens if the cells start to differentiate (Figure 5). To ensure immaturity of cells, the seeding density guidelines should be strictly followed (Table 1). In addition, care must be taken to not let the cells grow to confluency as this will trigger differentiation. In case the clonogenicity is significantly reduced, it is better to start a new culture from early-passage stem cells, preferably from passage 2 or 3.

Problem

ALI-derived epithelium is damaged.

Potential Solution

The loss of structural integrity may be a result of bad condition of seeded lung stem cellss or damage induced during medium changes. The seeding density of lung stem cells on Transwell filters should be strictly adhered to (Table 1). The apical medium should be carefully removed after the culture attains confluency. If leakage in the ALI is observed, the experiment should be started again.

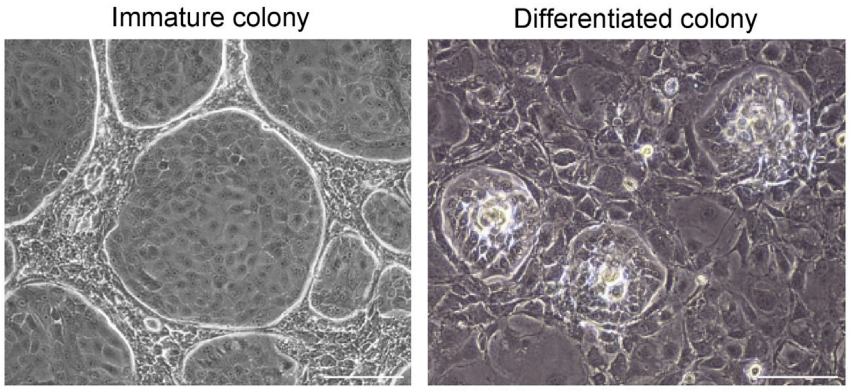


Figure 5. Inappropriate Lung Stem Cell Differentiation

Comparison between immature lung stem cell clones (left) and clones undergoing spontaneous differentiation (right). Scale bar, 100 μm. The images were taken at 7 days after the lung stem cells were seeded onto lawns of 3T3-J2 feeder cells. If the procedures described in this protocol are followed strictly, more than 80% of the stem cell colonies remain immature as shown in the left panel. If more than 50% of the colonies display the morphology shown in the right panel, the culture should be discarded.

Problem

Xenograft nodule shows incomplete differentiation.

Potential Solution

The timing of *in vivo* differentiation is key for appropriate differentiation. Based on our experience, 3 weeks seem to be ideal to collect the xenografts. One or two weeks of differentiation may not be sufficient for terminal differentiation. In addition, if nodules are left for longer than a month, the epithelia in these xenografts may diminish.

RESOURCE AVAILABILITY

Lead Contact

Further information and requests for resources and reagents should be directed to and will be fulfilled by the Lead Contact Wa Xian (wxian@uh.edu).

Materials Availability

The unique/stable reagents generated in this study are available from the Lead Contact with a completed Materials Transfer Agreement.

Data and Code Availability

This protocol does not include any datasets or code.

SUPPLEMENTAL INFORMATION

Supplemental Information can be found online at https://doi.org/10.1016/j.xpro.2020.100063.

ACKNOWLEDGMENTS

This work was supported by grants from the Cancer Prevention Research Institute of Texas (CPRIT; RR150104 to W.X. and RR1550088 to F.M.), the National Institutes of Health (1R01DK115445-01A1 to W.X., 1R01CA241600-01 and U24CA228550 to F.M.), the US Dept. of Defense (W81XWH-17-1-0123 to W.X.), and the American Gastroenterology Association Research and Development Pilot Award in Technology (to W.X.). W.X. and F.D.M. are CPRIT Scholars in Cancer Research. We thank all the members in the Xian-McKeon laboratory for helpful discussions and support. We thank H. Green and J. Rosen for advice and support.

STAR Protocols
Protocol

CellPress
OPEN ACCESS

AUTHOR CONTRIBUTIONS

Experimental design and conception were done by W.X., M.V., W.R., and F.D.M. Human lung stem cell cloning and analysis *in vitro* and *in vivo* were performed by W.R. and S.N. S.W. and W.R. performed bioinformatics analyses. W.X., W.R., S.N., and F.D.M. wrote the manuscript with input from all other authors. W.X. and F.D.M. supervised the research.

DECLARATION OF INTERESTS

W.X., F.D.M., W.R., S.W., and M.V. have filed patents related to technologies used in the present work. M.V., F.D.M., and W.X. have financial interests in Nüwa Medical Systems, Inc., Houston, TX, USA, a trademark of Tract pharmaceuticals, Inc., Houston, TX, USA.

REFERENCES

Kumar, P.A., Hu, Y., Yamamoto, Y., Hoe, N.B., Wei, T.S., Mu, D., Sun, Y., Joo, L.S., Dagher, R., Zielonka, E.M., et al. (2011). Distal airway stem cells yield alveoli in vitro and during lung regeneration following H1N1 influenza infection. Cell *147*, 525–538.

Rao, W., Wang, S., Duleba, M., Niroula, S., Goller, K., Xie, J., Mahalingam, R., Neupane, R., Liew, A.A., Vincent, M., et al. (2020). Regenerative metaplastic clones in COPD lung drive inflammation and fibrosis. Cell *181*, 848–864.

Senoo, M., Pinto, F., Crum, C.P., and McKeon, F. (2007). p63 Is essential for the proliferative potential of stem cells in stratified epithelia. Cell *129* (3), 523–536, https://doi.org/10.1016/j.cell.2007.02.045.

Zuo, W., Zhang, T., Wu, D.Z., Guan, S.P., Liew, A.A., Yamamoto, Y., Wang, X., Lim, S.J., Vincent, M., Lessard, M., et al. (2015). p63(+)Krt5(+) distal airway stem cells are essential for lung regeneration. Nature *517*, 616–620.

Rheinwald, J.G., and Green, H. (1975). Serial cultivation of strains of human epidermal keratinocytes: the formation of keratinizing colonies from single cells. Cell *6*, 331–343.

Green, H. (2008). The birth of therapy with cultured cells. BioEssays *30*, 897–903.

Hirsch, T., Rothoeft, T., Teig, N., Bauer, J.W., Pellegrini, G., De Rosa, L., Scaglione, D., Reichelt, J., Klausegger, A., Kneisz, D., et al. (2017). Regeneration of the entire human epidermis using transgenic stem cells. Nature *551*, 327–332.

Roy, A., Krzykwa, E., Lemieux, R., and Néron, S. (2001). Increased efficiency of gamma-irradiated versus mitomycin C-treated feeder cells for the expansion of normal human cells in long-term cultures. J. Hematother. Stem Cell Res. *10*, 873–880.

Fleischmann, G., Müller, T., Blasczyk, R., Sasaki, E., and Horn, P.A. (2009). Growth characteristics of the nonhuman primate embryonic stem cell line cjes001 depending on feeder cell treatment. Cloning Stem Cells *11*, 225–233.

Llames, S., García-Pérez, E., Meana, Á., Larcher, F., and del Río, M. (2015). Feeder layer cell actions and applications. Tissue Eng. Part B Rev. *21*, 345–353.